

Hysteresis, Avalanches, and Disorder Induced Critical Scaling: A Renormalization Group Approach

Karin Dahmen and James P. Sethna

Laboratory of Atomic and Solid State Physics,

Cornell University, Ithaca, NY, 14853-2501

Abstract

Hysteresis loops are often seen in experiments at first order phase transformations, when the system goes out of equilibrium. They may have a macroscopic jump (roughly as in the supercooling of liquids) or they may be smoothly varying (as seen in most magnets). We have studied the nonequilibrium zero-temperature random-field Ising-model as a model for hysteretic behavior at first order phase transformations. As disorder is added, one finds a transition where the jump in the magnetization (corresponding to an infinite avalanche) decreases to zero. At this transition we find a diverging length scale, power law distributions of noise (avalanches) and universal behavior. We expand the critical exponents about mean-field theory in $6 - \epsilon$ dimensions. Using a mapping to the pure Ising model, we Borel sum the $6 - \epsilon$ expansion to $O(\epsilon^5)$ for the correlation length exponent. We have developed a new method for directly calculating avalanche distribution exponents, which we perform to $O(\epsilon)$. Numerical exponents in three, four, and five dimensions are in good agreement with the analytical predictions. Some suggestions for further analyses and

experiments are also discussed.

PACS numbers: 75.60.Ej, 64.60.Ak, 81.30.Kf

I. INTRODUCTION

The modern field of disordered systems has its roots in dirt. An important effect of disorder is the slow relaxation to equilibrium seen in many experimental systems [1]. This paper is an attempt to unearth *universal, nonequilibrium* collective behavior buried in the muddy details of real materials and inherently due to their tendency to remain far from equilibrium on experimental time scales. In particular, we focus on two distinctly nonequilibrium effects: (a) the avalanche response to an external driving force and (b) the internal history dependence of the system (hysteresis).

Systems far from equilibrium often show interesting memory effects not present in equilibrium systems. Far from equilibrium, the system will usually occupy some metastable state that has been selected according to the history of the system. Jumps over large free energy barriers to reach a more favorable state are unlikely. The system will move through the most easily accessible local minima in the free energy landscape as an external driving field is ramped, because it cannot sample other, probably lower lying minima, from which its current state is separated by large (free energy) barriers. The complexity of the free energy landscape is usually greatly enhanced by the presence of disorder. It is well known [1–5], that disorder can lead to diverging barriers to relaxation and consequent nonequilibrium behavior and glassiness.

(a) Avalanches: In some systems, collective behavior in the form of avalanches is found when the system is pushed by the driving field into a region of descending slope in the free energy surface. In experiments avalanches are often associated with crackling noises as in acoustic emission and Barkhausen noise [6–9]. There are other nonequilibrium systems where no such collective behavior is seen. Bending a copper bar for example causes a sluggish, creeping response due to the entanglement of dislocation lines. In contrast, wood snaps and crackles under stress due to “avalanches” of fiber breakings [10].

Although avalanches are collective events of processes happening on microscales, in many systems they can become monstrously large so that we - in spite of being large, slow creatures

- can actually perceive them directly without technical devices. This reminds one of the behavior observed near continuous phase transitions, where critical fluctuations do attain human length and time scales if a tunable parameter is close enough to its critical value. Correspondingly one might expect to find universal features when the sizes and times of the avalanches get large compared to microscopic scales.

In fact, interesting questions concerning the *distribution* of avalanche sizes arise. Many experiments show power law distributions over several decades. For example, experiments measuring Barkhausen-pulses in an amorphous alloy, iron and alumeel revealed several decades of power law scaling for the distribution of pulse areas, pulse durations and pulse-energies [11]. Similarly, Field, Witt, and Nori recorded superconductor vortex avalanches in $Nb_{47\%}Ti_{53\%}$ in the Bean-state as the system was driven to the threshold of instability by the slow ramping of the external magnetic field. The avalanche sizes ranged from 50 to 10^7 vortices. The corresponding distribution of avalanche sizes revealed about three decades of power law scaling. Numerous other systems show similar power law scaling behavior [11–15].

Why should there be avalanches of many sizes? Power laws suggest a scaling relationship between different length scales with universal exponents.

There has been much recent progress studying avalanches near (continuous) *depinning transitions*. In these systems a single, preexisting interface or “rubber sheet” is pushed through a disordered medium by an external driving force. When the randomness is in some sense weak, the interface distorts elastically without breaking over a wide range of length scales [16]. The distortions occur in the form of avalanches on increasing size as the external driving force is raised to a critical threshold field at which the interface starts to slide (“depins”). Examples studied include charge density waves [17–22], weakly pinned Abrikosov flux lattices [23], single vortex-lines [24–26], preferentially wetting fluids invading porous media [27,28], a single advancing domain wall in weakly disordered magnets [28–30] and fluids advancing across dirty surfaces [31]. Their analytical description turns out to be rather involved, demanding functional renormalization groups (see appendix G). If the disorder is in some sense strong, the elastic interface can tear. It then responds much more

inhomogeneously and like a plastic or fluid, to the external driving force. This is the case for strongly pinned vortex lines in the mixed state of superconducting films [32,25], the invasion of nonwetting fluids into porous media [33,28] and nonlinear fluid flow across dirty surfaces [34], and others.

Many hysteretic systems exhibit a wide distribution of avalanche sizes *without* an underlying depinning transition. They usually have *many* interacting advancing interfaces and in some cases also new interfaces created spontaneously in the bulk. We propose that the large range of observed avalanche sizes in these systems might be a manifestation of a nearby critical point with both disorder and external magnetic field as tunable parameters. In the class of models, which we have been studying near the critical point, we find not only universal scaling behavior in the avalanche size distribution, but also in the shape of the associated hysteresis loops.

(b) Hysteresis (response lags the force): Hysteresis is often observed at first order transitions, when the system goes out of equilibrium. It probably has been best studied in magnetic systems. The origin of magnetic hysteresis lies in the spontaneous magnetization of the microscopic Weiss-domains [35]. In the demagnetized state, the Weiss domains are irregularly oriented in different directions. The orientation of the magnetization of each domain is a function of the energy of the magnetic field and the elastic energy in the crystal (magnetostriction) and it is chosen such that the free energy is at a (local) minimum. Since there are many minima available, the specific choice depends on the history of the system. Thermal vibrations of the lattice are usually not sufficient to rotate the magnetization of a Weiss-domain into another preferred direction, since in most cases these directions are separated from each other by large energy barriers. As a weak magnetic field is applied, first those Weiss-domains which are most closely aligned with the field will grow at the expense of the others. At higher fields, up to saturation, entire domains will rotate in the direction of the field. The ultimate cause for hysteresis are the irreversible domain wall motion and domain rotation, which happen suddenly, as “avalanches” without further field increase, when the corresponding threshold fields are exceeded. The resulting jumps in the magnetization are

called Barkhausen jumps. Under a magnifying glass the magnetization curve looks like a staircase: the slope of the flat parts is due to the reversible part of the susceptibility, the step height is given by the irreversible avalanche-like changes of the magnetization. If the magnetization curve has the shape of a rectangle, the change of the magnetization happens in enormous, system sweeping avalanches, the so called large Barkhausen effect. Experimentally the Barkhausen jumps can be observed by magnetic induction or through the associated acoustic emission.

Analogous effects are found in ferroelectric materials, where avalanches of flipping ferroelectric domains can be observed in response to a changing external electric field [36,37]. Hysteresis curves with step-like noise are also found in elastic transformations, for example in athermal shape-memory alloys ramping temperature or stress. The noise is due to avalanches of regions transforming from martensite to austenite or vice versa [13]. Similar behavior has been observed for vortices moving in avalanches in type II superconductors as the external magnetic field is increased [12], for liquid helium leaving Nuclepore in avalanches as the chemical potential is reduced [15], and for some earthquake models [38–40,14]. In section II we discuss recent experiments performed in some of these systems.

We have modeled the long wavelength, low frequency behavior of these systems using the nonequilibrium zero temperature random field Ising model (RFIM). Some of our results have been published previously [41,42]. In contrast to some other hysteresis models, like the Preisach model [43] and the Stoner-Wohlfarth model [7], where interactions between the individual hysteretic units (grains) are not included and collective behavior is not an issue, in the RFIM the intergrain coupling is the essential ingredient and cause for hysteresis and avalanche effects. Tuning the amount of disorder in the system we find a second order critical point with an associated diverging length scale, measuring the spatial extent of the avalanches of spin flips.

(c) Avalanches in the RFIM: A power law distribution with avalanches of *all* sizes is seen only at the critical value of the disorder. However, our numerical simulations indicate that the critical region is remarkably large: almost three decades of power law scaling in

the avalanche size distribution remain when measured 40% away from the critical point. At 2% away, we extrapolate seven decades of scaling. One reason for this large critical range is trivial: avalanche sizes are expressed in terms of volumes rather than lengths, so one decade of length scales translates to at least three decades of size (or more if the avalanches are not compact, *i.e.* if the Hausdorff dimension is less than three). Some experiments that revealed three decades of power law scaling have been interpreted as being spontaneously self-similar (“self-organized critical”) [12,11,44].¹ Our model suggests that many of the samples might just have disorders within 40% of the critical value. Tuning the amount of disorder in these systems might reveal a plain old critical point rather than self organized criticality.

(d) Hysteresis in the RFIM: At the critical disorder we also find a transition in the shape of the associated hysteresis loops: Systems with low disorder relative to the coupling strength, have rectangle-shaped hysteresis loops and a big (Barkhausen) discontinuity, while systems with large disorder relative to the coupling show smooth hysteresis loops without macroscopic jumps. At the critical disorder R_c separating these two regimes, the size of the jump seen in the low disorder hysteresis loops shrinks to a point at a critical magnetic field $H_c(R_c)$, where the magnetization curve $M(H)$ has infinite slope. The power law with which it approaches this point is universal.

(e) Results: We have extracted the universal exponents near this transition point from a history dependent renormalization group (RG) description for the nonequilibrium zero

¹The name “self-organized critical” is in fact an oxymoron: ”Critical” means that you have to be just at the right place, ”self-organized” indicates that the system does not need to be tuned anywhere special. While it is true that many “self organized critical” systems are regular critical points where the boundary conditions stabilize the system at the transition, the same is true of ice in a glass of water. The tools for studying the critical point are the RG methods in development over many years. We discuss here our doubts that the experiments are self-organized even in this limited sense.

temperature random field Ising model. The calculation turns out to be much simpler than for related depinning transitions [19,20,29–31,26] (see also appendix G). Above 6 dimensions the exponents are described by mean field theory. We expand the critical exponents around mean-field theory in $6 - \epsilon$ dimensions and discover a mapping to the perturbation expansion for the critical exponents in the pure equilibrium Ising model in two lower dimensions. The mapping does not, however, apply to the exponents governing the avalanche size distribution, which to our knowledge, have not yet been calculated directly in the depinning transitions. The simplicity of the RG calculation allowed us to develop a new method to calculate these avalanche exponents directly in the ϵ -expansion, involving replicas of the system in a very physical way. We have used it to calculate the avalanche exponents to first order in ϵ . We report under separate cover [45] extensive numerical simulations used to extract exponents in 3, 4, and 5 dimensions (see section X). We find good agreement between the two approaches.

This paper is organized as follows: In section II we discuss several experiments in magnetic systems, shape memory alloys, porous media and superconductors that have close connections to the model studied here. The model is introduced in section III and a summary of our results is given in section IV. In section V we pause for a moment and reflect upon our real motives. In section VI the RG description is set up using the Martin-Siggia-Rose formalism, and a description of the perturbative expansion and the results for the exponents to $O(\epsilon)$ is given in section VII. section VIII contains a discussion of the mapping of the expansion to the expansion for the thermal RFIM. We extract corrections to $O(\epsilon^5)$ for most of the exponents and show a comparison between the Borel resummation of the ϵ -expansion and numerical results. In section IX a new method to calculate avalanche exponents directly in an ϵ -expansion is described and performed to $O(\epsilon)$. Finally, in section X we compare the results to our numerical simulation [45].

Some of the details of the mean-field calculation are given in appendix A. The expected tilting of the scaling axes in finite dimensions is discussed in appendix B. Details on the implementation of the history in the RG calculation are given in appendix C. Appendix D contains a description of the Borel summation of the results for η and $1/\nu$ to $O(\epsilon^5)$ (which

is relevant also for the pure Ising model). The behavior near the infinite avalanche line in systems with less than critical randomness is discussed in appendix E. Appendix F renders details on the calculation of the avalanche exponents by the use of replicas. Related problems are finally discussed in appendix G.

II. EXPERIMENTS

In this section we will discuss several experiments that reveal scaling behavior which might be related to the critical point studied in this paper. The critical exponents found in real experiments do not necessarily have to be the same as in our model, since long-range interactions, different conserved quantities and other changes are likely to alter the universality class in some cases. We do propose however that the qualitative features, in particular the existence of an underlying plain old critical point with disorder and driving field as tunable parameters are likely to be the same as in our model (see also appendix G). A more detailed discussion of these and other Barkhausen experiments [91–96,99,97], and related experiments in non-magnetic avalanching systems (in shape memory alloys [13,46], superconductors [12,49], liquid helium in Nuclepore [15], and others), and a quantitative comparison with our theory will be given in a forthcoming publication [98,128,126].

A. Magnetic hysteresis loops for different annealing temperatures

A beautiful, qualitative illustration of the crossover from smooth hysteresis loops at large disorder to hysteresis loops with macroscopic jumps at low disorder is shown in figure 1. The hysteresis loops were measured by Berger [47,48] for a 60 nm thick Gd film which had been grown onto a tungsten single crystal with a (110) surface orientation. The substrate as well as the film are highly purified (contaminants are less than 1/20 of a monolayer). Gd films prepared in this way exhibit a hcp structure with the (0001) direction perpendicular to the surface. The substrate temperature during deposition was $T = 350K$, which results in smooth films with large atomically flat terraces, but also produces films with locally varying

strain and therefore with locally varying anisotropy. Subsequent annealing at higher temperatures improves the crystallographic order, which is accompanied by a strain relaxation. Thus, by varying the annealing temperature the authors are able to change the variation of the anisotropy defect density, which is somewhat analogous to the disorder parameter R in our model. Higher annealing temperatures correspond to lower values of R . If there is a second order critical point of the kind described in the introduction underlying the crossover from hysteresis loops with a jump to smooth hysteresis loops, it should be possible to extract a scaling form for the magnetization curves similar to the one given in eq. (9). (The annealing temperature minus some critical value would play the role of the tunable reduced disorder parameter r .) Under appropriate rescaling of the axes near the critical point the magnetization curves should all collapse one onto another. The necessary amount of rescaling as a function of distance from the critical point determines the (presumably universal) exponents [45]. Further measurements near the crossover to extract potential scaling behavior are currently being performed by Berger [47].

B. Barkhausen noise for different annealing temperatures

Scaling behavior has also been recorded in the Barkhausen pulse duration and pulse area distribution in a related experiment [6]. The pulse area gives the total change in the magnetization due to the corresponding Barkhausen pulse. It is analogous to the avalanche size given by the number of spins participating in an avalanche in our model. It was found that the distribution of pulse areas integrated over the hysteresis loop of an 81% Ni-Fe wire (50 cm long, 1mm diameter) was well described by a power law up to a certain cutoff size (see figure 2). The cutoff appeared to be smaller at higher annealing temperatures. It would be interesting to see whether the cutoff takes a system-size dependent maximum value at a critical annealing temperature T_c^{ann} and decreases again at higher and lower annealing temperatures. This would be expected if varying the annealing temperature would correspond to tuning the system through a critical region with a diverging length scale at

T_c^{ann} . Near T_c^{ann} the Barkhausen pulse area distributions should then be described by a scaling form that would allow a scaling collapse of all distributions onto one single curve for appropriate stretching of the axes. Again, potentially universal critical exponents could be extracted from such a collapse. They would be predicted by our avalanche critical exponents if our model is in the same universality class.

C. Barkhausen pulse size distributions at fixed disorder

There are other experiments which revealed power law decays for Barkhausen pulse size distributions in various samples, as we have mentioned earlier [11,44]. To our knowledge the amount of disorder (or another parameter) was not varied in these experiments. The power law scaling over several decades found in these systems has in some cases been interpreted as a manifestation of self-organized criticality [11]. According to our simulations however, three decades of scaling occur when the disorder is as far as 40% away from the critical value. Tuning the amount of disorder in the system (for example by annealing the sample as in the previous two experiments, or by introducing random strain fields) might lead to a larger (or smaller) cutoff in the power law pulse size distribution. It seems rather plausible that the observed scaling behavior would be due to a plain old critical point rather than self-organized criticality.

D. Remarks

The first experiment that showed the crossover in the shape of the magnetic hysteresis loops was performed in an effectively two dimensional system, while the experiments on Barkhausen noise used effectively three dimensional systems. Interestingly, two might be the lower critical dimension of the transition which we are studying in this paper.² These

²In one dimension there will still be a crossover from hysteresis loops with a macroscopic jump to smooth hysteresis loops for a *bounded* distribution of random fields [51], however the potential

conjectures are currently being tested with our numerical simulations [45].

Real experiments may involve long-range fields which may in principle alter the universality class. Different kinds of disorder, such as correlated disorder rather than point disorder and random anisotropies or random bonds rather than random fields, may also be present. Furthermore, the symmetries can be changed if there are more than two available (“spin”) states at each site in the lattice. In appendix G we discuss related models, and which of these changes are expected to change the universality class relative to our model.

What is the moral of this story? Power laws with cutoffs are anything but sufficient evidence for self-organized criticality. In the systems discussed here, they are more likely due to a nearby *plain old critical* point with disorder as a tunable parameter and a large critical region, than spontaneous self-organization towards a self-similar state. For related future experiments and analysis one would recommend the search for tunable parameters other than system size that allow to change the cutoff in the power law distributions. For the analysis of our simulation results, scaling collapses and other techniques from equilibrium critical phenomena turned out to be very useful for extracting critical exponents [45].

III. THE MODEL

As we have explained in the introduction, the goal is to describe the long-wavelength behavior of hysteretic systems with noise due to microscopic avalanches triggered by the external driving field. We will focus in particular on the scaling regime, where collective behavior is observed on many length scales. Conventional hysteresis models like the Preisach model [43], which do not take into account interaction between the smallest hysteretic units (grains), would not be suitable for this purpose. The Preisach model could only be used to fit a certain measured distribution of avalanche sizes — the power law scaling would be

scaling behavior found near the transition will not be universal, but rather depend on the exact shape of the tails of the distribution of random fields.

the *input* determining free parameters of the model rather than the *output* with universal predictive power.

The key ingredient is interaction.³ As is well known from equilibrium phenomena, behavior on long length scales can often be well described by simple microscopic models that only need describe a few basic properties correctly, such as symmetries, interaction range and effective dimensions. This notion has been successfully applied in particular to equilibrium magnetic systems: the scaling behavior found in some pure anisotropic ferromagnets near the Curie-temperature is mimicked reliably by the regular Ising model [53,54]. At each site i in a simple cubic lattice there is a variable s_i , in this context called a spin, which can take two different values, $s_i = +1$ or $s_i = -1$ [55]. (This corresponds to a real magnet where a crystal anisotropy prefers the magnetic moments (spins) to point along a certain easy axis.) Each spin interacts with its nearest neighbors on the lattice through an exchange interaction, $J_{ij} = J/z$, which favors parallel alignment. z is the coordination number of the lattice and J is a positive constant. (For the behavior on long length scales the exact range of the microscopic interaction is irrelevant, so long as it is finite.) One can write the Hamiltonian as

$$\mathcal{H} = - \sum_{ij} J_{ij} s_i s_j - H \sum_i s_i, \quad (1)$$

where it is understood that the sum runs over nearest neighbor pairs of spins on sites i and j . H is a homogeneous external magnetic field. In two and higher dimensions this model

³For systems exhibiting return-point-memory (also called “subloop-closure” or “wiping-out” property) [41,52,43] there is in fact a well established method to verify whether interactions play an important role, and whether the Preisach model is applicable at all. It involves testing for subloop-congruency. For further details we refer the reader to the literature [52,43,15]. This test has been conducted for the experiment on liquid He in Nuclepore [15] revealing the importance of interactions between the pores, and the failure of the conventional Preisach model to describe the hysteresis curve.

exhibits an equilibrium ferromagnetic state at temperatures $T < T_c$, where T_c is the Curie temperature. Figure 3 shows the corresponding equilibrium magnetization curve at zero temperature: All spins are pointing up at positive external magnetic fields, and all spins are pointing down at negative external magnetic fields. At $H = 0$ the curve is discontinuous.

What would the magnetization curve look like for the same model, but far from equilibrium, as is the case for most real magnets? The answer is shown in figure 4. We have imposed a certain local dynamics, assuming that each spin s_i will flip only when the total effective field at its site, given by

$$h_i^{\text{eff}} = - \sum_j J_{ij} s_j - H, \quad (2)$$

changes sign. We find that the resulting magnetization curve becomes history dependent. The system will typically be in some metastable state rather than the ground state. The upper branch of the hysteresis curve in figure 4 corresponds to the case where we have monotonically and adiabatically lowered the external magnetic field, starting from $H = +\infty$, where all spins were pointing up. At the coercive field $H_c^l = -2dJ_{ij} \equiv -J$ all spins flip in a single system spanning event or “avalanche”. Similarly, for increasing external magnetic field, they all flip at $H_c^u = 2dJ_{ij} \equiv +J$. It becomes clear that the underlying cause for hysteresis in this model is the interaction between the spins.

So far, however, an essential feature of real materials is missing: there is no account for *dirt*. Usually there will be inhomogeneities and disorder in the form of defects, grain boundaries, impurities, leading to random crystal anisotropies, and varying interaction strengths in the system. Consequently not all spins will flip at the same value of the external magnetic field. Instead, they will flip in avalanches of various sizes that can be broken up or stopped by strongly “pinned” spins or clusters of previously flipped spins.

If the disorder in the system is small, the picture will not deviate dramatically from the pure case. One would expect only a few small precursors to the macroscopic avalanche of figure 4. If however, the disorder is large compared to the coupling strength in the system, one might expect no system sweeping avalanche at all, but only small clusters of spins

flipping over a broad range of the external magnetic field.

A simple way to implement a certain kind of uncorrelated, quenched disorder is by introducing uncorrelated random fields into the model. (Other kinds of disorder are discussed in appendix G.) The energy function is replaced by

$$\mathcal{H} = - \sum_{ij} J_{ij} s_i s_j - \sum_i (H + f_i) s_i. \quad (3)$$

The local dynamics remains unchanged, except for a modification in the expression for the total effective field at site i , which now also has to take into account the random field f_i :

$$h_i^{\text{eff}} = - \sum_j J_{ij} s_j - H - f_i. \quad (4)$$

We assume a Gaussian distribution $\rho(f_i)$ of standard deviation R for the fields f_i , which is centered at $f_i = 0$:

$$\rho(f_i) = \frac{1}{\sqrt{2\pi}R} \exp\left(-\frac{f_i^2}{2R^2}\right). \quad (5)$$

As we will show, the critical exponents do not depend on the exact shape of the distribution of random fields. To pick a Gaussian is a standard choice, which (due to the central limit theorem [56]) is also more likely to be found in some real experiments than, for example, rectangular distributions [57].

In magnets the random fields might model frozen-in magnetic clusters with net magnetic moments that remain fixed even if the surrounding spins change their orientation. In contrast to random anisotropies they break time reversal invariance by coupling to the order parameter (rather than its square). In shape memory alloys, ramping temperature, the random fields can be thought of as concentration fluctuations that prefer martensite over the austenite phase [58]. In the martensitic phase, ramping stress, they model strain fields that prefer one martensitic variant over another [58].

In appendix G we discuss related systems with different kinds of disorder, symmetries, interactions and dynamics, and the possible effects of such changes on the associated long-wavelength behavior and critical properties at transitions analogous to the one studied here.

IV. RESULTS

It is relatively easy to solve the nonequilibrium model of eq. (3) in the mean-field approximation where every spin interacts equally strongly with every other spin in the system. The coupling is of size $J_{ij} = J/N$, where N is the total number of spins⁴ (*i.e.* all spins act as nearest neighbors). The Hamiltonian then takes the form

$$\mathcal{H} = - \sum_i (JM + H + f_i) s_i, \quad (6)$$

Just as in the Curie-Weiss mean field theory for the Ising model, the interaction of a spin with its neighbors is replaced by its interaction with the magnetization of the system.

It turns out that the mean-field theory already reflects most of the essential features of the long-length scale behavior of the system in finite dimensions: Sweeping the external field through zero, the model exhibits hysteresis. As disorder is added, one finds a continuous transition where the jump in the magnetization (corresponding to an infinite avalanche) decreases to zero. At this transition power law distributions of noise (avalanches) and universal behavior are observed.

As we will show later in an RG description of the model, the critical exponents describing the scaling behavior near the critical point are correctly given by mean-field theory for systems in 6 and higher spatial dimensions. The RG allows us to calculate their values in $(6 - \epsilon)$ dimensions in a power series expansion in $\epsilon > 0$ around their mean-field values at $\epsilon = 0$. In the following we briefly present the results from mean-field theory, from the ϵ -expansion and from numerical simulations in 3 dimensions. More details will be given in later sections.

⁴We warn the reader that in all plots of *numerical simulation* results in finite dimensions J will denote the strength of the nearest neighbor coupling J_{ij} in the simulated crystal, while in the analytic calculation and in mean-field theory it denotes $\sum_j J_{ij}$, *i.e.* the two definitions differ by the coordination number of the lattice.

A. Results on the magnetization curve

Figure 5 shows the hysteresis curve in mean field theory at various values of the disorder $R < R_c = \sqrt{(2/\pi)J}$, $R = R_c$, and $R > R_c$. For $R < R_c$, where the coupling is important relative to the amount of disorder in the system, the hysteresis curve displays a jump due to an infinite avalanche of spin flips, which spans the system. Close to R_c the size of the jump scales as $\Delta M \sim r^\beta$, with $r = (R_c - R)/R$, and $\beta = 1/2$ in mean field theory. Using a mapping to the pure Ising model, we find in $6 - \epsilon$ dimensions [59]

$$\begin{aligned} \beta = 1/2 - \epsilon/6 + 0.00617685\epsilon^2 - 0.035198\epsilon^3 + 0.0795387\epsilon^4 \\ - 0.246111\epsilon^5 + O(\epsilon^6). \end{aligned} \quad (7)$$

At $R = R_c$ the magnetization curve scales as $M - M(H_c(R_c)) \sim h^{(1/\delta)}$, where $h = H - H_c(R_c)$ and $H_c(R_c)$ is the (nonuniversal) magnetic field value at which the magnetization curve has infinite slope. In this mean field theory $H_c(R_c) = 0$, and $M(H_c(R_c)) = 0$, and $\beta\delta = 3/2$. In $6 - \epsilon$ dimensions [59]

$$\beta\delta = 3/2 + 0.0833454\epsilon^2 - 0.0841566\epsilon^3 + 0.223194\epsilon^4 - 0.69259\epsilon^5 + O(\epsilon^6). \quad (8)$$

Numerical simulations in 3 dimensions yield $\beta = 0.036 \pm 0.036$ and $\beta\delta = 1.81 \pm 0.36$ [45].

For $R > R_c$ the disorder can be considered more important than the coupling. Consequently there are no system spanning avalanches (for infinite system size) and the magnetization curve is smooth.

Note that the hard spin mean-field theory does not show any hysteresis for $R \geq R_c$. This is only an artifact of its particularly simple structure and not a universal feature. For example, the analogous soft spin model, which is introduced for the RG description in section VI, has the same exponents in mean-field theory, but shows hysteresis at *all* disorders R , even for $R > R_c$ as seen in figure 6.

Close to R_c and $H_c(R_c)$ the magnetization curve is described by a scaling form:

$$M - M(H_c(R_c)) \equiv m(r, h) \sim r^\beta \mathcal{M}_\pm(h/r^{\beta\delta}) \quad (9)$$

where \mathcal{M}_\pm is a universal scaling function (\pm refers to the sign of r). It is computed in mean-field theory in appendix A. Corrections⁵ to the mean-field equation of state in $6 - \epsilon$ dimensions are calculated to $O(\epsilon)$ in section VII B 4. Results to $O(\epsilon^2)$ are quoted in section VIII.

B. Results on the mean-field phase diagram

Figure 7 shows the phase diagram for the lower branch of the hysteresis curve as obtained from the simple hard spin mean-field theory, defined through eq. (6). The bold line with the critical endpoint $(R_c, H_c(R_c))$ indicates the function $H_c^u(R)$ for the onset of the infinite avalanche for the history of an *increasing* external magnetic field. The dashed line describes $H_c^l(R)$ for a *decreasing* external magnetic field. The three dotted vertical lines marked (a), (b), and (c) describe the paths in parameter space which lead to the corresponding hysteresis loops shown in figure 5. Figure 8 shows the corresponding phase diagram for the soft-spin model. As before, the three dotted vertical lines marked (a), (b) and (c) indicate the paths through parameter space associated with the three hysteresis loops shown in figure 6. Note that in the soft-spin model as well as in simulations in finite dimensions the two infinite avalanche lines $H_c^u(R)$ and $H_c^l(R)$ do not touch at R_c — this is another way of saying that in these cases there is hysteresis at $R = R_c$, and, because of continuity also at $R > R_c$.

C. Results on scaling near the onset $H_c(R)$ of the infinite avalanche line ($R < R_c$)

The mean-field magnetization curve scales near the onset of the infinite avalanche as

⁵The scaling form in finite dimensions may depend not on r and h , but on rotated variables r' and h' , which are linear combinations of r and h . This applies to all scaling relations derived in the infinite range model. The amount by which the scaling axes $r' = 0$ and $h' = 0$ are turned relative to $r = 0$ and $h = 0$ is a nonuniversal quantity and has no effect on the critical exponents (see appendix B).

$$(M - M_c(H_c(R))) \sim (H - H_c(R))^\zeta \quad (10)$$

with $\zeta = 1/2$. (In the following $H_c(R)$ always stands for $H_c^u(R)$ for the history of an increasing external magnetic field, and for $H_c^l(R)$ for a decreasing external magnetic field.)

Curiously we do not observe this scaling behavior in numerical simulations with short range interactions in 2, 3, 4 and 5 dimensions. Indeed, the RG description suggests that the onset of the infinite avalanche would be an abrupt (“first order” type) transition for all dimensions $d < 8$ (see appendix E), and a continuous transition for $d > 8$. We [45] have performed initial numerical simulations in 7 and 9 dimensions for system sizes 7^7 and 5^9 at less than critical disorders. The simulation results do in fact seem to confirm the RG prediction [45]. In the following we will mostly focus on the critical endpoint at $(R_c, H_c(R_c))$, where the mean-field scaling behavior is expected to persist in finite dimensions with slightly changed critical exponents.

D. Results on avalanches

Figure 9 shows the magnetization curves from simulations of two 3 dimensional systems with only 5^3 spins. The curves are not smooth. They display steps of various sizes. Each step in the magnetization curve corresponds to an avalanche of spin flips during which the external magnetic field is kept constant. Figure 10 shows histograms $D(S, r)$ of all avalanche sizes S observed in mean-field systems at various disorders r when sweeping through the entire hysteresis loop. For small r the distribution roughly follows a power law $D(S, r) \sim S^{-(\tau+\sigma\beta\delta)}$ up to a certain cutoff size $S_{max} \sim |r|^{-1/\sigma}$ which scales to infinity as r is taken to zero.

In appendix A we derive a scaling form for the avalanche size distribution for systems near the critical point: Let $D(S, r, h)$ denote the probability to find an avalanche of size S in a system with disorder r at magnetic field h upon an infinitesimal increase of the external magnetic field. For large S one finds

$$D(S, r, h) \sim 1/S^\tau \mathcal{D}_\pm(Sr^{1/\sigma}, h/r^{\beta\delta}). \quad (11)$$

The scaling form for $D(S, r)$ of the histograms in figure 10 is obtained by integrating $D(S, r, h)$ over the external magnetic field.

In mean field theory we find $\sigma = 1/2$ and $\tau = 3/2$. In $6 - \epsilon$ dimensions we obtain from the RG calculation $\sigma = 1/2 - \epsilon/12 + O(\epsilon^2)$ and $\tau = 3/2 + O(\epsilon^2)$. Numerical simulations in 3 dimensions [45] render $\sigma = 0.238 \pm 0.017$ and $\tau = 1.60 \pm 0.08$ [45].

E. Results on correlations near $(R_c, H_c(R_c))$

With the mean field approximation we have lost all information about length scales in the system. The RG description, which involves a coarse graining transformation to longer and longer length scales, provides a natural means to extract scaling forms for various correlation functions and the correlation length of the system.

1. Avalanche correlations

The avalanche correlation function $G(x, r, h)$ measures the probability for the configuration of random fields in the system to be such that a flipping spin will trigger another at relative distance x through an avalanche of spin flips. Close to the critical point and for large x the function $G(x, r, h)$ scales as

$$G(x, r, h) \sim 1/x^{d-2+\eta} \mathcal{G}_{\pm}(x/\xi(r, h)), \quad (12)$$

where η is called “anomalous dimension” and \mathcal{G}_{\pm} is a universal scaling function. The correlation length $\xi(r, h)$ is the important (macroscopic) length scale of the system. At the critical point, where it diverges, the correlation function $G(x, 0, 0)$ decays algebraically — there will be avalanches on all length scales. Close to the critical point the correlation length scales as

$$\xi(r, h) \sim r^{-\nu} \mathcal{Y}_{\pm}(h/r^{\beta\delta}), \quad (13)$$

where \mathcal{Y}_{\pm} is the corresponding scaling function. From the ϵ -expansion one obtains [59]

$$1/\nu = 2 - \epsilon/3 - 0.1173\epsilon^2 + 0.1245\epsilon^3 - 0.307\epsilon^4 + 0.951\epsilon^5 + O(\epsilon^6), \quad (14)$$

and

$$\eta = 0.0185185\epsilon^2 + 0.01869\epsilon^3 - 0.00832876\epsilon^4 + 0.02566\epsilon^5 + O(\epsilon^6). \quad (15)$$

The numerical values in 3 dimensions are $1/\nu = 0.704 \pm 0.085$ and $\eta = 0.79 \pm 0.29$.

2. Spin-spin (“cluster”) correlations

There is another correlation function which measures correlations in the fluctuations of the spin orientation at different sites. It is related to the probability that two spins s_i and s_j at two different sites i and j , that are distanced by x , have the same value [53]. It is defined as

$$C(x, r, h) = \langle (s_i - \langle s_i \rangle_f)(s_j - \langle s_j \rangle_f) \rangle_f, \quad (16)$$

where $\langle \rangle_f$ indicates the average over the random fields. From the RG description we find that for large x it has the scaling form

$$C(x, r, h) \sim x^{-(d-4+\bar{\eta})} \mathcal{C}_{\pm}(x/\xi(r, h)), \quad (17)$$

where $\xi(r, h)$ scales as given in eq. (13) and \mathcal{C}_{\pm} is a universal scaling function. At the critical point $C(x, 0, 0)$ decays algebraically — there will be clusters of equally oriented spins on all length scales. The ϵ -expansion renders [59]

$$\bar{\eta} = 0.0185185\epsilon^2 + 0.01869\epsilon^3 - 0.00832876\epsilon^4 + 0.02566\epsilon^5 + O(\epsilon^6). \quad (18)$$

which is in fact the same perturbation expansion as for η to all orders in ϵ . (The two exponents do not have to be equal beyond perturbation theory, see also [126,129]).

F. Results on avalanche durations

Avalanches take a certain amount of time to spread, because the spins are flipping sequentially. The further the avalanche spreads, the longer it takes till its completion. The

RG treatment suggests that there is a scaling relation between the duration T of an avalanche and its linear extent l

$$T(l) \sim l^z \tag{19}$$

with $z = 2 + 2\eta$ to $O(\epsilon^3)$ [60], *i.e.*

$$z = 2 + 0.037037\epsilon^2 + 0.03738\epsilon^3 + O(\epsilon^4). \tag{20}$$

Our numerical result in 3 dimensions is $z = 1.7 \pm 0.3$.⁶

The fractal dimension for the biggest avalanches $S_{max} \sim r^{-1/\sigma} \sim \xi^{1/(\sigma\nu)}$ is

$$d_{fractal} = 1/(\sigma\nu), \tag{21}$$

so that the time for the biggest finite avalanches scales as $T(S_{max}) \sim S_{max}^{\sigma\nu z}$.

G. Results on the area of the hysteresis loop

In some analogy to the free energy density in equilibrium systems, one can extract the scaling of the area of the hysteresis loop for this system near the critical endpoint. (This is the energy dissipated in the loop per unit volume.) From the fact that the singular part of the magnetization curve scales as $m(h, r) \sim r^\beta \mathcal{M}_\pm(h/r^{\beta\delta})$ (see eq. (9)) we conjecture that the singular part of the area would scale as $A_{sing} \sim \int m(h, r) dh \sim r^{2-\alpha}$ with $2 - \alpha = \beta + \beta\delta$. (The scaling form for the total area A_{tot} will also have an analytical piece: $A_{tot} = c_0 + c_1 r^n +$

⁶While we expect the $6 - \epsilon$ results for the static exponents $\beta, \delta, \nu, \eta, \bar{\eta}, \tau, \sigma$, etc. to agree with our hard-spin simulation results close to 6 dimensions, this is not necessarily so for the dynamical exponent z . There are precedences for the dynamics being sensitive to the exact shape of the potential, sometimes only in mean-field theory [17,19,20] (charge density waves in a smooth-potential versus a linear cusp potential), and sometimes even in the ϵ -expansion [20,127] (charge density waves in a sawtooth potential).

$c_2 r^{(n+1)} + \dots + A_{sing}$; for any data analysis one needs to keep all terms with $n \leq 2 - \alpha$.) In mean field theory $\alpha = 0$. Numerical and analytical results can be derived from the results for β and $\beta\delta$ quoted earlier.

H. Results on the number of system-spanning avalanches at the critical disorder

$$R = R_c$$

In percolation in any dimensions less than 6, there is at most *one* infinite cluster present at any value of the concentration parameter p , in particular also at its critical value p_c [61]. In contrast, in our system at the critical point $R = R_c$ the number N_∞ of “infinite avalanches” found during one sweep through the hysteresis loop, diverges with system size as $N_\infty \sim L^\theta$ in all dimensions $d > 2$.

The ϵ -expansion for our system yields

$$\theta\nu = 1/2 - \epsilon/6 + O(\epsilon^2) \tag{22}$$

Numerical simulations [45] show clearly that $\theta > 0$ in 4 and 5 dimensions. In three dimensions one finds $\theta\nu = 0.021 \pm 0.021$ and $\theta = 0.015 \pm 0.015$. (For more details on θ see [126,129].)

I. List of exponent relations

In the following sections we list various exponent relations, for which we give detailed arguments in references [126,129].

1. Exponent equalities

The exponents introduced above are related by the following exponent equalities:

$$\beta - \beta\delta = (\tau - 2)/\sigma \quad \text{if } \tau < 2, \tag{23}$$

$$(2 - \eta)\nu = \beta\delta - \beta, \quad (24)$$

$$\beta = \frac{\nu}{2}(d - 4 + \bar{\eta}), \quad (25)$$

and

$$\delta = (d - 2\eta + \bar{\eta})/(d - 4 + \bar{\eta}). \quad (26)$$

(The latter three equations are not independent and are also valid in the equilibrium random field Ising model [62,125,101]).⁷

2. Incorrect exponent equalities

a. Breakdown of hyperscaling In our system there are two different violations of hyperscaling.

1. In references [126,129], we show that the connectivity hyperscaling relation $1/\sigma = d\nu - \beta$ from percolation is violated in our system. There is a new exponent θ defined by $1/\sigma = (d - \theta)\nu - \beta$ with $\theta\nu = 1/2 - \epsilon/6 + O(\epsilon^2)$ and $\theta\nu = 0.021 \pm 0.021$ in three dimensions [45]. θ is related to the number of system spanning avalanches observed during a sweep through the hysteresis loop.

2. As we will discuss in section VIII there is a mapping of the perturbation theory for our problem to that of the equilibrium random field Ising model to all orders in ϵ . From that mapping we deduce the breakdown of an infamous (“energy”)-hyperscaling relation, which has caused much controversy in the case of the *equilibrium* random-field Ising model [62]

$$\beta + \beta\delta = (d - \tilde{\theta})\nu, \quad (27)$$

⁷Also, using these relations one finds that the inequality $\nu/\beta\delta \geq 2/d$ (which applies in our model [129,126,104]) goes over into the Schwartz-Soffer inequality $\bar{\eta} \leq 2\eta$ that has been derived for the corresponding equilibrium model [63].

with a new exponent $\tilde{\theta}$. In [126,129] we discuss the relation of the exponent $\tilde{\theta}$ to the energy output of the avalanches. The ϵ -expansion yields $\tilde{\theta} = 2$ to all orders in ϵ . Non-perturbative corrections are expected to lead to deviations of $\tilde{\theta}$ from 2 as the dimension is lowered. The same is true as is the case in the equilibrium RFIM [126,129]. The numerical result in three dimensions is $\tilde{\theta} = 1.5 \pm 0.5$ [45]. (In the three-dimensional Ising model it is $\tilde{\theta}_{eq} = 1.5 \pm 0.4$ [62,100].)

b. Breakdown of perturbative exponent equalities There is another strictly perturbative exponent equality, which is also obtained from the perturbative mapping to the random-field Ising-model [126,129],

$$\bar{\eta} = \eta. \quad (28)$$

It, too, is expected to be violated by non-perturbative corrections below 6 dimensions.

3. Exponent inequalities

In references [126,129] we give arguments for the following two exponent-inequalities⁸:

$$\nu/\beta\delta \geq 2/d, \quad (29)$$

which is formally equivalent to the ‘‘Schwartz-Soffer’’ inequality, $\bar{\eta} \leq 2\eta$, first derived for the equilibrium random field Ising model [63], and

$$\nu \geq 2/d, \quad (30)$$

which is a weaker bound than eq. (29) so long as $\beta\delta \geq 1$, as appears to be the case both theoretically and numerically at least for $d \geq 3$.

⁸From the normalization of the avalanche size distribution $D(s, r, h)$ (see eq. (11)) follows that $\tau > 1$.

J. Results on the upper critical dimension of the critical endpoint $(R_c, H_c(R_c))$

The consistency of the mean-field theory exponents for $d \geq 6$ can be shown by a Harris criterion type of argument [53], which also leads to eq. (29) [128,126]. Approaching the critical point along the $r' = 0$ line, one finds a well defined transition point only if the fluctuations $\delta h'$ in the critical field H_c due to fluctuations in the random fields are always small compared to the distance h' from the critical point, i.e. $\delta h'/h' \ll 1$ as $h' \rightarrow 0$. With $\delta h' \sim \xi^{-d/2}$ and $\xi \sim (r')^{-\nu} f_{\pm}(h'/(r')^{\beta\delta}) \sim (h')^{-\nu/(\beta\delta)}$ at $r' = 0$, one obtains $\delta h'/h' \sim \xi^{-d/2}/\xi^{-\beta\delta/\nu} \ll 1$, or $\nu/\beta\delta \geq 2/d$. For $\nu = 1/2$ and $\beta\delta = 3/2$ this is only fulfilled if $d \geq 6$, *i.e.* $d = 6$ is the upper critical dimension.

V. WHY AN ϵ -EXPANSION?

Perturbation theory has proven an invaluable tool for practical calculations in many branches of physics. The asymptotic expansion in powers of the electronic charge in electrodynamics is an example where perturbation theory not only gives extremely accurate results but also provides a qualitative insight in the underlying physical processes such as absorption and emission of photons. Critical phenomena in general are among the cases where perturbation theory cannot be applied (at least not below a certain “upper critical dimension” d_c). The fluctuations in the order parameter near the critical point become too large to extract useful information from a perturbation expansion in some physical coupling constant.

The RG has been developed specifically for such cases. It is a means to extend the derivation of critical scaling forms from mean-field theory to finite dimensions, and to obtain information about the effective behavior of the system on long length scales. The Wilson-Fisher momentum shell renormalization group is an iterative coarse graining transformation. In each step the shortest wavelength degrees of freedom are integrated out, leading to an effective action for the modes on longer length scales. If a theory is renormalizable, the

coarse grained action will be in the same form as the original action, but with rescaled parameters.

Under coarse graining many of these parameters will flow to a certain fixed point, which is independent of their original microscopic value. The properties of the system on long length scales only depend on the fixed point. This is the key to universality: different microscopic systems flow to the same fixed point and are therefore described by the same effective action on long length scales. They will consequently show the same critical behavior.

Second order critical points are fixed points of the coarse graining transformation. They are characterized by a diverging correlation length and consequent scale invariance. There are fluctuations (such as clusters, avalanches, etc.) on all length scales. In the same sense power laws are scale free functions.⁹ It is therefore not surprising that systems near their critical point are described by power laws. One of the triumphs of the RG is to show from first principles that near the critical point the interesting long-wavelength properties are given by *homogeneous functions*¹⁰ with respect to a change of length scale in the system. This observation leads to Widom scaling forms for the various macroscopic quantities, some of which we already obtained from simple expansions in mean field theory.

The RG thus provides a formal justification of the scaling ansatz used in the data analysis and an explanation for the universality of the critical exponents. It is the ultimate

⁹When a function $f(x) \sim x^{|\alpha|}$ is measured over three pairs of octaves, say over the intervals $[1, 4]$, $[10, 40]$, and $[100, 400]$, the ratio of the largest to the smallest value is always $4^{|\alpha|}$, so the three graphs of $f(x)$ can be superimposed by simple change of scale. In this sense, power laws are scale invariant [64].

¹⁰A function $f(x_1, \dots, x_n)$ is homogeneous of degree D in the variables x_1, \dots, x_n , if on multiplying each x_i by an arbitrary factor b the value of f is multiplied by b^D , *i.e.* $f(bx_1, \dots, bx_n) = b^D f(x_1, \dots, x_n)$ [64]. Here we use the definition $f(b^{\lambda_1} x_1, \dots, b^{\lambda_n} x_n) = b^y f(x_1, \dots, x_n)$ for $\lambda_1, \dots, \lambda_n$ real constants.

justification for the attempt to extract useful predictions about real complex materials from extremely simple caricatures of the microscopic physics.

In particular it has been used to derive an expansion for the critical exponents around their mean-field values in powers of the dimensional parameter $\epsilon = d_c - d$, where d is the dimension of the system. Note that the ϵ -expansion is an asymptotic expansion in terms of a quite unphysical parameter. Nevertheless it has proven very successful for mathematical extrapolations. In this paper we shall apply its basic ideas to our problem and refer the reader for further details to excellent reviews in the existing literature [65,66,53,64,67–70].

The calculation turns out to be interesting in its own right. In contrast to RG treatments of equilibrium critical phenomena, a calculation for our hysteresis problem has to take into account the entire history of the system. It reveals formal similarities to related *single interface* depinning transitions [19,20,29–31,26]. Although our problem deals with the seemingly more complex case of *many* advancing interfaces or domain walls, the calculation turns out to be rather simple, much simpler in fact than in the single interface depinning problem. More details are given in appendix G. The techniques employed here are likely to be applicable to other nonequilibrium systems as well.

VI. ANALYTICAL DESCRIPTION

In equilibrium systems one defines a partition function as the sum over the thermal weights or probabilities of all possible states. From this partition function all ensemble averaged correlation functions can be obtained. It is also usually the quantity used to calculate the critical exponents in an RG treatment. Our system is at zero temperature and far from equilibrium. For a given configuration of random fields, the system will follow a deterministic path through the space of spin microstates as the external magnetic field is raised adiabatically. Systems with different configurations of random fields will follow different paths. If we assign a δ -function weight to the correct path for each configuration and then average over the distribution of random fields, we obtain a probability distribution

for the possible *paths* of the system, which is the analogue of the probability distributions for the possible states in equilibrium systems. The analogue of ensemble averaging for equilibrium systems, is random field averaging in our system. The sum over all possible paths weighted by their corresponding probability will play the role of a partition function for our nonequilibrium system when we set up a Wilson-Fisher momentum shell renormalization group transformation to calculate the critical exponents.

How can one formally describe the path that a system takes for a specific configuration of random fields as the external magnetic field is increased from $-\infty$ to $+\infty$? A convenient way is to introduce a time t into the otherwise adiabatic problem via $H(t) = H_0 + \Omega t$. H_0 is the magnetic field at time $t = 0$. $\Omega > 0$ is the sweeping rate for a monotonically increasing external magnetic field. The idea is to write down an equation of motion for each spin such that the resulting set of coupled differential equations has a unique solution which corresponds to the correct path the system takes for a given history. By taking Ω to zero in the end one obtains the adiabatic or “static” limit, in which we are interested. For convenience we introduce soft spins that can take values ranging from $-\infty$ to $+\infty$. Later on this will allow us to replace traces over all possible spin configurations by path integrals over the range of definition of the spins. We assume that each spin is moving in a double well potential $V(s_i)$ with minima at the “discrete” spin values $s_i = \pm 1$:

$$V(s_i) = \begin{cases} k/2 (s_i + 1)^2 & \text{for } s < 0 \\ k/2 (s_i - 1)^2 & \text{for } s > 0 \end{cases} \quad (31)$$

To guarantee that the system takes a finite magnetization at any magnetic field, one needs $k > 0$ and $k/J > 1$. The Hamiltonian of the soft spin model is then given by:

$$\mathcal{H} = - \sum_{ij} J_{ij} s_i s_j - \sum_i (f_i s_i + H s_i - V(s_i)). \quad (32)$$

All terms in the Hamiltonian are as before, except for the additional $V(s_i)$ term. A spin flip in this model corresponds to a spin moving from the lower to the upper potential well. ¹¹

¹¹We believe the calculation could just as well have been performed for discrete spins, maybe

We impose purely relaxational dynamics, given by

$$(1/\Gamma_0)\partial_t s_i(t) = -\delta\mathcal{H}/\delta s_i(t). \quad (33)$$

Γ_0 is a “friction constant”.

This model shows qualitatively similar behavior to real magnets: As the external magnetic field is ramped, we observe spin flips, which correspond to irreversible domain wall motions. The linear relaxation between the spin flips corresponds to the reversible domain wall motion, which we have described in the introduction.

The soft spin mean-field theory, where every spin interacts equally with every other spin yields the same static critical exponents as we have obtained earlier for the hard spin model. We have also checked that replacing the linear cusp potential by the more common, smooth s^4 double well potential does not change the static mean field exponents.¹²

A. Formalism

We use the formalism introduced by Martin Siggia and Rose [73] to treat dynamical critical phenomena, which is similar to the Bausch–Janssen–Wagner method [74]. One defines the generating functional Z for the dynamical problem as an integral over a product of δ -functions (one for each spin), each of which imposes the equation of motion at all times on its particular spin [19]:

by using the ideas of Lubensky *et al.* [71]. At the time it seemed easier to use the established formalism for continuous spins. However, in mean-field theory the formulas look very similar to the hard-spin model. The new parameter k from the double well potential never seems to come into play for any of the universal properties of the system.

¹²The form of the potential does change the (dynamical) mean-field exponents in the CDW depinning transition at zero temperature [19]. In finite dimensions it changes some properties that are associated with the thermal rounding of the CDW transition [72].

$$1 \equiv Z = \int [ds] \mathcal{J}[s] \prod_i \delta(\partial_t s_i / \Gamma_0 + \delta\mathcal{H} / \delta s_i). \quad (34)$$

$[ds]$ symbolizes the path integral over all spins in the lattice at all times, and $\mathcal{J}[s]$ is the necessary Jacobian, which fixes the measure of the integrations over the s_i such that the integral over each delta-function yields 1 [19]. One can show that $\mathcal{J}[s]$ merely cancels the equal time response functions [75,19].¹³

In order to write Z in an exponential form in analogy to the partition function in equilibrium problems, we express the δ -functions in their Fourier-representation, introducing an unphysical auxiliary field $\hat{s}_j(t)$:

$$\delta(\partial_t / \Gamma_0 s_i(t) + \delta\mathcal{H} / \delta s_i(t)) \sim 1/2\pi \int d\hat{s} \exp(i \sum_j \hat{s}_j(t) (\partial_t s_j(t) / \Gamma_0 + \delta\mathcal{H} / \delta s_j(t))). \quad (35)$$

Absorbing any constants into $\mathcal{J}[s]$, this yields for the (not yet random-field averaged) generating functional (in continuous time):

$$1 \equiv Z = \int \int [ds][d\hat{s}] \mathcal{J}[s] \exp(i \sum_j \int dt \hat{s}_j(t) (\partial_t s_j(t) / \Gamma_0 + \delta\mathcal{H} / \delta s_j(t))), \quad (36)$$

or

$$1 = Z = \int \int [ds][d\hat{s}] \mathcal{J}[s] \exp(W), \quad (37)$$

with the action

¹³To that end, one chooses the following regularization (when discretizing in time): Let $t = n\epsilon$ with ϵ a small number taken to zero later when n is taken to infinity, such that their product remains fixed. Then $\partial_t s_i(t)$ becomes $(s_i(n\epsilon) - s_i((n-1)\epsilon)) / \epsilon$ and we integrate over $ds_i(n\epsilon)$. Because of the analyticity we are free to take the rest of the argument of the δ -function at the lower value $s_i((n-1)\epsilon)$, or the average value $(s_i(n\epsilon) + s_i((n-1)\epsilon)) / 2$, or the upper value $s_i(n\epsilon)$. If we choose the first possibility, one finds that the Jacobian will be only a constant, since each argument only depends on $s_i(n\epsilon)$, and is independent of any other $s_j(n\epsilon)$ with $i \neq j$. This corresponds to allowing a force at time $(n-1)\epsilon$ to have an effect only *after* some time ϵ , i.e. equal times response functions are manifestly zero.

$$\begin{aligned}
W &= i \sum_j \int dt \hat{s}_j(t) (\partial_t s_j(t) / \Gamma_0 + \delta \mathcal{H} / \delta s_j(t)) \\
&= i \sum_j \int dt \hat{s}_j(t) (\partial_t s_j(t) / \Gamma_0 - \sum_l J_{jl} s_l - H - f_j + \delta V / \delta s_j).
\end{aligned} \tag{38}$$

We can express correlation and response functions of $s_j(t)$ as path integrals in terms of W , because solely the unique deterministic path of the system for the given configuration of random fields makes a nonzero contribution to the path integral over $[ds]$ in eq. (36). For example the value of spin s_j at time t' is given by

$$s_j(t') = Z^{-1} \int \int [ds'] [d\hat{s}'] \mathcal{J}[s'] s'_j(t') \exp(W). \tag{39}$$

Similarly, correlation functions are given by

$$s_j(t') s_k(t'') = Z^{-1} \int \int [ds'] [d\hat{s}'] \mathcal{J}[s'] s'_j(t') s'_k(t'') \exp(W). \tag{40}$$

To calculate the response of s_j at time t' to a perturbative field $J_{\epsilon_k}(t', t'')$ switched on at site k at time t'' , we add the perturbation to the magnetic field at site k , such that the action becomes

$$\begin{aligned}
W_\epsilon &= i \sum_{j \neq k} \int dt \hat{s}_j(t) (\partial_t s_j(t) / \Gamma_0 - \sum_l J_{jl} s_l - H - f_j + \delta V / \delta s_j) \\
&\quad + i \int dt \hat{s}_k(t) (\partial_t s_k(t) / \Gamma_0 - \sum_l J_{kl} s_l - H - f_k + \delta V / \delta s_k - J_{\epsilon_k}(t, t'')).
\end{aligned} \tag{41}$$

Taking the derivative with respect to J_{ϵ_k} and the limit $\epsilon_k \rightarrow 0$ afterwards¹⁴ one obtains

$$\delta s_j(t') / \delta \epsilon_k(t'') = (-i) Z^{-1} \int \int [ds] [d\hat{s}] \mathcal{J}[s] s_j(t') \hat{s}_k(t'') \exp(W), \tag{42}$$

so \hat{s} acts as a “response field”. Henceforth we shall suppress $\mathcal{J}[s]$, keeping in mind that its only effect is to cancel equal time response functions (see previous footnote).

Since $Z = 1$ independent of the random fields, we could have left out the Z^{-1} factors in eqs. (39), (40), and (42). This greatly facilitates averaging over the random fields: The

¹⁴An exact definition of the functional derivative which is consistent with the history of a monotonically increasing magnetic field is given in appendix C.

average response and correlation functions are generated by averaging Z directly over the random fields. Unlike in equilibrium problems with quenched randomness it is not necessary to calculate the (more complicated) average of $\ln Z$. One obtains for the random field averaged correlation functions

$$\langle s_j(t') s_k(t'') \rangle_f = \int \int [ds][d\hat{s}] s_j(t') s_k(t'') \langle \exp(W) \rangle_f, \quad (43)$$

and similarly

$$\delta s_j(t') / \delta \epsilon_k(t'') = \langle s_j(t') \hat{s}_k(t'') \rangle_f = \int \int [ds][d\hat{s}] s_j(t') \hat{s}_k(t'') \langle \exp(W) \rangle_f. \quad (44)$$

It is not obvious how to calculate $\langle \exp(W) \rangle_f$ directly, since W involves terms like $J_{ij} s_i \hat{s}_j$ which couple different sites. Following Sompolinsky and Zippelius [76], and Narayan and Fisher [19], we can circumvent this problem by performing a change of variables from the spins s_j to local fields $J\tilde{\eta}_i = \sum_j J_{ij} s_j$. (We introduce the coefficient J on the left hand side to keep the dimensions right.) At the saddle point of the associated action the new variables $\tilde{\eta}_j$ (for all j) are given by the mean-field magnetization and the different sites become decoupled. A saddle point expansion becomes possible, because the coefficients in the expansion can be calculated in mean-field theory — they are also the same for all sites j .

Here is how it works: we insert into Z the expression

$$1 = 1/2\pi \int \int [d\hat{\eta}][d\tilde{\eta}] \mathcal{J}[\tilde{\eta}] \exp(i \sum_j \int dt \hat{\eta}_j(t) (s_j(t) - \sum_i J_{ij}^{-1} J \tilde{\eta}_i(t))) \quad (45)$$

where $\mathcal{J}[\tilde{\eta}]$ stands for the suitable Jacobian, which is simply a constant and will be suppressed henceforth. Integrating out the auxiliary fields $\hat{\eta}_j$, one recovers that the expression in eq. (45) is the integral over a product of δ -functions which impose the definitions $J\tilde{\eta}_i(t) = \sum_j J_{ij} s_j(t)$ at all times for all i .

After some reshuffling of terms and introducing some redefinitions that are motivated by the attempt to separate the nonlocal from the local terms, one obtains

$$Z = \int \int [d\hat{\eta}][d\tilde{\eta}] \prod_j \bar{Z}_j[\tilde{\eta}_j, \hat{\eta}_j] \exp[- \int dt \hat{\eta}_j(t) (\sum_l J_{jl}^{-1} J \tilde{\eta}_l(t))] \quad (46)$$

where $\bar{Z}_j[\tilde{\eta}_j, \hat{\eta}_j]$ is a *local* functional

$$\begin{aligned} \bar{Z}_j[\tilde{\eta}_j, \hat{\eta}_j] = \int [ds_j][d\hat{s}_j] \langle \exp\{J^{-1} \int dt [J\hat{\eta}_j(t)s_j(t) + \\ i\hat{s}_j(t)(\partial_t s_j(t)/\Gamma_0 - J\tilde{\eta}_j(t) - H - f_j + \delta V/\delta s_j)]\} \rangle_f \end{aligned} \quad (47)$$

(we have absorbed a factor i in the definition of $\hat{\eta}_j$). In short this can also be written as

$$Z \equiv \int [d\tilde{\eta}][d\hat{\eta}] \exp(\tilde{S}_{eff}) \quad (48)$$

with the effective action \tilde{S}_{eff} , now expressed in terms of the “local field” variables $\tilde{\eta}$ and $\hat{\eta}$

$$\tilde{S}_{eff} = - \int dt \sum_j \hat{\eta}_j(t) \sum_l J_{jl}^{-1} J \tilde{\eta}_l(t) + \sum_j \ln(\bar{Z}_j[\tilde{\eta}_j, \hat{\eta}_j]). \quad (49)$$

Physically we can interpret the functional

$$\Phi[\eta] \equiv \int [d\hat{\eta}] \exp(\tilde{S}_{eff}) \quad (50)$$

as the random field averaged probability distribution for the possible paths the system can take through the spin configuration space as the external magnetic field is slowly increased. Each path is specified by a set of N effective field functions $J\eta_i(t)$ (i runs over the lattice with $N \rightarrow \infty$ spins). Z is the integral of this (normalized) probability distribution over all possible paths of the system and is therefore equal to 1.

The stationary point $[\tilde{\eta}_j^0, \hat{\eta}_j^0]$ of the effective action is given by

$$[\delta \tilde{S}_{eff} / \delta \tilde{\eta}_j]_{\tilde{\eta}_j^0, \hat{\eta}_j^0} = 0, \quad (51)$$

and

$$[\delta \tilde{S}_{eff} / \delta \hat{\eta}_j]_{\tilde{\eta}_j^0, \hat{\eta}_j^0} = 0. \quad (52)$$

With eqs. (47) and (49) we find the saddle-point equations:

$$(-i) \langle \hat{s}_i \rangle_{l, \tilde{\eta}^0, \hat{\eta}^0} - \sum_j J J_{ij}^{-1} \hat{\eta}_j^0 = 0, \quad (53)$$

and

$$\langle s_i \rangle_{l, \hat{\eta}^0, \tilde{\eta}^0} - \sum_j J J_{ij}^{-1} \tilde{\eta}_j^0 = 0. \quad (54)$$

The notation $\langle \rangle_{l, \hat{\eta}^0, \tilde{\eta}^0}$ here denotes a *local* average, obtained from the *local* partition function \bar{Z}_i , after having fixed $\hat{\eta}_i$ and $\tilde{\eta}_i$ to their stationary-point solutions $\hat{\eta}_i^0$ and $\tilde{\eta}_i^0$.

For example (from eqs. (47), (49), (52), and (54))

$$\begin{aligned} \langle s_i(t) \rangle_{l, \hat{\eta}^0, \tilde{\eta}^0} &= \left[\frac{\delta}{\delta \hat{\eta}_i} \sum_j \ln(\bar{Z}_j[\tilde{\eta}_j, \hat{\eta}_j]) \right]_{\hat{\eta}^0, \tilde{\eta}^0} = \frac{1}{\bar{Z}_i} \int \int [ds][d\hat{s}] s_i(t) \\ &\langle \exp \{ J^{-1} \int dt [\sum_j J \hat{\eta}_j^0(t) s_j(t) \\ &+ i \hat{s}_j(t) (\partial_t s_j(t) / \Gamma_0 - J \tilde{\eta}_j^0(t) - H - f_j + \delta V / \delta s_j)] \} \rangle_f. \end{aligned} \quad (55)$$

Eq. (53) and eq. (54) have the self-consistent solution

$$\hat{\eta}_i^0(t) = 0, \quad (56)$$

and

$$\tilde{\eta}_i^0(t) = M(t) = \langle s_i(t) \rangle_{l, \hat{\eta}^0, \tilde{\eta}^0}, \quad (57)$$

where $M(t)$ is the random field average of the solution of the mean field equation of motion

$$\partial_t s_j(t) / \Gamma_0 = J \tilde{\eta}_j^0(t) + H + f_j - \delta V / \delta s_j. \quad (58)$$

(This can be seen by setting $\hat{\eta}^0 = 0$ in eq. (55). Integrating out the \hat{s} fields we see that \bar{Z}_j is the random field average over a product of δ -functions which impose eq. (58) by their argument. Eq. (57) is the self-consistency condition for this mean-field equation of motion.)

We can now expand the effective action \tilde{S}_{eff} in the variables $\hat{\eta}_j \equiv (\hat{\eta}_j - \hat{\eta}_j^0)$ and $\eta_j \equiv (\tilde{\eta}_j - \tilde{\eta}_j^0)$, which corresponds to an expansion around mean-field-theory:

$$Z = \int \int [d\eta][d\hat{\eta}] \exp(S_{eff}) \quad (59)$$

with an effective action (expressed in the new variables η and $\hat{\eta}$):

$$\begin{aligned} S_{eff} &= - \sum_{j,l} \int dt J_{jl}^{-1} J \hat{\eta}_j(t) \eta_l(t) + \sum_j \sum_{m,n=0}^{\infty} \frac{1}{m!n!} \int dt_1 \cdots dt_{m+n} \\ &u_{mn}(t_1, \dots, t_{m+n}) \hat{\eta}_j(t_1) \cdots \hat{\eta}_j(t_m) \eta_j(t_{m+1}) \cdots \eta_j(t_{m+n}) \end{aligned} \quad (60)$$

Here, as seen by inspection from eq. (49) and eq. (47)

$$\begin{aligned}
u_{m,n} &= \frac{\partial}{\partial \eta_j(t_{m+1})} \cdots \frac{\partial}{\partial \eta_j(t_{m+n})} \left[\frac{\delta^m [\ln \bar{Z}_j - \hat{\eta}_j(t) \eta_j^0(t)]}{\delta \hat{\eta}_j(t_1) \cdots \delta \hat{\eta}_j(t_m)} \right]_{\hat{\eta}=0, \eta=0} \\
&= \frac{\partial}{\partial \epsilon(t_{m+1})} \cdots \frac{\partial}{\partial \epsilon(t_{m+n})} \langle (s(t_1) - \eta^0(t_1)) \cdots (s(t_m) - \eta^0(t_m)) \rangle_{l, \hat{\eta}^0, \eta^0},
\end{aligned} \tag{61}$$

i.e., the coefficients u_{mn} are equal to the local (l), connected responses and correlations in mean field theory.

Again, *local* (l) means [19] that we do not vary the local field η_j^0 in the mean-field equation

$$\frac{1}{\Gamma_0} \partial_t s_j(t) = J \eta_j^0(t) + H + f_j - \frac{\delta V}{\delta s_j(t)} + J \epsilon(t) \tag{62}$$

when we perturb with the infinitesimal force $J \epsilon(t)$.

B. Source terms

Correlations of s and \hat{s} can be related to correlations of η and $\hat{\eta}$ [19]. If we introduce the source terms

$$\int dt (s_j(t) \hat{l}_j(t) - i \hat{s}_j(t) l_j(t)) \tag{63}$$

into the action, we can write the correlations of s and \hat{s} as functional derivatives with respect to \hat{l} and l at $l = \hat{l} = 0$. A shift in the variables η and $\hat{\eta}$ by l and \hat{l} respectively leads to a source term of the kind

$$J J_{ij}^{-1} (\hat{\eta}_i(t) - \hat{l}_i(t)) (\eta_j(t) - l_j(t)) \tag{64}$$

so that derivatives with respect to l and \hat{l} give correlation functions of $\hat{\eta}$ and η . For low momentum behavior the factor $J J_{ij}^{-1}$ can be replaced by one since $\sum_i J_{ij}^{-1} = J^{-1}$.

C. Implementing the history

Up to here the effective action S_{eff} manifestly involves the entire magnetic field range $-\infty < H < +\infty$. As we discuss in appendix C it turns out, however, that in the adiabatic

limit a separation of time scales emerges. The relaxation rate $k\Gamma_0$ in response to a perturbation is fast compared to the driving rate Ω/k of the external magnetic field. The static critical exponents can then be extracted self-consistently from a RG calculation performed at a single, fixed value H of the external magnetic field. The analysis is much simpler than one might have expected. Instead of dealing with the entire effective action which involves *all* field values H , it suffices in the adiabatic limit to calculate all coefficients u_{mn} in eq. (60) at one single fixed magnetic field H , and then to coarse grain the resulting action $S_{eff}(H) \equiv S_H$. There are no corrections from earlier values of the external magnetic field.

Physically this corresponds to the statement that increasing the magnetic field within an infinite ranged model (mean field theory) and then tuning the elastic coupling to a short ranged form (RG) would be equivalent to the physical relevant critical behavior, which actually corresponds to *first* tuning the elastic coupling to a short ranged form and *then* increasing the force within a short ranged model [20]. In their related calculation for CDWs below the depinning threshold [20], Narayan and Middleton give an argument that this approach is self-consistent for their problem. In the appendix C we first show that their argument applies to our system as well, and then discuss the consistency of the magnetic field decoupling within the RG treatment of the entire history for separated time scales.

Where did the history dependence go? Note that the values of the coefficients u_{mn} at field H are still history dependent (in the way the mean-field solution is). Also, causality must be observed by the coarse graining transformation, so that even in the adiabatic limit the intrinsic history dependence of the problem does not get lost.

D. Calculating some of the u_{mn} coefficients at field H

In appendix C we show that u_{mn} basically assume their static values in the adiabatic limit. In this section we will briefly outline their derivation and quote the relevant results.

We have to be consistent with the history of an increasing external magnetic field, when expanding around the “mean-field-path” $\eta^0(t)$. This implies that for calculating responses

from eq. (61) we must only allow a perturbing force $J\epsilon(t)$ that *increases* with time in eq. (62). For example, for $u_{1,1}$ we add a force $J\epsilon(t) \equiv J\epsilon\Theta(t-t')$ in eq. (62), where $\Theta(t-t')$ is the step function, and solve for $\langle s(t)|_{H+J\epsilon(t)} \rangle_f$. The local response function is then given by the derivative of $\lim_{\epsilon \rightarrow 0} [\langle \langle s(t)|_{H+J\epsilon(t)} \rangle_f - \langle s(t)|_H \rangle_f] / \epsilon$ with respect to $(-t')$. The higher response functions are calculated correspondingly. (The most important ones are calculated in appendix C.) One obtains in the low frequency approximation for the first few terms of the effective action of eq. (60) at field H

$$\begin{aligned}
S_H = & - \sum_{j,l} \int dt J_{jl}^{-1} J \hat{\eta}_j(t) \eta_l(t) - \sum_j \int dt \hat{\eta}_j(t) [-a\partial_t / \Gamma_0 - u_{11}^{stat}] \eta_j(t) \\
& + \sum_j \int dt \frac{1}{6} u \hat{\eta}_j(t) (\eta_j(t))^3 \\
& + \sum_j \int dt_1 \int dt_2 \frac{1}{2} u_{2,0} \hat{\eta}_j(t_1) \hat{\eta}_j(t_2), \tag{65}
\end{aligned}$$

with

$$a = (J/k + 4\rho(-J\eta^0 - H + k))/k, \tag{66}$$

$$u_{11}^{stat} = 2J\rho(-J\eta^0 - H + k) + J/k, \tag{67}$$

$$w = -2J^2\rho'(-J\eta^0 - H + k), \tag{68}$$

$$u = 2J^3\rho''(-J\eta^0 - H + k), \tag{69}$$

and

$$\begin{aligned}
u_{2,0} = & R^2/k^2 + 4\left(\int_{-\infty}^{-H-\eta^0+k} \rho(h)dh\right) - 4\left(\int_{-\infty}^{-H-\eta^0+k} \rho(h)dh\right)^2 \\
& - 4\left(\int_{-\infty}^{-H-\eta^0+k} (h/k)\rho(h)dh\right). \tag{70}
\end{aligned}$$

Eq. (70) implies that $u_{2,0} \geq 0$ for any normalized distribution $\rho(f)$.

VII. PERTURBATIVE EXPANSION

A. The Gaussian theory for $d > d_c$: response and correlation functions

One can show [53,66] that for systems with dimension d above the upper critical dimension d_c , the nonquadratic terms in the action become less and less important on longer and longer length (and time) scales. Near the critical point, where the behavior is dominated by fluctuations on long length scales, the system is then well described by the quadratic parts of the action, and the calculation of correlation and response functions amounts to the relatively simple task of solving Gaussian integrals. It should come as no surprise that the mean-field exponents are recovered, since the quadratic parts of the action represent the lowest order terms in the saddle-point expansion around mean-field theory.

In our problem the action S_H of eq. (65) has the quadratic part

$$\begin{aligned}
 Q(\eta, \hat{\eta}) = & - \sum_{j,l} \int dt J_{jl}^{-1} J \hat{\eta}_j(t) \eta_l(t) - \sum_j \int dt \hat{\eta}_j(t) [-a\partial_t/\Gamma_0 - u_{11}^{stat}] \eta_j(t) \\
 & + (1/2) \sum_j \int dt_1 \int dt_2 \hat{\eta}_j(t_1) \hat{\eta}_j(t_2) u_{2,0}.
 \end{aligned} \tag{71}$$

In the long-wavelength limit we can write $J^{-1}(q) = 1/J + J_2 q^2$ [64].

Rescaling $\hat{\eta}$, ω and q we can replace the constants $J_2 J$ and a by 1. The low frequency part of the $\hat{\eta}\eta$ -term in $Q(\eta, \hat{\eta})$ is then given by

$$- \int d^d q \int dt \hat{\eta}(-q, t) (-\partial_t/\Gamma_0 + q^2 - \chi^{-1}/J) \eta(q, t) \tag{72}$$

where

$$\chi^{-1} = J(u_{11}^{stat} - 1) = 2J^2 \rho(-JM - H + k) - J(k - J)/k \tag{73}$$

is the negative static response to a monotonically increasing external magnetic field, calculated in mean-field-theory.¹⁵

¹⁵Note that $\chi^{-1} = J(k - J)/kt$, where t is a parameter used in the mean-field scaling functions

In frequency space, it can be written as

$$- \int d^d q \int dt (-i\omega/\Gamma_0 + q^2 - \chi^{-1}/J) \hat{\eta}(-q, -\omega) \eta(q, \omega). \quad (74)$$

The $\hat{\eta}\hat{\eta}$ term in $Q(\eta, \hat{\eta})$, given by

$$\int d^d q \int dt_1 \int dt_2 1/2 u_{2,0} \hat{\eta}(-q, t_1) \hat{\eta}(q, t_2) \quad (75)$$

can also be expressed in frequency space

$$\int d^d q \int d\omega (1/2) u_{2,0} \delta(\omega) \hat{\eta}(-q, -\omega) \hat{\eta}(q, \omega). \quad (76)$$

The expressions from eq. (74) and eq. (76) can be written together as

$$Q(\eta, \hat{\eta}) = - \int d\omega \int d^d q \quad (77)$$

$$(\hat{\eta}(-q, -\omega), \eta(-q, -\omega)) \begin{pmatrix} -1/2 u_{2,0} \delta(\omega) & (i\omega/\Gamma_0 + q^2 - \chi^{-1}/J) \\ (-i\omega/\Gamma_0 + q^2 - \chi^{-1}/J) & 0 \end{pmatrix} \begin{pmatrix} \hat{\eta}(q, \omega) \\ \eta(q, \omega) \end{pmatrix}$$

This can be used to determine the response and correlation functions at field H at low frequencies to lowest order in the expansion around mean field theory [77]. Inverting the matrix one obtains [19]

$$G_{\hat{\eta}\eta}(q, \omega) = \langle \hat{\eta}(-q, -\omega) \eta(q, \omega) \rangle \approx 1/(-i\omega/\Gamma_0 + q^2 - \chi^{-1}/J) \quad (78)$$

and

$$G_{\hat{\eta}\hat{\eta}}(q, \omega) = \langle \hat{\eta}(-q, -\omega) \hat{\eta}(q, \omega) \rangle \approx u_{2,0} \delta(\omega) / |-i\omega/\Gamma_0 + q^2 - \chi^{-1}/J|^2. \quad (79)$$

The $\delta(\omega)$ in eq. (79) is a consequence of the underlying separation of time scales. It will lead to an essentially static character of the RG analysis of the problem. This might have been expected, since the critical phenomena we set out to describe are essentially static

in appendix A. It is defined for the soft spin model in eq. (A29). In particular, this implies that near the critical point χ^{-1} scales with the original parameters r and h in the same way as t , see eq. (A4) in the same appendix.

in nature. At the critical point $\chi^{-1} = 0$ we have $G_{\hat{\eta}\eta}(q, \omega = 0) \sim q^{2-\eta}$ with $\eta = 0$ and $G_{\eta\eta}(q, \omega = 0) \sim q^{4-\bar{\eta}}$ with $\bar{\eta} = 0$ at lowest order in perturbation theory. One can Fourier transform the correlation functions back to time

$$G_{\hat{\eta}\eta}(q, t, t') \equiv \langle \hat{\eta}(q, t) \eta(-q, t') \rangle \quad (80)$$

$$= \begin{cases} \Gamma_0 \exp\{-\Gamma_0(q^2 - \chi^{-1}/J)(t' - t)\} & \text{for } t' > t \\ 0 & \text{for } t' \leq t \end{cases}$$

and

$$G_{\eta\eta}(q, t, t') = \int dt_1 \int dt_2 G_{\hat{\eta}\eta}(q, -(t' - t) + t_1 + t_2) u_{2,0} G_{\hat{\eta}\eta}(q, t_2)$$

$$= u_{2,0}/(q^2 - \chi^{-1}/J)^2. \quad (81)$$

B. The RG analysis

In dimension $d < d_c$ the nonquadratic parts of the action are no longer negligible near the critical point. One obtains corrections to the mean-field behavior.

The Wilson-Fisher coarse graining procedure is an iterative transformation to calculate the effective action for the long wavelength and low frequency degrees of freedom of the system. In each coarse graining step [78,65,19,66] one integrates out high momentum modes of *all* frequencies $\hat{\eta}(q, \omega)$ and $\eta(q, \omega)$, with q in a momentum shell $[\Lambda/b, \Lambda]$, $b > 1$, and afterwards rescales according to $q = b^{-1}q'$, $\omega = b^{-1}\omega'$, $\hat{\eta}(q, \omega) = b^{\hat{c}_p} \hat{\eta}'(q, \omega)$, and $\eta(q, \omega) = b^{c_p} \eta'(q, \omega)$. As usual, the field rescalings \hat{c}_p and c_p are chosen such that the quadratic parts of the action at the critical point ($\chi^{-1} = 0$) remain unchanged, so that the rescaling of the response and the cluster correlation function under coarse graining immediately gives their respective power law dependence on momentum (*i.e.* this is an appropriate choice of the scaling units.) Without loop corrections this implies that $z = 2$, $\hat{\eta}(x, t) = b^{-d/2-z} \hat{\eta}'(x, t)$ and $\eta(x, t) = b^{-d/2+2} \eta'(x, t)$.

Performing one coarse graining step for the expansion for S_H or eq. (65) yields a coarse grained action which can be written in the original form, with “renormalized” vertices $u'_{m,n}$.

Without loop corrections, the vertices of the coarse-grained action are simply rescalings of the original vertices, which can be easily read off using the rescalings of q , ω , η , and $\hat{\eta}$. Taking into account that each $\delta/\delta\epsilon(t)$ involves a derivative with respect to time, and therefore another factor b^{-z} under rescaling, we arrive at

$$u'_{m,n} = b^{[-(m+n)+2]d/2+2n} u_{m,n}. \quad (82)$$

This shows that above 8 dimensions all vertices that are coefficients of terms of higher than quadratic order in the fields, shrink to zero under coarse-graining and are therefore “irrelevant” for the critical behavior on long length scales and at low frequencies.

The “mass” term χ^{-1} in the action actually grows under rescaling in any dimension:

$$(\chi^{-1})' = b^2(\chi^{-1}) \quad (83)$$

(without loop corrections). At $\chi^{-1} = 0$ and if all irrelevant coefficients are set to zero, the action does not change under coarse graining. This case is obviously a fixed point of the coarse graining transformation, where the system looks the same on all length scales. There is no finite (correlation) length determining the long wavelength behavior, which is just what one would expect at a critical point.

The critical exponents can be extracted from a linearization of the transformation around the associated fixed point. In the RG sense “relevant” eigenvectors of the linearized transformation (*i.e.* coefficients like χ^{-1} that grow under coarse graining) render the corresponding scaling fields or tunable parameters.

Below eight dimensions the vertex $u_{1,2} \equiv w = 2J\rho'(-J\eta^0 - H + k)$ is the first coefficient of a nonquadratic term to become relevant. An action with the original parameters $\chi^{-1} = 0$ and $w \neq 0$ corresponds to a system with less than critical randomness $R < R_c$ at the onset field of the infinite avalanche. In appendix E we show how to extract the mean-field exponents for the infinite avalanche line from the scaling above eight dimensions and that the RG treatment suggests a first order transition for the same systems in less than 8 dimensions.

In systems where the bare value of w is zero at the critical fixed point with $\chi^{-1} = 0$, all nonquadratic terms are irrelevant above *six* dimensions. As can be seen from appendix A, this case constitutes the interesting “critical endpoint” at $R = R_c$ and $H = H_c(R_c)$, which we have discussed in the introduction. The corresponding “upper critical dimension” is $d_c = 6$. For any dimension higher than 6, the mean-field exponents should describe the behavior on long length scales correctly [53]. For $d < 6$, the vertex $u_{1,3} = u$ becomes relevant, while all higher vertices remain irrelevant. We are left with the effective action which includes all vertices relevant for an expansion around 6 dimensions:

$$\begin{aligned} \tilde{S} = & - \int d^d q \int dt \hat{\eta}(-q, t) [-\partial_t / \Gamma_0 + q^2 - \chi^{-1} / J] \eta(q, t) \\ & + (1/6) \sum_j \int dt \hat{\eta}_j(t) (\eta_j(t))^3 u + (1/2) \sum_j \int dt_1 \int dt_2 \hat{\eta}_j(t_1) \hat{\eta}_j(t_2) u_{2,0} \end{aligned} \quad (84)$$

Below 6 dimensions, where u does not scale to zero, we will perform the coarse graining transformation in perturbation theory in u . At the fixed point, in $6 - \epsilon$ dimensions, u will be of $O(\epsilon)$. The perturbation series for the parameters in the action and thus also for the critical exponents, becomes a perturbation series in powers of ϵ . From the form of the action one can derive Feynman rules (see appendix C), which enable us to write down the perturbative corrections in a systematic scheme. Examples of their derivation for the ϕ^4 model are given elsewhere [66,53,64].

1. Loop corrections

In the remaining parts of this section we perform a coarse graining transformation to first order in ϵ .¹⁶ From the integration over the short wavelength degrees of freedom (of all

¹⁶In principle this is not necessary, since we can read off the corrections to $O(\epsilon^5)$ from the mapping to the ϵ -expansion of the pure Ising model in two lower dimensions, which we discuss in the next section. However we will need the techniques introduced here later for the calculation of the avalanche exponents.

frequencies) one obtains loop corrections to various vertices. Figure 11 (a) and (b) shows the corrections to χ^{-1} and u which are important for an $O(\epsilon)$ calculation. The dots correspond to the vertices with the indicated names. An outgoing arrow corresponds to an $\hat{\eta}$ operator, an incoming arrow corresponds to an η operator.

We consider the $\hat{\eta}\eta$ term in the action as propagator and all other terms as vertices. An internal line in a diagram corresponds to the contraction

$$\langle \hat{\eta}(q, t)\eta(-q, t') \rangle = \begin{cases} \Gamma_0 \exp\{-\Gamma_0(q^2 - \chi^{-1}/J)(t' - t)\} & \text{for } t' > t \\ 0 & \text{for } t' \leq t \end{cases} \quad (85)$$

with q in the infinitesimal momentum shell $\Lambda/b < q < \Lambda$ ($b > 1$) over which is integrated. This expression can be approximated by $\delta(t - t')$ in the low frequency approximation [19]. Note, however, that causality must be obeyed, *i.e.* $t' > t$. Figure 11 (c) shows an example of a diagram that violates causality and is therefore forbidden. External (loose) ends in a diagram correspond to operators that are not integrated out, *i.e.* modes of momentum $q < \Lambda/b$ outside of the momentum shell. Each internal line carrying momentum contributes a factor

$$1/(q^2 - \chi^{-1}/J). \quad (86)$$

The entire loop in diagram 11 (a) contributes the integral

$$I_1 = \int_{\Lambda/b}^{\Lambda} d^d q / (2\pi)^d 1/(q^2 - \chi^{-1}/J)^2 \quad (87)$$

(integration over time is already performed). Similarly the loop diagram in figure 11 (b) yields the integral

$$I_2 = \int_{\Lambda/b}^{\Lambda} d^d q / (2\pi)^d 1/(q^2 - \chi^{-1}/J)^3. \quad (88)$$

After each integration step we also have to rescale momenta, frequencies and fields. Thus the recursion relations for χ^{-1}/J and u become

$$(\chi^{-1}/J)' = b^2 \left(\chi^{-1}/J + \frac{u_{2,0}}{2!} \frac{u}{3!} 6I_1 \right) \quad (89)$$

and

$$u' = b^\epsilon \left(\frac{u}{3!} + \frac{u_{2,0}}{2!} \left[\frac{u}{3!} \right]^2 36I_2 \right). \quad (90)$$

(There are no loop corrections to $u_{2,0}$ at this order, so $u'_{2,0} = u_{2,0}$.) The integrals I_1 and I_2 have to be computed in $6 - \epsilon$ dimensions. To that end one uses the relation [53]

$$I = \int \frac{d^d q}{(2\pi)^d} f(q^2) = \frac{S_d}{(2\pi)^d} \int dq q^{d-1} f(q^2), \quad (91)$$

where S_d is the surface area of a unit sphere in d dimensions:

$$S_d = 2\pi^{d/2} / \Gamma(d/2). \quad (92)$$

In performing this analytic continuation in dimension we make the very strong assumption that the physical properties vary smoothly with dimension. It has been justified by its great success in many problems (although it gives an asymptotic expansion in ϵ which is not well behaved, see appendix D). Disregarding potential complications we then expand [53]

$$I_{1,2} = I_{1,2}(0) + \epsilon I'_{1,2}(0) + O(\epsilon^2). \quad (93)$$

Since both I_1 and I_2 are multiplied by u in the recursion relations, which will be of $O(\epsilon)$ at the fixed point, we only need $I_{1,2}(0)$ for an $O(\epsilon)$ calculation. With $K_d = S_d / (2\pi)^d$ we obtain [53]

$$\begin{aligned} I_1 &= \int_{\Lambda/b}^{\Lambda} d^d q / (2\pi)^d 1 / (q^2 - \chi^{-1}/J)^2 \\ &= \int_{\Lambda/b}^{\Lambda} d^d q / (2\pi)^d (1/q^4) (1 + 2(\chi^{-1}/J)/q^2 + O((\chi^{-1}/J)^2)) \\ &= K_6 \Lambda^2 (1 - 1/b^2) / 2 + 2K_6 (\chi^{-1}/J) \ln b + O((\chi^{-1}/J)^2, \epsilon). \end{aligned} \quad (94)$$

Similarly

$$I_2 = K_6 \ln b + O((\chi^{-1}/J)^2, \epsilon). \quad (95)$$

2. Recursion relations to $O(\epsilon)$

With $v \equiv u_{2,0}u$ and $b^\epsilon = e^{\epsilon \ln b} = 1 + \epsilon \ln b + O(\epsilon^2)$ the recursion relations then become

$$(\chi^{-1}/J)' = b^2 \left(\chi^{-1}/J + v/(4\pi)^3 \Lambda^2 (1 - 1/b^2)/4 + v/(4\pi)^3 (\chi^{-1}/J) \ln b \right) \quad (96)$$

and

$$v' = v + v[\epsilon + 3v/(4\pi)^3 v] \ln b. \quad (97)$$

There are two fixed points of these relations. The Gaussian fixed point $(\chi^{-1}/J)^* = 0, v^* = 0$, and a new, nontrivial fixed point at

$$(\chi^{-1}/J)^* = -\epsilon \Lambda^2/12 \quad (98)$$

and

$$v^* = -(4\pi)^3 \epsilon/3, \quad (99)$$

which is sometimes called the Wilson-Fisher (WF) fixed point. We linearize the recursion relations around these fixed points to calculate the critical exponents. At the Gaussian fixed point the corresponding matrix is

$$\begin{pmatrix} \partial \left(\frac{\chi^{-1}}{J} \right)' / \partial (\chi^{-1}/J) & \partial (\chi^{-1}/J)' / \partial v \\ \partial v' / \partial (\chi^{-1}/J) & \partial v' / \partial v \end{pmatrix} = \begin{pmatrix} b^2 & \frac{\Lambda^2}{4} (b^2 - 1) / (4\pi)^3 \\ 0 & b^\epsilon \end{pmatrix} \quad (100)$$

At the Wilson-Fisher fixed point it is

$$\begin{pmatrix} b^{(2-\epsilon/3)} & \frac{3\Lambda^2}{2} (b^2 - 1) / (4\pi)^3 \\ 0 & b^{-\epsilon} \end{pmatrix} \quad (101)$$

The eigenvalues of the transformation linearized around the Gaussian fixed point are given by $e_{\chi^{-1}} = b^{y_t}$ with $y_t = 2$ and $e_2 = b^\epsilon$ with eigendirections $e_{\chi^{-1}} = (1, 0)$ and $e_2 = (\Lambda^2/(4(4\pi)^3), 1)$ in the $(\chi^{-1}/J, v)$ plane.

The eigendirections of the transformation linearized around the Wilson-Fisher fixed point are $e_{\chi^{-1}} = (1, 0)$ and $e_2 = (-\epsilon \Lambda^2/12, -(4\pi)^3 \epsilon/3)$. The corresponding eigenvalues, called $\Lambda_{(\chi^{-1})}$ and Λ_2 are given by

$$\Lambda_{(\chi^{-1})} = b^{y_t} \quad (102)$$

with $y_t = 2 - \epsilon/3$ and

$$\Lambda_2 = b^{-\epsilon}. \quad (103)$$

3. Flows and exponents

a. For $\epsilon < 0$, i.e. $d > 6$: the Gaussian fixed point is unstable along the $e_{\chi^{-1}}$ direction, but stable along the e_2 direction. Thus v (or equivalently u) is an irrelevant variable. The correlation length scales as $\xi(\chi^{-1}/J) = b\xi((\chi^{-1}/J)')$ since under coarse graining the coordinates scale as $x' = bx$. From the appendices A and C we know that $w = 0$ implies that $h = 0$ and $\chi^{-1} \sim r$.¹⁷ One obtains (along $h = 0$)

$$\xi(r) \sim b\xi(b^{y_t}r). \quad (104)$$

Choosing $b = r^{-1/y_t}$ it follows that

$$\xi = r^{-1/y_t}\xi(1). \quad (105)$$

Since $\xi \sim r^{-\nu}$ along $h = 0$, one obtains

$$\nu = 1/y_t. \quad (106)$$

Therefore $\nu = 1/2$ for $d > 6$.

b. For $\epsilon > 0$, i.e. $d < 6$: the Gaussian fixed point becomes unstable along both $e_{\chi^{-1}}$ and e_2 . Along the e_2 direction the flow is towards the attractive WF fixed point, which will govern the critical behavior of all systems that do not initially sit at the Gaussian fixed point $u = J\rho''(-JM - H) = 0$. For those systems one then obtains (see eq. (102))

¹⁷See appendix A, eq. (A13) in particular, keeping in mind that the parameter t given there is proportional to χ^{-1} , apart from some irrelevant adjustments for the soft-spin model.

$$\nu = 1/y_t = 1/2 + \epsilon/12 \quad (107)$$

The corresponding flows in the $(\chi^{-1}/J, \nu)$ plane are shown in figure 12.

As in the RG treatment of the standard Ising model, the anomalous dimension η is equal to zero to first order in ϵ , since the field rescalings acquire no loop corrections to first order in ϵ [53]. (The coefficient of the q^2 -term in the propagator and the $u_{2,0}$ -term only receive $O(\epsilon^2)$ and higher order loop corrections.) Since the $i\omega$ term also receives no corrections to $O(\epsilon)$, we have $z = 2 + O(\epsilon^2)$.

4. Equation of state

We can also calculate $O(\epsilon)$ corrections to the equation of state [79], and consequently for the entire scaling *function* of the magnetization in eq. (9). Following Wallace [79] we replace the field $\tilde{\eta}(x)$ in the Hamiltonian by a new field $L(x)$ with zero expectation value

$$\tilde{\eta}(x) = L(x) + M \quad (108)$$

with

$$\langle L \rangle = 0. \quad (109)$$

In other words, in contrast to the preceding analysis, here we expand the action around the *true*, not mean-field, magnetization M at the considered order. At tree level $[L(x) = \eta(x)]_{tree-level}$ and $[M = \eta^0]_{tree-level}$ and $[u_{1,0}(M) = 0]_{tree-level}$. At higher order however, unlike in an expansion around mean-field theory, $u_{1,0}(M)$ is no longer zero. Its role is to cancel off all tadpole graphs [79,19], so that $\langle L \rangle = 0$ at any given order. The lowest order tadpole correction is shown in figure 13. Here we follow Wallace's calculation in [79]. Instead of performing an iterative integration over successive momentum shells, as we have done before, all momentum modes are taken into account in one step in which the integration extends from 0 up to the cutoff Λ [68]. The analytic expression to be added to $u_{1,0}$, corresponding to the lowest order correction of figure 13, is then given by

$$(1/2)u_{2,0}w \int_0^\Lambda 1/(q^2 - \chi^{-1})^2 d^d q. \quad (110)$$

As we have explained, the true magnetization M is chosen such that

$$u_{1,0}(M) + (1/2)u_{2,0}w \int_0^\Lambda 1/(q^2 - \chi^{-1})^2 d^d q + \dots = 0 \quad (111)$$

where \dots stands for all higher order corrections. Eq. (111) then constitutes the equation of state at the given order. In an expansion around $\eta^0 = M$ (where M is now the true magnetization), $u_{1,0}(M)$ is given by eq. (61), eq. (62) and section VIC to be

$$u_{1,0}(M) = (k + H)/k - (k - J)M/k - 2 \int_{-\infty}^{-JM-H+k} \rho(h) dh. \quad (112)$$

Close to the critical point the integral can be expanded around $-JM-H+k = -Jm-h = 0$, where $m = M - M_c$ is the deviation of the magnetization M from the mean-field critical value $M_c = +1$, and $h = H - H_c(R_c)$, with the mean-field value $H_c(R_c) = k - J$, and $r = (R_c - R)/R$ with $R_c = 2kJ/(\sqrt{2\pi}(k - J))$. One obtains

$$u_{1,0} = \frac{h}{k} + \frac{\chi^{-1}}{J} r m + \frac{2J^3}{3!} \rho''(0) m^3 + \dots, \quad (113)$$

where $\rho''(h)$ denotes the second derivative of the distribution of random fields with respect to its argument and \dots stands for higher order corrections. To calculate the equation of state at one loop order we insert into eq. (111) the expressions $\chi^{-1} = -2Jr/(\sqrt{2\pi}R) + 1/2um^2 + \dots$ (see eq. (73)), $w = um + \dots$ (see eq. (68)) and $u = 2J^3\rho''(0) + \dots$ (see eq. (69)), where \dots denotes higher orders in m and h . One then finds that the calculation is analogous to the one done for the Ising model in two lower dimensions. For details on solving the integral etc. we refer the reader to the article on the equation of state for the Ising model in $4 - \epsilon$ dimensions by D.J. Wallace in reference [79], especially equation (3.35). (In fact, with the following formal identifications, the resulting equations of state in the two systems can be mapped onto each other: $h/k = -h_w$, $2Jr/(\sqrt{2\pi}R) = -t_w$, $2J^3\rho''(0) = -(u_0)_w$, $m = -m_w$. We have denoted the quantities in Wallace's article by an index "w".)

We find for the equation of state to one loop order:

$$u_{1,0} \equiv 0 = \frac{h}{k} + 2J/(\sqrt{2\pi}R)rm + \frac{2J^3}{3!}\rho''(0)m^3 + \frac{1}{6}\epsilon m(2J/(\sqrt{2\pi}R)r + J^3\rho''(0)m^2) \ln(-2J/(\sqrt{2\pi}R)r - J^3\rho''(0)m^2). \quad (114)$$

Here $\epsilon = 6 - d$ and r and m are the reduced randomness and magnetization respectively.

5. The exponents β and δ

This equation allows us to extract the critical exponents β and δ by taking the corresponding limits: The exponent δ can be obtained by setting $r = 0$. That leaves one with

$$0 \equiv u_{1,0} = h/k + 1/3J^3\rho''(0)m^{3+\epsilon}. \quad (115)$$

Since by definition of δ one has $|h| \sim |m|^\delta$, we find

$$\delta = 3 + \epsilon. \quad (116)$$

Similarly one sets $h = 0$ to get β and finds from $|r| \sim |m|^{1/\beta}$ (for $R < R_c$) that

$$\beta = \frac{1}{2} - \frac{\epsilon}{6}. \quad (117)$$

6. The entire scaling function

From eqs. (114), (116) and (117) one can construct the entire scaling function $\tilde{f}(r/m^{1/\beta})$ to $O(\epsilon)$ in

$$|h/k| = |m|^\delta \tilde{f}(r/|m|^{1/\beta}) \quad (118)$$

directly, as shown in reference [79]. With the redefinitions

$$m_{new}^2 = -(1/3)J^3\rho''(0)m^2 \quad (119)$$

and

$$x = -(2Jr)/(\sqrt{2\pi}R|m_{new}|^{1/\beta}) \quad (120)$$

(for $r > 0$), one obtains

$$f(x) = x + 1 + \frac{\epsilon}{6}((x + 3) \ln(x + 3) - 3(x + 1) \ln(3) + 2x \ln(2)) + O(\epsilon^2), \quad (121)$$

in

$$|h/k| = |m_{new}|^\delta f(x). \quad (122)$$

In the next section we discuss a formal mapping of our ϵ expansion to the ϵ expansion of the pure Ising model in two lower dimensions, which allows us to copy the $O(\epsilon^2)$ correction to the equation of state from previous calculations for the pure Ising model [80].

VIII. MAPPING TO THE THERMAL RANDOM FIELD ISING MODEL

A. Perturbative mapping and dimensional reduction

We notice that the results found for ν , β and δ in $6 - \epsilon$ dimensions (eqs. (107), (117), and (116)) are the same as those for the regular equilibrium Ising model in $4 - \epsilon$ dimensions. In fact, this equivalence actually extends to *all* orders in ϵ : We will show that the ϵ -expansion for our model is the same as the ϵ -expansion for the *equilibrium* random field Ising model to all orders in ϵ [130]. Once this equivalence is established, we can use that the $(6 - \epsilon)$ -expansion of the *equilibrium* random field Ising has been mapped to *all* orders in ϵ to the corresponding expansion of the regular Ising model in two lower dimensions [81,82].

The easiest way to recognize that the ϵ -expansion for our model and for the *equilibrium* RFIM should really be the same is by comparing the corresponding effective actions. In a dynamical description of the *equilibrium* RFIM at zero external magnetic field the following effective Langevin equation of motion for the spin-field $\phi(r, t)$ was used [60]

$$\partial_t \phi(x, t) = -\Gamma_0(-\nabla^2 \phi(x, t) + r_0 \phi(x, t) + 1/6 g_0 \phi^3(x, t) - h_R(x)). \quad (123)$$

$h_R(x)$ represents spatially uncorrelated quenched random fields distributed according to a Gaussian of width Δ_0 and mean zero. $h_T(r, t)$ is the thermal noise field, which is taken to be gaussian with vanishing mean value and the variance

$$\langle h_T(r, t)h_T(r', t') \rangle = 2kT/\Gamma_0\delta(r - r')\delta(t - t'). \quad (124)$$

The corresponding Martin Siggia Rose generating functional is

$$\begin{aligned} Z_{H_0}^{thermal} &= \int [d\hat{\phi}] \int [d\phi] \exp\left\{- \int d^d q \int dt (\hat{\phi}(-q, t)(-\partial_t/\Gamma_0 + q^2 + r_0)\phi(q, t)) \right. \\ &\quad + \int d^d x \int dt (\hat{\phi}(x, t)(-1/6g_0)\phi(x, t)^3) \\ &\quad \left. + \int d^d x \int dt (\hat{\phi}(x, t)(h_R(x) + h_T(r, t)))\right\}. \end{aligned} \quad (125)$$

Since again $Z_{H_0}^{thermal} = 1$, we can average the partition function directly over the random fields h_R and the thermal noise h_T :

$$\bar{Z}_{H_0}^{thermal} = \langle Z_{H_0}^{thermal} \rangle_{h_R}. \quad (126)$$

The average over the random fields at each x and over the thermal noise fields at each x and t yields, (after completing the square):

$$\begin{aligned} \bar{Z}_{H_0}^{thermal} &= \int [d\hat{\phi}] \int [d\phi] \exp\left\{- \int d^d q \int dt \hat{\phi}(-q, t)(-\partial_t/\Gamma_0 + q^2 + r_0)\phi(q, t) \right. \\ &\quad + \int d^d x \int dt \hat{\phi}(x, t)(-\frac{1}{6}g_0)\phi^3(x, t) \\ &\quad + \int d^d x \int dt_1 \int dt_2 \hat{\phi}(x, t_1)\hat{\phi}(x, t_2)\Delta^2/2 \\ &\quad \left. + \int d^d x \int dt \hat{\phi}^2(x, t)(2kT)/\Gamma_0\right\}. \end{aligned} \quad (127)$$

With the identifications $r_0 = -\chi^{-1}(H_0)$, $u = -1/6g_0$, $u_{2,0} = \Delta^2$ and $T = 0$, we see that the argument of the exponential function is the same action as the effective action for our zero temperature, nonequilibrium model in eq. (65). Setting T to zero in the action for the equilibrium RFIM does not change the expansion for the static behavior, since it turns out that corrections involving temperature are negligible compared to those involving the random magnetic field [82,60,83] — the *temperature* dependence is irrelevant in the *thermal* RFIM and the *time* dependence is irrelevant in our zero-temperature *dynamical* RFIM,

leaving us with the same starting point for the calculation! This equivalence implies that in $6 - \epsilon$ dimensions we should obtain the same critical exponents to all orders in ϵ for our model, as were calculated for the thermal random field Ising model, which in turn are the same as those of the pure equilibrium Ising model in $4 - \epsilon$ dimensions [81,82].

This observation is rather convenient, since it provides us with results from the regular Ising model to $O(\epsilon^5)$ for free. In $6 - \epsilon$ dimensions we read off [59]

$$1/\nu = 2 - \epsilon/3 - 0.1173\epsilon^2 + 0.1245\epsilon^3 - 0.307\epsilon^4 + 0.951\epsilon^5 + O(\epsilon^6) \quad (128)$$

$$\eta = 0.0185185\epsilon^2 + 0.01869\epsilon^3 - 0.00832876\epsilon^4 + 0.02566\epsilon^5 + O(\epsilon^6) \quad (129)$$

$$\begin{aligned} \beta &= 1/2 - \epsilon/6 + 0.00617685\epsilon^2 - 0.035198\epsilon^3 + 0.0795387\epsilon^4 \\ &\quad - 0.246111\epsilon^5 + O(\epsilon^6) \end{aligned} \quad (130)$$

$$\begin{aligned} \beta\delta &= 3/2 + 0.0833454\epsilon^2 - 0.0841566\epsilon^3 + 0.223194\epsilon^4 - 0.69259\epsilon^5 \\ &\quad + O(\epsilon^6). \end{aligned} \quad (131)$$

β and δ have been calculated from η and ν using the perturbative relations: $\beta = (\nu/2)(d - 4 + \bar{\eta})$ and $\delta = (d - 2\eta + \bar{\eta})/(d - 4 + \bar{\eta})$ [84], with $\eta = \bar{\eta}$ to all orders in ϵ [60].

By the same mapping we obtain the universal scaling function for the magnetization to $O(\epsilon^2)$ [80,79]. We set

$$h = m^\delta f(x = r/m^{1/\beta}) \quad (132)$$

in which the normalizations of x and the universal scaling function f are chosen such that

$$f(0) = 1, \quad f(-1) = 0. \quad (133)$$

The expansion to second order in ϵ is then

$$f(x) = 1 + x + \epsilon f_1(x) + \epsilon^2 f_2(x) \quad (134)$$

with

$$f_1(x) = \frac{1}{6} [(x+3) \ln(x+3) - 3(x+1) \ln(3) + 2x \ln(2)] \quad (135)$$

and

$$\begin{aligned}
f_2(x) = & \left[\frac{1}{18} \right]^2 \{ [6 \ln 2 - 9 \ln 3] [3(x+3) \ln(x+3) + 6x \ln 2 - 9(x+1) \ln 3] \\
& + \frac{9}{2}(x+1)[\ln^2(x+3) - \ln^2 3] \\
& + 36[\ln^2(x+3) - (x+1) \ln^2 3 + x \ln^2 2] \\
& - 54 \ln 2 [\ln(x+3) + x \ln 2 - (x+1) \ln 3] \\
& + 25[(x+3) \ln(x+3) + 2x \ln 2 - 3(x+1) \ln 3] \} .
\end{aligned} \tag{136}$$

The scaling function $f(x)$ has actually been calculated up to order ϵ^3 [67]. As it stands the expression (134) meets the Griffith analyticity requirements [85] only within the framework of the ϵ -expansion, but not explicitly. These subtleties can be avoided by writing it in a parametric form [80], which can then be compared directly with our numerical results for the universal scaling function of dM/dH in 5, 4, 3, and 2 dimensions. We will present the results in a forthcoming paper [45].

The dynamic exponent z cannot be extracted from the mapping to the regular Ising model. It was calculated separately to $O(\epsilon^3)$ for the equilibrium RFIM [60] and found to be given to this order by¹⁸¹⁹

$$z = 2 + 2\eta = 2 + 0.037037\epsilon^2 + 0.03738\epsilon^3 + O(\epsilon^4). \tag{137}$$

¹⁸Eq. (137) is only a perturbative result for z which does not reveal the presence of diverging barrier heights that lead to the observed slow relaxation towards equilibrium [2,62,3–5]. Nonperturbative corrections are expected to be important in the equilibrium random field Ising model.

¹⁹While we expect the $6 - \epsilon$ results for the static exponents $\beta, \delta, \nu, \eta, \bar{\eta}, \tau, \sigma$, etc. to agree with our hard-spin simulation results close to 6 dimensions, this is not necessarily so for the dynamical exponent z . There are precedences for the dynamics being sensitive to the exact shape of the potential, at least in mean-field theory. Such differences have been found for example in the case of charge density waves [17,19,20,127], if studied for smooth potentials, for cusp-potentials, or for sawtooth potentials.

Because of the perturbative mapping of our model to the equilibrium RFIM, eq. (137) also gives the result for z in our nonequilibrium hysteretic system.

We have performed a Borel resummation (see also appendix D) of the corrections to $O(\epsilon^5)$ for η , ν , and the derived [84] exponent $\beta\delta$. The exponent β is then given through $\beta = \beta\delta - (2 - \eta)\nu$ (eq. (24)). Figure 14 shows a comparison with our numerical results in 3, 4, and 5 dimensions.

The agreement is rather good near 6 dimensions. However the apparent dimensional reduction through the perturbative mapping to the Ising exponents in 2 lower dimensions gradually loses its validity at lower and lower dimensions. It is after all only due to the equivalence of two asymptotic series, both of which have radius of convergence zero. Table I shows a comparison between the numerical exponents for our model and for the equilibrium RFIM in three dimensions.

B. Nonperturbative corrections

The mapping of the ϵ -expansion for the thermal random field Ising model to the expansion for the Ising model in two lower dimensions has caused much controversy when first discovered. The problem was that it had to break down at the lower critical dimension, where the transition disappears. There is no transition in the pure Ising model in $d = 1$, but the equilibrium RFIM is known rigorously to have a transition in $d = 3$ [102,103]. The same is true for our model: numerical simulations indicate [45,98] that the lower critical dimension is lower than three — probably equal to two.

In the case of the equilibrium random field Ising model it was finally agreed [62,82] that this breakdown might be due to nonperturbative corrections. The point is that proving a relation to all orders in ϵ does not make it true. In the equilibrium RFIM there are at least two sources of nonperturbative corrections:

a. The “embarrassing” correction: It was found that there was a calculational error in the $(6 - \epsilon)$ -expansion for the RFIM. The perturbation series was tracing over many

unphysical metastable states of the system, instead of just taking into account the ground state, which the system occupies in equilibrium. There were indications that this error leads to nonperturbative corrections, which would destroy the dimensional reduction outside of perturbation theory [82].

In our calculation we have avoided the embarrassing source of nonperturbative corrections found in the equilibrium random field Ising problem. Given the initial conditions and a history $H(t)$, the set of coupled equations of motion for all spins will have only one solution. In the Martin Siggia Rose formalism, the physical state is selected as the only solution that obeys causality, there are no unphysical metastable states coming in. Therefore we believe our results should also apply to systems below the critical randomness, at least before the onset of the infinite avalanche.

b. Instanton corrections: Even without the embarrassing correction, there is no reason why a perturbative mapping of the expansions about the upper critical dimensions should lead to a mapping of the lower critical dimensions also. The ϵ -expansion is only an asymptotic expansion — it has radius of convergence zero. As we discuss in appendix D, there is no known reason to assume that the ϵ -expansion uniquely determines an underlying function. It leaves room for functions subdominant to the asymptotic power series: If the series $\sum_0^\infty f_k z^k$ is asymptotic to some function $f(z)$ in the complex plane as $z \rightarrow 0$, then it is also asymptotic to any function which differs from $f(z)$ by a function $g(z)$ that tends to zero more rapidly than all powers of z as $z \rightarrow 0$ [90]. An example of such a subdominant function would be $g(z) = \exp(-1/z)$. While some asymptotic expansions can be proven to uniquely define the underlying function, this has not been shown for the ϵ -expansion (appendix D) — not for our problem, nor for the equilibrium pure Ising model, nor for the equilibrium thermal random field Ising model.

At this point, the ϵ -expansion for our model is on no worse formal footing than that for the ordinary Ising model. We believe, the asymptotic expansion is valid for both models, despite the fact that their critical exponents are different: the exponents for the Ising model

in $\epsilon = 4 - d$ and the exponents for our model in $\epsilon = 6 - d$ are different analytic functions with the same asymptotic expansion. The ϵ -expansion can not be used to decide whether the lower critical dimension is at $\epsilon = 3$ or at $\epsilon = 4$.

We conclude that because of instanton corrections the dimensional reduction breaks down for the equilibrium RFIM as well as for our nonequilibrium, deterministic zero temperature RFIM. In addition there is another “embarrassing” source of non-perturbative corrections in the equilibrium RFIM, which we do not have in our problem. There is no reason to expect our exponents to be the same as those of the equilibrium RFIM [86], though the perturbation series can be mapped. There might actually be three different underlying functions for the same ϵ -expansion for any exponent: one for the pure Ising model, one for the equilibrium random field Ising model, and one for our model, so that the exponents in all three models would still be different although their ϵ -expansions are the same.

IX. ϵ -EXPANSION FOR THE AVALANCHE EXPONENTS

The exponents whose ϵ -expansion we have calculated so far using the mapping to the equilibrium RFIM are ν , η , $\bar{\eta}$, β , $\beta\delta$, $\tilde{\theta}$ and z . Unfortunately, we cannot extract the avalanche exponents τ , $1/\sigma$, and θ from this mapping. The two exponent relations involving these exponents

$$\tau - 2 = \sigma\beta(1 - \delta) \tag{138}$$

and

$$1/\sigma = (d - \theta)\nu - \beta \tag{139}$$

are not enough to determine all three exponents from the information already obtained.

In the following we will compute τ and σ directly in an ϵ -expansion. The method employed makes use of the scaling of the higher moments of the avalanche size distribution. They are being calculated using n replicas of the system for the n 'th moment.

A. The second moment of the avalanche size distribution

When calculating η and ν we have already used all information from the scaling behavior of the first moment $\langle S \rangle$ of the avalanche size distribution: In [129,126] we show that $\langle S \rangle$ scales as the spatial integral over the avalanche-response-correlation function, which in turn scales as the “upward susceptibility” dM/dh calculated consistently with the history of the system.

In the Martin-Siggia-Rose formalism it is given by²⁰

$$\langle S \rangle \sim \int dt_0 \int d^d x \langle \hat{s}(t_0, x_0) s(t, x) \rangle_f = \int dt_0 \int d^d x \langle \delta s(t, x) / \delta \epsilon(t_0, x_0) \rangle_f. \quad (141)$$

The second moment $\langle S^2 \rangle$ of the avalanche size distribution is the random field average of the squared avalanche response. Note that it is not simply the square the expression in eq. (141) for the first moment — the product rule for taking derivatives gets in the way: A quantity such as

$$\langle \hat{s}(t_0, x_0) s(t_1, x_1) \hat{s}(t_2, x_0) s(t_3, x_3) \rangle_f \equiv A + B \quad (142)$$

not only contains the term which we need, namely

$$A = \left\langle \frac{\delta s(t_1, x_1)}{\delta \epsilon(t_0, x_0)} \frac{\delta s(t_3, x_3)}{\delta \epsilon(t_2, x_0)} \right\rangle_f \quad (143)$$

but also the terms

²⁰As we explain in section VI A and in [129,126] the expression

$$\int dt_0 \langle \hat{s}(t_0, x_0) s(t, x) \rangle_f \quad (140)$$

gives the random-field-averaged static response of the system at time t and position x to a positive θ -function pulse applied at position x_0 an infinitely long time before t (so that all transients have died away). The integral over all space will then give the *total* static random-field averaged response of the system to a θ -function pulse applied at site x_0 . This should scale in the same way as the first moment of the avalanche size distribution, *i.e.* as the average avalanche size.

$$B = \left\langle \frac{\delta^2 s(t_1, x_1)}{\delta \epsilon(t_0, x_0) \delta \epsilon(t_2, x_0)} s(t_3, x_3) \right\rangle_f + \left\langle s(t_1, x_1) \frac{\delta^2 s(t_3, x_3)}{\delta \epsilon(t_0, x_0) \delta \epsilon(t_2, x_0)} \right\rangle_f, \quad (144)$$

which are not related to $\langle S^2 \rangle$.

How can we separate A from B ?

One possibility is to introduce a second replica of the system with the identical configuration of random fields, the same initial conditions, and the same history of the external magnetic field. One can then calculate the response in each of the two replicas separately, multiply the results and afterwards take the average over the random fields. Denoting the quantities in the first replica with superscript α and those in the second replica with superscript β one obtains

$$\begin{aligned} A_2 &\equiv \langle \hat{s}^\alpha(t_0, x_0) s^\alpha(t_1, x_1) \hat{s}^\beta(t_2, x_0) s^\beta(t_3, x_3) \rangle_f \\ &= \left\langle \frac{\delta s^\alpha(t_1, x_1)}{\delta \epsilon^\alpha(t_0, x_0)} \frac{\delta s^\beta(t_3, x_3)}{\delta \epsilon^\beta(t_2, x_0)} \right\rangle_f, \end{aligned} \quad (145)$$

since

$$\frac{\delta s^\alpha}{\delta \epsilon^\beta} = 0, \quad (146)$$

and

$$\frac{\delta s^\beta}{\delta \epsilon^\alpha} = 0. \quad (147)$$

Similarly for the n 'th moment $\langle S^n \rangle$ of the avalanche size distribution one would use n replicas of the system. In appendix F we make this argument more precise and derive the scaling relation between $\langle S^2 \rangle$ and A_2

$$\langle S^2 \rangle_f \sim \int dt_1 \int dt_\alpha dt_\beta d^d x_\alpha d^d x_\beta \langle \hat{s}^\alpha(t_\alpha, x_\alpha) s^\alpha(t_0, x_\alpha) \hat{s}^\beta(t_\beta, x_\beta) s^\beta(t_1, x_\beta) \rangle_f. \quad (148)$$

In the following we generalize the RG treatment from previous sections to the case of two replicas, and extract the scaling behavior of $\langle S^2 \rangle$ from eq. (148) near the critical point. We will compare the result to the scaling relation

$$\begin{aligned} \langle S^2 \rangle &= \int S^2 D(S, r, h) dS \sim \int S^2 / S^\tau \mathcal{D}_\pm(S r^{1/\sigma}, h/r^{\beta\delta}) dS \\ &\sim r^{(\tau-3)/\sigma} \mathcal{S}_\pm^{(2)}(h/r^{\beta\delta}), \end{aligned} \quad (149)$$

where $\mathcal{S}_{\pm}^{(2)}$ is the corresponding scaling function, and obtain the missing information to compute the exponents τ and σ .

B. Formalism for two replicas

The generalization of the MSR generating functional to two replicas is rather straightforward. The equation of motion for each spin is the same in both replicas.

$$\partial_t s_i^\alpha / \Gamma_0 - \delta \mathcal{H}(s^\alpha) / \delta s_i^\alpha = 0 \quad (150)$$

and

$$\partial_t s_i^\beta / \Gamma_0 - \delta \mathcal{H}(s^\beta) / \delta s_i^\beta = 0 \quad (151)$$

where the Hamiltonian \mathcal{H} is given by eq. (32).

The new generating functional is a double path integral over two δ -functions which impose the equations of motion for both replicas. Again we can write the δ -functions in their ‘‘Fourier’’ representation by introducing two auxiliary fields \hat{s}^α and \hat{s}^β .

One obtains simply the square of the generating functional from eq. (34), expressed in terms of two replicas:

$$\begin{aligned} Z^{\alpha\beta} = & \int \int [ds^\alpha][d\hat{s}^\alpha] \int \int [ds^\beta][d\hat{s}^\beta] J[s^\alpha] J[s^\beta] \\ & \exp(i \sum_j \int dt \hat{s}_j^\alpha(t) (\partial_t s_j^\alpha(t) / \Gamma_0 - \delta \mathcal{H}(s^\alpha) / \delta s_j^\alpha(t))) \\ & \exp(i \sum_j \int dt \hat{s}_j^\beta(t) (\partial_t s_j^\beta(t) / \Gamma_0 - \delta \mathcal{H}(s^\beta) / \delta s_j^\beta(t))). \end{aligned} \quad (152)$$

We note that the two replicas do not interact before the average over the random fields is taken. Since $Z = 1$ we can again average Z directly over the random fields.

We rewrite the action using the same kinds of transformations to the local fields $\tilde{\eta}^\alpha$, $\hat{\tilde{\eta}}^\alpha$, $\tilde{\eta}^\beta$ and $\hat{\tilde{\eta}}^\beta$ which we introduced previously (see eq. (46)) *i.e.*

$$\begin{aligned} Z^{\alpha\beta} = & \int [d\tilde{\eta}^\alpha][d\hat{\tilde{\eta}}^\alpha][d\tilde{\eta}^\beta][d\hat{\tilde{\eta}}^\beta] \prod_j \bar{Z}_j[\tilde{\eta}_j^\alpha, \hat{\tilde{\eta}}_j^\alpha, \tilde{\eta}_j^\beta, \hat{\tilde{\eta}}_j^\beta] \\ & \exp \left\{ - \int dt \sum_j \hat{\tilde{\eta}}_j^\alpha(t) \left(\sum_\ell J_{j\ell}^{-1} J \tilde{\eta}_\ell^\alpha(t) \right) - \int dt \sum_j \hat{\tilde{\eta}}_j^\beta(t) \left(\sum_\ell J_{j\ell}^{-1} J \tilde{\eta}_\ell^\beta(t) \right) \right\}, \end{aligned} \quad (153)$$

where $\bar{Z}_j[\tilde{\eta}_j^\alpha, \hat{\eta}_j^\alpha, \tilde{\eta}_j^\beta, \hat{\eta}_j^\beta]$ is a local functional

$$\bar{Z}_j[\tilde{\eta}_j^\alpha, \hat{\eta}_j^\alpha, \tilde{\eta}_j^\beta, \hat{\eta}_j^\beta] = \int [ds^\alpha][d\hat{s}^\alpha][ds^\beta][d\hat{s}^\beta] \langle \exp \tilde{S}_{\text{eff}_j}^{\alpha\beta} \rangle_f, \quad (154)$$

and

$$\begin{aligned} \tilde{S}_{\text{eff}_j}^{\alpha\beta} = & \frac{1}{J} \int dt \left\{ J\hat{\eta}_j^\alpha(t) s_j^\alpha(t) + i\hat{s}_j^\alpha(t) \left(\partial_t s_j^\alpha(t) - J\tilde{\eta}_j^\alpha - H - f_j + \frac{\delta V^\alpha}{\delta s_j^\alpha} \right) \right\} \\ & + \frac{1}{J} \int dt \left\{ J\hat{\eta}_j^\beta(t) s_j^\beta(t) \right. \\ & \left. + i\hat{s}_j^\beta(t) \left(\partial_t s_j^\beta(t) - J\tilde{\eta}_j^\beta - H - f_j + \frac{\delta V^\beta}{\delta s_j^\beta} \right) \right\}. \end{aligned} \quad (155)$$

Here V^α and V^β are given by the linear cusp potential V defined in eq. (31), to be understood as a function of s^α and s^β respectively.

Again, we expand the action around its stationary point. It is specified by four coupled equations, which turn out to be solved self consistently by the replica symmetric mean field solution, which we found earlier when studying just one replica:

$$\hat{\eta}_0^\alpha = 0, \quad (156)$$

$$\hat{\eta}_0^\beta = 0, \quad (157)$$

$$\tilde{\eta}_0^\alpha = \langle s^\alpha \rangle_f, \quad (158)$$

$$\tilde{\eta}_0^\beta = \langle s^\beta \rangle_f. \quad (159)$$

Analogously to before [42] we will now expand around the mean-field solution $\tilde{\eta}_0^\alpha, \tilde{\eta}_0^\beta$ ($J\tilde{\eta}_0^\alpha$ and $J\tilde{\eta}_0^\beta$ denote the local field configurations about which the log of the integrand in equation (153) is stationary). Introducing shifted fields $\eta^\alpha \equiv \tilde{\eta}^\alpha - \tilde{\eta}_0^\alpha$ so that $\langle \eta^\alpha \rangle_f = 0$, and $\hat{\eta}^\alpha \equiv \hat{\eta}^\alpha$ (and correspondingly for η^β , and $\hat{\eta}^\beta$), leaves one with the generating functional

$$\bar{Z} = \int [d\eta^\alpha][d\hat{\eta}^\alpha][d\eta^\beta][d\hat{\eta}^\beta] \exp(S^{\alpha\beta}) \quad (160)$$

with an effective action

$$\begin{aligned}
S^{\alpha\beta} &= - \sum_{j,l} \int dt J_{jl}^{-1} J \hat{\eta}_j^\alpha(t) \eta_l^\alpha(t) - \sum_{j,l} \int dt J_{jl}^{-1} J \hat{\eta}_j^\beta(t) \eta_l^\beta(t) \\
&+ \sum_j \sum_{m,n,p,q=0}^{\infty} \frac{1}{m!n!p!q!} \int dt_1 \cdots dt_{m+n+p+q} u_{mnpq}^{\alpha\beta}(t_1, \dots, t_{m+n+p+q}) \\
&\hat{\eta}_j^\alpha(t_1) \cdots \hat{\eta}_j^\alpha(t_m) \eta_j^\alpha(t_{m+1}) \cdots \eta_j^\alpha(t_{m+n}) \\
&\hat{\eta}_j^\beta(t_{m+n+1}) \cdots \hat{\eta}_j^\beta(t_{m+n+p}) \eta_j^\beta(t_{m+n+p+1}) \cdots \eta_j^\beta(t_{m+n+p+q}). \tag{161}
\end{aligned}$$

Here, the $u_{mnpq}^{\alpha\beta}$ are the derivatives of $\ln \bar{Z}_j^{\alpha\beta}$ with respect to the fields $\hat{\eta}_j^\alpha$, η_j^α , $\hat{\eta}_j^\beta$ and η_j^β and thus are equal to the local, connected responses and correlations in mean-field theory:

$$\begin{aligned}
u_{mnpq}^{\alpha\beta} &= \frac{\partial}{\partial \epsilon^\alpha(t_{m+1})} \cdots \frac{\partial}{\partial \epsilon^\alpha(t_{m+n})} \frac{\partial}{\partial \epsilon^\beta(t_{m+n+p+1})} \cdots \frac{\partial}{\partial \epsilon^\beta(t_{m+n+p+q})} \\
&\langle s^\alpha(t_1) \cdots s^\alpha(t_m) s^\beta(t_{m+n+1}) \cdots s^\beta(t_{m+n+p}) \rangle_{f,l,c}. \tag{162}
\end{aligned}$$

As before, local [19] (l) means that we do not vary the local field $(\eta_0^\alpha)_j$ in the mean-field equation

$$\partial_t s_j^\alpha(t) = J(\eta_0^\alpha)_j(t) + H + f_j - \frac{\delta V^\alpha}{\delta s_j^\alpha(t)} + J\epsilon^\alpha(t) \tag{163}$$

when we perturb the replica α with the infinitesimal force $J\epsilon^\alpha(t)$ (and correspondingly for replica β). The index c to the average in eq. (162) is a reminder that these are *connected* correlation and response functions. In the same way as we discussed in section VID the force $J\epsilon^\alpha(t)$ is only allowed to *increase* with time consistently with the history we have chosen. From eq. (162) one sees that $u_{0npq} = 0$ if $n \neq 0$, $u_{mn0q} = 0$ if $q \neq 0$, and $u_{0n0q} = 0$, just as we had $u_{0n} = 0$ in our earlier calculation for just one replica.

C. Coarse graining transformation

The coarse graining transformation is defined in the same way as in the single replica case. In the appendix F we give the Feynman rules for loop corrections, and derive the canonical dimensions of the various operators in the action.

D. The scaling of the second moment of the avalanche size distribution

In appendix F we derive the scaling expression (eq. (148)) for the second moment of the avalanche size distribution

$$\langle S^2 \rangle \sim \int dt_1 \int dt_\alpha dt_\beta d^d x_\alpha d^d x_\beta \langle \hat{s}^\alpha(t_\alpha, x_\alpha) s^\alpha(t_0, x_\alpha) \hat{s}^\beta(t_\beta, x_\beta) s^\beta(t_1, x_\beta) \rangle_f. \quad (164)$$

In order to find the scaling dimension of $\langle S^2 \rangle$ we need to know how

$$\langle \hat{s}^\alpha(t_\alpha, x_\alpha) s^\alpha(t_0, x_\alpha) \hat{s}^\beta(t_\beta, x_\beta) s^\beta(t_1, x_\beta) \rangle_f \quad (165)$$

scales under coarse graining. The topology of the diagrams permits no $O(\epsilon)$ loop corrections to the corresponding vertex function. Since the anomalous dimensions of the external legs (*i.e.* Greens functions) in the two replicas are also zero at $O(\epsilon)$ it is sufficient to use the plain field rescalings to extract the scaling behavior of $\langle \hat{s}^\alpha \hat{s}^\beta s^\alpha s^\beta \rangle$ under coarse graining. As shown in appendix F one obtains

$$\langle \hat{s}^\alpha \hat{s}^\beta s^\alpha s^\beta \rangle \sim \Lambda^{(2(d+z))-4} \quad (166)$$

where Λ is the cutoff in the momentum shell integrals.

Inserting this result into eq. (164) along with the canonical dimensions of the various times $[t] \sim \Lambda^{-z}$ and coordinates $[x] \sim \Lambda^{-1}$, one obtains

$$\langle S^2 \rangle \sim \Lambda^{-(4+z)} \quad (167)$$

(Formally including the anomalous dimensions $\eta = \bar{\eta} = 0 + O(\epsilon^2)$, one obtains (to first order in ϵ) $\langle S^2 \rangle \sim \Lambda^{-(z+(2-\eta)2)}$. Similarly, one finds for the higher moments $\langle S^n \rangle \sim \Lambda^{-((n-1)z+(2-\eta)n)}$.)

On the other hand, from eq. (149) we know that $\langle S^2 \rangle \sim r^{(\tau-3)/\sigma} \mathcal{S}_\pm^{(2)}(h/r^{\beta\delta})$. If we use that r has scaling units $\Lambda^{1/\nu}$, and that $\tau - 2 = \sigma\beta(1 - \delta)$ (see section IVI, and [129,126]), we find by comparison with eq. (167) that $1/\sigma = z\nu + (2 - \eta)\nu$ to first order in ϵ . One gets the same relation from comparing the dimensions for the n 'th moment, which scales as $\langle S^n \rangle \sim r^{(\tau-(n+1))/\sigma} \mathcal{S}_\pm^{(n)}(h/r^{\beta\delta})$.

E. Results

We've seen that

$$1/\sigma = z\nu + (2 - \eta)\nu = 2 + \epsilon/3 + O(\epsilon^2). \quad (168)$$

If one inserts the result for $1/\sigma = z\nu + (2 - \eta)\nu = 2 + \epsilon/3 + O(\epsilon^2)$ into the relation $\tau - 2 = \sigma\beta(1 - \delta)$, one obtains

$$\tau = 3/2 + O(\epsilon^2). \quad (169)$$

From the violated hyperscaling relation $1/\sigma = (d - \theta)\nu - \beta$ one finds

$$\theta\nu = 1/2 - \epsilon/6 + O(\epsilon^2). \quad (170)$$

This concludes the perturbative approach to the problem.

X. COMPARISON WITH NUMERICAL SIMULATIONS IN 2, 3, 4, AND 5 DIMENSIONS

Figure 15 shows a comparison between the theoretical predictions for various exponents and their values as obtained from numerical simulations in 2, 3, 4, and 5 dimensions. These prepublication results are courtesy of Olga Perković. A complete list of the numerical exponents that were measured in the simulations, and a detailed description of the algorithm that allowed to simulate systems with up to 1000^3 spins is given in a forthcoming publication [45]. A quantitative comparison of the results to experiments can be found in [126,128]. Some first results and conjectures about the behavior in in two dimensions, which is likely the lower critical dimension of our critical point, are presented elsewhere [98]. As is seen in the figure, the agreement between the numerics and the results from the ϵ expansion is surprisingly good, even down to $\epsilon = 3$.

The numerical values in 3 dimensions for β , $\beta\delta$, ν and η seem to have overlapping error bars with the corresponding exponents of the equilibrium RFIM. Maritan *et al* [86]

conjectured that the exponents might be equal in a comment to our first publication [41] on this system. Why this should be is by no means obvious. The physical states probed by the two systems are very different. While the equilibrium RFIM will be in the lowest free energy state, our system will be in a history dependent metastable state. Nevertheless, as we have seen, the perturbation expansions for the critical exponents can be mapped onto another to all orders in ϵ . In appendix G 3 we discuss possible connections between the two models that might become clear if temperature fluctuations are introduced in our zero-temperature avalanche model.

Acknowledgements

We acknowledge the support of DOE Grant #DE-FG02-88-ER45364 and NSF Grant #DMR-9118065. We would like to thank Olga Perković very much for providing the beautiful numerical results in two, three, four, and five dimensions to which the analytical results of this paper compare favorably. Furthermore we thank Andreas Berger, Lincoln Chayes, Daniel Fisher, Stuart Field, Sivan Kartha, Bill Klein, Eugene Kolomeisky, James A. Krumhansl, Onuttom Narayan, Mark Newman, Jordi Ortín, Antoni Planes, Mark Robins, Bruce Roberts, Jean Souletie, Uwe Tauer, Eduard Vives, and Jan von Delft for helpful conversations, and NORDITA where this project was started. This research was conducted using the resources of the Cornell Theory Center, which receives major funding from the National Science Foundation (NSF) and New York State. Additional funding comes from the Advanced Research Projects Agency (ARPA), the National Institutes of Health (NIH), IBM Corporation, and other members of the center's Corporate Research Institute. Further pedagogical information using Mosaic is available [131].

APPENDIX A: HARD-SPIN AND SOFT-SPIN MEAN-FIELD THEORY

1. Hard-Spin Mean-Field Theory

In this appendix we derive the scaling forms near the critical point for the magnetization and the avalanche size distribution in the hard-spin mean-field theory. At the end we briefly discuss changes of nonuniversal quantities for the soft-spin mean-field theory.

We start from the hard-spin mean-field Hamiltonian:

$$\mathcal{H} = - \sum_i (JM + H + f_i) s_i \quad (\text{A1})$$

where the interaction with the nearest neighbors from the short range model eq. (3) has been replaced by an interaction with the average spin value or magnetization $M = (\sum s_i)/N$. This would be the correct Hamiltonian if every spin would interact equally strongly with every other spin in the lattice *i.e.* for infinite range interactions.

2. Mean-field magnetization curve

Initially, at $H = -\infty$, all spins are pointing down. The field is slowly increased to some finite value H . Each spin s_i flips, when it gains energy by doing so, *i.e.* when its local effective field $h_i^{\text{eff}} = JM + H + f_i$ changes sign. At any given field H all spins with $h_i^{\text{eff}} < 0 \Leftrightarrow f_i < -JM - H$ will still be pointing down, and all spins with $h_i^{\text{eff}} > 0 \Leftrightarrow f_i > -JM - H$ will be pointing up. Self-consistency requires that $M = \int \rho(f) s_i df$. Therefore

$$M = (-1) \int_{-\infty}^{-JM-H} \rho(f) df + \int_{-JM-H}^{\infty} \rho(f) df = 1 - 2 \int_{-\infty}^{-JM-H} \rho(f) df \quad (\text{A2})$$

is the self-consistency equation from which we can extract the mean-field magnetization as a function of H . As in the main text $\rho(f) = \exp(-f^2/2R^2)/(\sqrt{2\pi}R)$ is the distribution of random fields.

For $R \geq \sqrt{2/\pi}J \equiv R_c$ the solution $M(H)$ of eq. (A2) is analytic at all values of H . For $R = R_c$ there is a critical magnetic field $H_c(R_c) = 0$ where the magnetization curve

$M(H)$ has diverging slope. For $R < R_c$ the solution $M(H)$ is unique only for H outside a certain interval $[H_c^l(R), H_c^u(R)]$. For H in the range between the two “coercive fields” $H_c^l(R)$ and $H_c^u(R)$, the equation has three solutions, two that are stable and one that is unstable. Unlike equilibrium systems, which will always occupy the solution with the lowest overall free energy, our nonequilibrium (zero temperature) system is forced by the *local* dynamics to stay in the current local energy minimum until it is destabilized by the external magnetic field. For increasing external magnetic field this implies that the system will always occupy the metastable state with the lowest possible magnetization. Conversely, for decreasing external magnetic field, the system will occupy the metastable state with highest possible magnetization. One obtains a hysteresis loop for $M(H)$ with a jump, or “infinite avalanche” at the upper and lower coercive fields $H_c^u(R)$ and $H_c^l(R)$ respectively (see figure 5).

From eq. (A2) follows that $dM/dH = 2\rho(x)/(-t(x))$ with $x = -JM - H$ and

$$t(x) = 2J\rho(-JM - H) - 1. \quad (\text{A3})$$

dM/dH diverges if $t(x_c) = 0$, which defines x_c . For $R > R_c$ the slope dM/dH is always finite, and $t < 0$ at all $H \in [-\infty, +\infty]$. For $R \leq R_c$ however the condition $t(x_c) = 0$ is fulfilled at the critical field $H_c(R)$. To obtain potential scaling behavior near this point, we expand $t(x)$ around $x_c = -JM(H_c(R)) - H_c(R)$

$$t = 2J\rho(x) - 1 = 2J(\rho(x_c) - 1) + \rho'(x_c)(x - x_c) + 1/2\rho''(x_c)(x - x_c)^2 + \dots, \quad (\text{A4})$$

where

$$2J\rho(x_c) - 1 = 0. \quad (\text{A5})$$

Then

$$\chi \equiv dM/dH = (-\rho(x_c))/(J(\rho'(x_c)(x - x_c) + 1/2\rho''(x_c)(x - x_c)^2 + \dots)). \quad (\text{A6})$$

For a general analytic distribution of random fields $\rho(x)$ with one maximum with nonvanishing second derivative ($\rho''(x_c) < 0$) this suggests two different scaling behaviors corresponding to the cases $\rho'(x_c) = 0$ and $\rho'(x_c) \neq 0$.

Let us consider the case $\rho'(x_c) = 0$ first. For a Gaussian distribution of width $R \equiv R_c$ with zero mean this implies that $x_c = -JM(H_c) - H_c = 0$ and consequently $\rho(x_c) = 1/(\sqrt{2\pi}R_c)$ and $\rho''(x_c) = 1/(2\pi R_c^3)$. With eq. (A5) one obtains $R_c = \sqrt{2/\pi}J$. This is in fact the largest possible value of R for which $M(H)$ has a point of diverging slope.

Integrating eq. (A6) leads to a cubic equation for M and the leading order scaling behavior

$$M(r, h) \sim |r|^\beta \mathcal{M}_\pm(h/|r|^{\beta\delta}), \quad (\text{A7})$$

for small $h = H - H_c(R_c)$ and $r = (R_c - R)/R$. In mean-field theory $\delta = 3$ and \mathcal{M}_\pm is given by the smallest real root $g_\pm(y)$ of the cubic equation

$$g^3 \mp \frac{12}{\pi}g - \frac{12\sqrt{2}}{\pi^{3/2}R_c}y = 0, \quad (\text{A8})$$

where here and throughout \pm refers to the sign of r .

The other case ($\rho(x_c) = 1/(2J)$ and $\rho'(x_c) \neq 0$) is found for distributions with $R < R_c$. Integrating eq. (A6) with $x_c = -JM(H_c(R)) - H_c(R)$ yields a quadratic equation for the magnetization and the scaling behavior

$$M - M(H_c(R)) \sim (H - H_c(R))^\zeta \quad (\text{A9})$$

with $\zeta = 1/2$ for H close to $H_c(R)$. From eq. (A2) and eq. (A5) one finds $H_c(R_c) = 0$, $H_c(R) \sim r^{\beta\delta}$ for small $r > 0$, with $\beta\delta = 3/2$ and $H_c(R = 0) = J$. The corresponding phase diagram was shown in figure 7.

Note that the scaling results for R close to R_c as given in eq. (A7) remind one of the scaling results of the Curie-Weiss mean-field theory for the equilibrium Ising model near the Curie-temperature ($T = T_c$). For $T < T_c$ however, the equilibrium model has a discontinuity in the magnetization at $H = 0$, while for $R < R_c$ our model displays a jump in the magnetization at a (history dependent) nonzero magnetic field $H_c(R)$, where the corresponding metastable solution becomes unstable. Our infinite avalanche line $H_c(R)$ is in fact similar to the spinodal line in spinodal decomposition [53].

Note also that this mean-field theory does not show any hysteresis for $R \geq R_c$ (see figure 5). This is only an artifact of its particularly simple structure and not a universal feature. For example, the continuous spin model, which we use for the RG description in section VI has the same exponents in mean-field theory, but shows hysteresis for *all* disorders R , even for $R > R_c$. In that case there are two critical fields $H_c^u(R_c)$ and $H_c^l(R_c)$ — one for each branch of the hysteresis curve (see figure 6, and figure 8).

3. Mean-field avalanche-size distribution

As we have already discussed in the main text, one finds avalanches of spin flips as the external field is raised adiabatically. Due to the ferromagnetic interaction a flipping spin may cause some of its nearest neighbors to flip also, which may in turn trigger some of their neighbors, and so on. In mean-field theory, where all spins act as nearest neighbors with coupling J/N , a spin flip from -1 to $+1$ changes the effective field of *all* other spins by $2J/N$. For large N , the average number of secondary spins that will be triggered to flip in response to this change in the effective local field is then given by $n_{trig} \equiv (2J/N)N\rho(-JM - H) = 2J\rho(-JM - H)$. If $n_{trig} < 1$, any avalanche will eventually peter out, and even in an infinite system all avalanches will only be of finite size. If $n_{trig} = 1$, the avalanche will be able to sweep the whole system, since each flipping spin triggers on average one other spin. This happens when the magnetic field H takes a value at the infinite avalanche line $H = H_c(R)$, with $R \leq R_c$, since $n_{trig} = 1$ is equivalent to $t = 0$ (see eq. (A3)).

Considering all possible configurations of random fields, there is a probability distribution for the number S of spins that flip in an avalanche. It can be estimated for avalanches in large systems, i.e. for $S \ll N$: For an avalanche of size S to happen, given that the primary spin has random field f_i , it is *necessary* that there are exactly $S - 1$ secondary spins with their random fields in the interval $[f_i, f_i + 2(J/N)S]$. Assuming that the probability density of random fields is approximately constant over this interval, the probability $P(S)$ for a corresponding configuration of random fields is given by the Poisson distribution, with the

average value $\lambda = 2JS\rho(-JM - H) = S(t + 1)$, where $t \equiv 2J\rho(-JM - H) - 1$:

$$P(S) = \frac{\lambda^{(S-1)}}{(S-1)!} \exp(-\lambda). \quad (\text{A10})$$

This includes cases in which the random fields of the s spins are arranged in the interval $[f_i, f_i + 2S(J/N)]$ in such a way that they do not flip in one big avalanche, but rather in two separate avalanches triggered at slightly different external magnetic fields. Imposing periodic boundary conditions on the interval $[f_i, f_i + 2S(J/N)]$ one can see that for any arrangement of the random fields in the interval there is exactly one spin which can trigger the rest in one big avalanche. In $1/S$ of the cases, the random field of this particular spin to trigger the avalanche will be the one with the lowest random field, as desired. Therefore we need to multiply $P(S)$ by $1/S$ to obtain the probability $D(S, t)$ for an avalanche of size S starting with a spin flip at random field $f_i = -JM - H$

$$D(S, t) = S^{(S-2)} / (S-1)! (t+1)^{(S-1)} e^{-S(t+1)}. \quad (\text{A11})$$

With Stirling's formula we find for large S the scaling form

$$D(S, t) \sim \frac{1}{\sqrt{2\pi} S^{3/2}} \exp(-St^2/2). \quad (\text{A12})$$

To obtain the scaling behavior near the two different critical points, we will insert into the expression in eq. (A12) the expansion of $t(x)$ around x_c from eq. (A4).

4. Avalanches near the critical endpoint

Near the critical point $(R_c, H_c(R_c))$, where $x_c = 0$ and $\rho'(x_c) = 0$ we obtain $t = 2J(\rho(0) - 1) + J\rho''(0)(-JM - H)^2$, which (by equation eq. (A7)) leads to the scaling form

$$t \sim r[1 \mp 1/4\pi g_{\pm}(h/|r|^{\beta\delta})^2]. \quad (\text{A13})$$

g_{\pm} was defined in eq. (A8), and \pm again refers to the sign of $r = (R_c - R)/R$. Inserting the result into eq. (A12) one obtains

$$D(S, r, h) \sim S^{-\tau} \mathcal{D}_{\pm}(S/|r|^{-1/\sigma}, h/|r|^{\beta\delta}), \quad (\text{A14})$$

with the mean-field results $\tau = 3/2$, $\sigma = 1/2$, $\beta\delta = 3/2$, and the mean-field scaling function

$$\mathcal{D}_{\pm}(x, y) = \frac{1}{\sqrt{2\pi}} e^{-x[1 \mp \frac{\pi}{4} g_{\pm}(y)]^2/2}. \quad (\text{A15})$$

5. Mean-field avalanche size distribution near the ∞ -avalanche line (“spinodal line”)

For $R < R_c$ one has $\rho'(x_c) \neq 0$, so that the expansion for t becomes

$$\begin{aligned} t &= 2J(\rho(x_c) - 1) + 2J\rho'(x_c)(x - x_c) + \dots = 2J\rho'(x_c)(x - x_c) \\ &= 2J\rho'(x_c)(-J(M - M(H_c(R))) - (H - H_c(R))) \end{aligned} \quad (\text{A16})$$

Following the steps that led to eq. (A9) we arrive at

$$t = -2\sqrt{J\rho'(x_c)(H - H_c(R))} + \text{higher orders in } (H - H_c(R)) \quad (\text{A17})$$

so that for H close to the onset to infinite avalanche (with $H \leq H_c^u(R)$ for increasing field H and $H > H_c^l(R)$ for decreasing field)

$$D(S, (H - H_c(R))) \sim \frac{1}{\sqrt{2\pi}S^{3/2}} \exp\{-2[\rho'(-JM - H)J]S|H - H_c(R)|\}. \quad (\text{A18})$$

or, written more generally,

$$D(S, H - H_c(R)) \sim 1/S^{\tau} \bar{\mathcal{F}}(S|H - H_c(R)|^{1/\kappa}) \quad (\text{A19})$$

with $\kappa = 1$ and $\tau = 3/2$ in mean-field theory, and $\bar{\mathcal{F}}$ the corresponding mean-field scaling function.

6. Modifications for the soft-spin mean-field theory

In section VI we have for calculational convenience switched from the hard-spin model, where each spin s_i could only take the values ± 1 , to a soft-spin model, where s_i can take

any value between $-\infty$ and $+\infty$. In realistic systems these soft-spins can be considered as coarse grained versions of the elementary spins. The corresponding Hamiltonian with the newly introduced double-well potential

$$V(s_i) = \begin{cases} k/2 (s_i + 1)^2 & \text{for } s < 0 \\ k/2 (s_i - 1)^2 & \text{for } s > 0 \end{cases} \quad (\text{A20})$$

to mimic the two spin states of the hard-spin model, was given in eq. (32). In the mean-field approximation, where the coupling term $-J_{ij}s_i s_j$ is replaced by $-\sum_i JM s_i$ with $M = \sum_j s_j/N$, we obtain

$$\mathcal{H} = - \sum_i \{ (JM + H + f_i) s_i - V(s_i) \} . \quad (\text{A21})$$

For adiabatically increasing external magnetic field the local dynamics introduced earlier implies that each spin will be negative so long as the lower well Hamiltonian

$$\mathcal{H}_- \equiv k/2 (s_i + 1)^2 - (H + JM + f_i) s_i \quad (\text{A22})$$

does have a local minimum with $\delta\mathcal{H}/\delta s = 0$ for negative s_i . This implies that $s_i < 0$ if

$$\frac{\delta}{\delta s_i} [k/2 (s_i + 1)^2 - (H + f_i + JM) s_i]_{s=0} \geq 0 , \quad (\text{A23})$$

else s_i will be stable only at the bottom of the positive potential well, where

$$\frac{\delta}{\delta s_i} \mathcal{H}_+ = \frac{\delta}{\delta s_i} [k/2 (s_i - 1)^2 - (H + JM + f_i) s_i] = 0 . \quad (\text{A24})$$

We conclude that for the given history

$$\begin{cases} s_i \leq 0 & \text{for } f_i \leq -JM - H + k \\ s_i > 0 & \text{for } f_i > -JM - H + k . \end{cases} \quad (\text{A25})$$

From the self-consistency condition

$$\langle s_i \rangle \equiv \int \rho(f_i) s_i df_i = M \quad (\text{A26})$$

we derive the mean-field self-consistency equation for the *soft-spin* magnetization M_u (for *increasing* external magnetic field):

$$M_u(H) = (k + H)/(k - J) - 2k/(k - J) \int_{-\infty}^{-JM-H+k} \rho(f)df. \quad (\text{A27})$$

Correspondingly one finds for the branch of *decreasing* external magnetic field:

$$M_l(H) = (k + H)/(k - J) - 2k/(k - J) \int_{-\infty}^{-JM-H-k} \rho(f)df. \quad (\text{A28})$$

Figure 6 shows the corresponding hysteresis loops in the three disorder regimes $R < R_c = \sqrt{2/\pi}J(k/(k - J))$, where the hysteresis loop has a jump, $R = R_c$, where the jump has shrunk to a single point of infinite slope dM/dH , and $R > R_c$, where the hysteresis loop is smooth. In contrast to the hard spin model, this model displays hysteresis even for $R \geq R_c$.

The critical magnetic fields $H_c^u(R)$ and $H_c^l(R)$ at which the slope of the static magnetization curve diverges are found by differentiating eqs. (A27) and (A28) with respect to H and by solving for dM_{stat}/dH . One finds (for increasing external magnetic field) that $dM_{stat}/dH \sim 1/\tau$ with

$$\tau = (2k/(k - J))J\rho(-JM_{stat} - H + k) - 1. \quad (\text{A29})$$

τ is defined analogously to the parameter t in eq. (A3). (It is worth mentioning that $t = \chi^{-1}k/(J(k - J))$, where χ^{-1} is the constant term in the propagator of the RG treatment, which was introduced in eq. (73) in the main text.) The critical field $H_c(R)$ is given by the solution to the condition $\tau = 0$. To find the scaling behavior near the critical point one can expand eq. (A27) around $H_c^u(R)$, and correspondingly eq. (A28) around $H_c^l(R)$. For increasing external magnetic field the critical point $R = R_c$, $H = H_c^u(R_c)$ and $M = M_c \equiv M_u(H_c^u(R_c))$ is characterized by the equation $\tau = 0$ and $\rho'(-JM_c - H_c + k) = 0$, *i.e.* $-JM_c - H_c + k = 0$. It follows that $R_c = \frac{1}{\sqrt{2\pi}}\frac{2kJ}{k-J}$. Inserting these results into eq. (A27) one obtains $M_c^u = 1$ and $H_c^u(R_c) = k - J$. Similarly for a decreasing external magnetic field one finds $H_c^l(R_c) = -(k - J)$ and $M_c^l = M_l(H_c^l(R_c)) = -1$. The corresponding modified phase diagram is depicted in figure 8, with $H_c^u(R = 0) = +k$ and $H_c^l(R = 0) = -k$.

In the same way as discussed in appendix A for the (static) hard-spin model, expanding eqs. (A27) and (A28) around M_c , H_c and R_c yields cubic equations for the magnetization and one obtains the scaling behavior near the critical point

$$m \sim h^{1/3} \quad (\text{A30})$$

for $m \equiv M - M_c$ and $h \equiv H - H_c(R_c)$. Consequently the slope of the magnetization as a function of h diverges at the critical point

$$dm/dh \sim h^{-2/3}. \quad (\text{A31})$$

It turns out that in fact none of the universal scaling features we discussed for the hard spin model is changed. The mean-field critical exponents β , δ , τ and σ , and the scaling forms near the critical point are the same as in the hard-spin model. (A “spin-flip” in the hard spin model corresponds to a spin moving from the lower to the upper potential well in the soft-spin model.) Apart from modifying some nonuniversal constants, the new parameter $k > J$ in the definition of the soft-spin potential does not appear to change the calculation in any important way.

a. Soft-Spin Mean-Field Theory at Finite Sweeping Frequency Ω

In section VIA, eq. (62), we have derived the following equation of motion for each spin in the dynamical soft-spin mean-field theory, as the external magnetic field $H(t) = H_0 + \Omega t$ is slowly increased

$$\frac{1}{\Gamma_0} \partial_t s_j(t) = J\eta_j^0(t) + H + f_j - \frac{\delta V}{\delta s_j(t)} + J\epsilon(t). \quad (\text{A32})$$

With the definition of the potential V from eq. (31) this becomes

$$1/(\Gamma_0 k) \partial_t s_j(t) = -s_j(t) + J\eta_j^0(t)/k + H(t)/k + f_j/k + \text{sgn}(s_j) + J\epsilon(t)/k. \quad (\text{A33})$$

From eq. (54) we know that $\eta^0(t) = \langle s \rangle \equiv M(t)$ is the time dependent mean-field magnetization of the system. It can be calculated by taking the random-field average of eq. (A33) and solving the resulting equation of motion for $\eta^0(t)$. One can show [126] that for driving rate Ω/k small compared to the relaxation rate $k\Gamma_0$ of the system, for all values of H_0 the solution $\eta^0(t)$ can be expanded in terms of (Ω/Γ_0) in the form

$$\eta^0(t) \equiv M(t) = M_{stat}(H_0) + (\Omega/\Gamma_0)^{p_1} f_1(H_0)t + (\Omega/\Gamma_0)^{p_2} f_2(H_0)t^2 + \dots \quad (\text{A34})$$

with $0 < p_1 < p_2 < \dots$. The p_i depend on whether $R < R_c$ or $R = R_c$. $M_{stat}(H_0)$ is the solution of the static mean-field theory equation (A27) for the given history. If the series converges for $\Omega \rightarrow 0$, it follows that $\eta^0(t)$ approaches the *constant* magnetization $M_{stat}(H_0)$ in the adiabatic limit. This is certainly expected for H_0 *away* from the critical field $H_c(R)$, where the static magnetization is non-singular: as Ω tends to zero the time dependent magnetization $M(t)$ simply lags less and less behind the static value $M_{stat}(H(t))$. The magnetization $M(t)$ can be expanded as $M(t) = M_{stat}(H_0) + [dM/dH]_{H_0}\Omega t + \dots$ and converges towards $M_{stat}(H_0)$ as $\Omega \rightarrow 0$, as long as all derivatives $[d^n M_{stat}/dH^n]_{H_0}$ are well defined and finite. This argument however does not obviously hold at the critical fields $H_0 = H_c(R)$ with $R \leq R_c$, where dM_{stat}/dH and all higher derivatives diverge. Using boundary layer theory one can show [126] that even at these singular points $M(t)$ converges toward its static limit $M(H_c(R))$ as $\Omega \rightarrow 0$, though with power laws smaller than one in Ω , as indicated in eq. (A34). Since we use $M_{stat}(H_0)$ as the foundation for our ϵ -expansion, this is reassuring.

APPENDIX B: TILTING OF THE SCALING AXES

In the appendix on mean-field theory we derived scaling forms for the magnetization and the avalanche size distribution, which depended on the (mean-field) scaling fields $r = (R - R_c)/R$ and $h = H - H_c$. In finite dimensions however, the corresponding scaling forms may depend not on r and h , but on rotated variables

$$r' = r + ah \quad (\text{B1})$$

and

$$h' = h + br. \quad (\text{B2})$$

The amount by which the scaling axes $r' = 0$ and $h' = 0$ are tilted relative to the $(r, 0)$ and $(0, h)$ direction in the (r, h) plane is a nonuniversal quantity and has no effect on the critical

exponents. Nevertheless it can be important in the data analysis. (The numerical results in 3, 4, and 5 dimensions do indeed seem to indicate a slight tilting [45].)

1. Extracting β and $\beta\delta$ from the magnetization curves

With $m(r', h') = M(r', h') - M_c$, where $M_c = M(0, 0)$ is the magnetization at the critical point, we obtain the scaling form

$$m \sim (r')^\beta \mathcal{M}_\pm(h'/(r')^{\beta\delta}). \quad (\text{B3})$$

In simulations and experiments however the magnetization is given as a function of r and h rather than r' and h' . We rewrite eq. (B3) in terms of r and h by inserting the definitions of r' and h' from eq. (B1) and eq. (B2) and use the fact that $\beta\delta > 1$ in the cases we are considering. One obtains for the leading order scaling behavior

$$M - (M_c + cr) \sim r^\beta \tilde{\mathcal{M}}_\pm((h + br)/r^{\beta\delta}) \quad (\text{B4})$$

(where c is a constant and $\tilde{\mathcal{M}}_\pm$ is the appropriate function). Equivalently this can be written as

$$dM/dH \sim r^{\beta-\beta\delta} \tilde{\mathcal{M}}_\pm((h + br)/r^{\beta\delta}). \quad (\text{B5})$$

To extract the critical exponents β and $\beta\delta$ one can then use collapses of dM/dH in the same way as if the mean-field scaling forms were valid in finite dimensions, except for the presence of a new tilting parameter b , that has to be varied to its correct value simultaneously with β and $\beta\delta$ to find the best collapse of the data curves. (A more detailed description of the procedure is given in reference [45]).

2. Extracting the correlation length exponents ν and $\nu/(\beta\delta)$

Similarly to eq. (B3) the scaling for the correlation length in finite dimensions takes the form

$$\xi \sim (r')^{-\nu} \mathcal{Y}_{\pm}(h'/(r')^{\beta\delta}), \quad (\text{B6})$$

Thus $\xi \sim (h')^{-\nu/(\beta\delta)}$ along $r' = 0$ and $\xi \sim (r')^{-\nu}$ along $h' = 0$. Figure 16 shows contour lines in the (r', h') plane for the correlation length. Since $\nu/(\beta\delta) < \nu$, ξ changes faster in the $(0, h')$ direction than in the $(r', 0)$ direction. This implies that the correlation length diverges with the dominant exponent $\nu/(\beta\delta)$ when the critical point is approached along any direction other than $h' = 0$. This can be used to extract $\nu/(\beta\delta)$ from collapses of numerical or experimental curves for the correlation function $G(x, h, r)$ measured as a function of h at fixed $R = R_c$:

$$G(x, h, r = 0) \sim 1/x^{(d-2+\eta)} \tilde{\mathcal{G}}_{\pm}(xh^{-\nu/(\beta\delta)}, 0) \quad (\text{B7})$$

with the appropriate scaling function $\tilde{\mathcal{G}}_{\pm}$. (Even in 3 dimensions $\nu/(\beta\delta) < \nu$ is still correct and the tilting is small.)

On the other hand it seems rather difficult to find the weaker scaling direction $(r', 0)$ accurately enough to be able to extract ν by approaching the critical point along this line. If, instead, we integrate the correlation function or the avalanche size distribution over h' , we obtain a scaling form that depends only on r' . From collapses of the integrated functions, the exponent ν can then be extracted, even without knowledge of the exact size of the tilting angle. Practically, in the analysis of our simulation data we actually integrate over the magnetic field H rather than h' . On long length scales this is equivalent to an integration over h' : The integration path $r = \text{const} \equiv c$ is written in the (h', r') plane through $r' = a_1c + b_1h$ and $h' = a_2c + b_2h$. Under coarse graining the h' component grows faster than the r' component, so that after several coarse graining steps the integration path is deformed into a straight line parallel to h' . This procedure yields the dominant contribution to an integrated scaling function $G_{int}(x, r) \equiv \int dh G(x, r, h)$ in the region near the critical point. It allows us to treat r as a scaling field and to extract the weaker exponent ν : we have $\xi \sim r^{-\nu}$ after integration over the hysteresis loop. For the integrated avalanche correlation function, for example, this means $G_{int}(x, r) \sim 1/x^{d+\beta/\nu} \mathcal{G}_{\pm}^{int}(xr^{-\nu})$, with the appropriate scaling function \mathcal{G}_{\pm}^{int} .

The rotation of the scaling axes (see also [45]) is not apparent from the ϵ -expansion. For the renormalization group calculation we have linearized the coarse graining transformation around the fixed point. The rotation of the scaling axes is due to nonlinear corrections introduced during the flow to the fixed point.

From the mapping of the perturbation series for the critical exponents in our model to the perturbation series for the critical exponents in the equilibrium random field Ising model, one might expect that for $R \geq R_c$ the $H \rightarrow (-H)$ symmetry of the fixed point in the thermal random field Ising model is mapped to an $(h') \rightarrow (-h')$ symmetry in our problem. (Nonperturbative corrections might destroy this of course.) Note that this symmetry only emerges on long length scales, near the critical point, where the mapping to the thermal random field Ising model holds.

APPENDIX C: SOME DETAILS OF THE RG CALCULATION

1. Calculating some u_{mn} coefficients

In section VIA in eq. (61) we have given an expression for the coefficients u_{mn} in the expansion around mean-field theory:

$$u_{m,n} = \frac{\partial}{\partial \epsilon(t_{m+1})} \cdots \frac{\partial}{\partial \epsilon(t_{m+n})} \langle (s(t_1) - \eta^0(t_1)) \cdots (s(t_m) - \eta^0(t_m)) \rangle_{l, \hat{\eta}^0, \eta^0}, \quad (\text{C1})$$

where $s_j(t)$ is the solution of the *local* mean-field equation

$$1/(\Gamma_0 k) \partial_t s_j(t) = -s_j(t) + J \eta_j^0(t)/k + H(t)/k + f_j/k + \text{sgn}(s_j) + J \epsilon(t)/k. \quad (\text{C2})$$

We need to insert the solution for $\eta^0(t)$ from appendix A 6 into eq. (C2) to calculate the higher response and correlation functions u_{mn} as given in eq. (C1).

a. The coefficient $u_{1,0}$

The vertex $u_{1,0}$ is defined as

$$u_{1,0}(t) = \langle s_j(t) \rangle_l - \eta^0(t). \quad (\text{C3})$$

From the stationary phase equation eq. (54) we have $\eta^0(t) = \langle s_i(t) \rangle_l$. Therefore (by construction)

$$u_{1,0}(t) = 0. \quad (\text{C4})$$

b. The coefficient $u_{1,1}(t_1, t_2)$

As is shown in appendix A 6, $\eta^0(t)$ can be expanded in terms of Ω (at least for $R \geq R_c$ and for $R < R_c$ before the jump up to $H_c(R)$):

$$\eta^0(t) = M(H_0) + \Omega^p t + \dots, \quad (\text{C5})$$

where $M(H_0)$ is the static magnetization, $p > 0$, and \dots implies higher orders in Ω . Inserting this expansion into eq. (C2) and eq. (C1) allows us to calculate the coefficients u_{mn} perturbatively in Ω . Only the lowest order remains as $\Omega \rightarrow 0$. The vertex function $u_{11}(t_1, t_2)$ is then given by

$$\lim_{\Omega \rightarrow 0} [\partial_t (\lim_{\epsilon \rightarrow 0} \langle s(t_2) |_{H(t_2) + J\epsilon\theta(t_2 - t_1)} - s(t_2) |_{H(t_2)} \rangle_f / \epsilon)]. \quad (\text{C6})$$

To evaluate $s(t_2) |_{H(t_2) + J\epsilon\theta(t_2 - t_1)}$ from the equation of motion eq. (C2) we have to consider three cases:

1. Neither $s_j(t) |_{H(t)}$ nor $s(t) |_{H(t) + J\epsilon\theta(t - t_1)}$ flip at any time t with $t_1 < t < t_2$. To lowest order in Ω the solution of eq. (C2) is then given by simple relaxation:

$$s_j^{no\ flip}(t) |_{H(t) + J\epsilon\theta(t - t_1)} - s_j(t) |_{H(t)} = (J\epsilon/k)(1 - \exp[-k\Gamma_0(t - t_1)])\theta(t - t_1). \quad (\text{C7})$$

2. The unperturbed $s_j(t) |_{H(t)}$ flips at some time t_J with $t_1 \leq t_J < t_2$. The fraction of spins for which this is the case is proportional to Ω . Thus, for $\Omega \rightarrow 0$ these spins will yield no contribution to u_{11} for finite $t_2 - t_1$. (This is true even if one chooses to keep

$H(t_2) - H(t_1) \equiv \Delta H_0 \neq 0$ fixed as $\Omega \rightarrow 0$. One finds that the resulting contribution to u_{11} involves terms of the form $\exp[-k\Gamma_0\Delta H/\Omega]$ which clearly vanish as $\Omega \rightarrow 0$.)

3. The unperturbed spin $s_j(t)|_{H(t)}$ does not flip at any time between t_1 and t_2 , but the perturbed spin $s(t)|_{H(t)+J\epsilon\theta(t-t_1)}$ does flip at time t_J with $t_1 \leq t_J < t_2$. For fixed, finite $t_2 - t_1$ we can again expand the contribution Δs to u_{11} in terms of Ω . In the adiabatic limit at fixed, finite $t_2 - t_1$ only the lowest order term survives, which is independent of Ω . It is calculated at constant $\eta^0(t_2) = \eta^0(t_1)$ and $H(t_2) = H(t_1) \equiv H$, as done in the following paragraph:

The time t_J with $t_1 \leq t_J < t_2$ at which a spin moves from the lower to the upper well is given by

$$s(t_J)|_{H+J\epsilon\theta(t_J-t_1)} = 0. \quad (\text{C8})$$

Before the perturbation is switched on, the static solution for the spin in the lower potential well is

$$s_i(t_1) = J\eta^0/k + H/k + f_i/k - 1. \quad (\text{C9})$$

As soon as the perturbation is switched on, the spin starts relaxing into its new equilibrium position according to eq. (C7). Its value will remain negative until time t_J , when it will flip to a positive value in the upper potential well. Thus (using eq. (C9) and eq. (C7))

$$0 = s_i(t_J) = (1 - \exp(-k(t_J - t_1)))J\epsilon/k + (J\eta^0/k + H/k + f_i/k - 1), \quad (\text{C10})$$

or

$$t_J = t_1 - 1/k\Gamma_0 \ln(1 + (J\eta^0/k + H/k + f_i/k - 1)k/J\epsilon). \quad (\text{C11})$$

The shift in $s_J(t)$ at time $t_2 > t_J$ will therefore not only consist of a contribution due to simple relaxation as given by eq. (C7) but also a contribution due to the spin flip. It is proportional to the distance of the equilibrium point of the upper well to the equilibrium point of the lower well, which is at all times two in our model. Solving eq. (C2) with $\text{sgn}(s_i(t < t_J)) = -1$ and $\text{sgn}(s_i(t > t_J)) = +1$, we find in this case

$$\begin{aligned}
s_i^{flip}(t_2)|_{H+J\epsilon(t_2)} - s_i(t_2)|_H &= J\epsilon/k(1 - \exp(-k\Gamma_0(t_2 - t_1)))\Theta(t_2 - t_1) \\
&+ 2(1 - \exp(-k\Gamma_0(t_2 - t_J)))\Theta(t_2 - t_J)\Theta(t_J - t_1). \tag{C12}
\end{aligned}$$

The first of the two terms on the right hand side of the equation also appears in eq. (C7). We can therefore separate the contribution solely due to the spin flip from the relaxational part:

From eq. (C7) and eq. (C12) one obtains

$$\Delta s \equiv s_i^{flip}(t_2) - s_i^{noflip}(t_2) = 2(1 - \exp(-k\Gamma_0(t_2 - t_J))). \tag{C13}$$

The disorder averaged shift in the local magnetization is then

$$\begin{aligned}
\langle s(t_2)|_{H+J\epsilon(t)} - s(t_2)|_H \rangle_f &\sim (s_i^{noflip}(t_2)|_{H+\epsilon(t)} - s_i(t_2)|_H) \\
&+ \int_{t_1}^{t_2} dt_J dN(t_J)/dt_J 2(1 - \exp(-k\Gamma_0(t_2 - t_J)))\Theta(t_2 - t_J). \tag{C14}
\end{aligned}$$

$dN(t_J)$ is the number of spins that are going to flip in the time interval $[t_J, t_J + dt_J]$ with $t_1 < t_J < t_2$. From eq. (C10) we find a relation between the random field f_i and t_J :

$$f_i = -J\eta^0 - H + k - J\epsilon(1 - \exp(-k\Gamma_0(t_J - t_1))). \tag{C15}$$

Therefore

$$\begin{aligned}
dN(t_J) &= \tag{C16} \\
dt_J |df_i/dt_J| \rho(f_i = -J\eta^0 - H + k - J\epsilon(1 - \exp(-k\Gamma_0(t_J - t_1)))) \\
&= dt_J (J\epsilon k\Gamma_0 \exp(-k\Gamma_0(t_J - t_1))) \\
&\quad \rho(f_i = -J\eta^0 - H + k - J\epsilon(1 - \exp(-k\Gamma_0(t_J - t_1)))) \\
&= dt_J (J\epsilon k\Gamma_0 \exp(-k\Gamma_0(t_J - t_1)) \rho(f_i = -J\eta^0 - H + k)) + O(\epsilon^2).
\end{aligned}$$

Eq. (C7), eq. (C12), and eq. (C14) then yield for the average shift (for $t_2 > t_1$) divided by ϵ , in the limit of small ϵ

$$\lim_{\epsilon \rightarrow 0} [\langle s_i(t_2)|_{H+J\epsilon(t_2)} - s_i(t_2)|_H \rangle] / \epsilon \tag{C17}$$

$$\begin{aligned}
&= [J/k + 2J\rho(f_i = -J\eta^0 - H + k) + \\
&\quad \exp(-k\Gamma_0(t_2 - t_1))(-J/k - 2J(1 + k\Gamma_0(t_2 - t_1))) \\
&\quad \rho(f_i = -J\eta^0 - H + k)]\Theta(t_2 - t_1),
\end{aligned}$$

which correctly goes to zero for $t_2 \rightarrow t_1$. (The terms proportional to ρ are due to spin flips and the others stem from simple relaxation.) For $(t_2 - t_1) \rightarrow \infty$ it approaches the static value $J/k + 2J\rho(f_i = J\eta^0 - H + k)$, which is the static response to a small perturbation. The $u_{1,1}(t_1, t_2)$ vertex is given by the negative time derivative of eq. (C17) with respect to t_1 , i.e.

$$\begin{aligned}
u_{1,1}(t_1, t_2) &= (J/k + 2J\rho(f_i = -J\eta^0 - H + k))\delta(t_2 - t_1) \tag{C18} \\
&+ \delta(t_2 - t_1)[\exp(-k\Gamma_0(t_2 - t_1))(-J/k - 2J(1 + k\Gamma_0(t_2 - t_1))) \\
&\quad \rho(f_i = -J\eta^0 - H + k)] \\
&+ \Theta(t_2 - t_1)\partial_{t_1}[\exp(-k\Gamma_0(t_2 - t_1))(-J/k - 2J(1 + k\Gamma_0(t_2 - t_1))) \\
&\quad \rho(f_i = -J\eta^0 - H + k)].
\end{aligned}$$

In the corresponding term in the action this is multiplied by $\eta(t_2)$ and $\hat{\eta}(t_1)$ and integrated over dt_1 and dt_2 . The terms multiplied by $\delta(t_2 - t_1)$ in eq. (C18) cancel exactly, so that there is only left the term multiplied by $\theta(t_2 - t_1)$. We perform an integration by parts in t_1 and obtain two terms: The boundary term which has a purely static integrand and leaves only one time integral, and a time dependent part with two time integrals.

The static term contributing to the action is then

$$- \int_{-\infty}^{+\infty} dt_1 \hat{\eta}(t_1) \eta(t_1) (-J/k - 2J\rho(f_i = -J\eta^0 - H + k)). \tag{C19}$$

The dynamical part can be written as

$$\begin{aligned}
&\int_{-\infty}^{+\infty} dt_2 \int_{-\infty}^{+\infty} dt_1 \Theta(t_2 - t_1) \hat{\eta}(t_2) (\partial_{t_1} \eta(t_1)) \exp(-k\Gamma_0(t_2 - t_1)) \\
&(-J/k - 2J(1 + k\Gamma_0(t_2 - t_1))) \rho(-J\eta^0 - H + k). \tag{C20}
\end{aligned}$$

In the low frequency approximation this becomes

$$\begin{aligned}
& \int_{-\infty}^{\infty} dt_1 \hat{\eta}(t_1) \partial_{t_1} \eta(t_1) [-J/k - 4J\rho(-J\eta^0 - H + k)] / (\Gamma_0 k) \\
& = - \int_{-\infty}^{\infty} dt_1 \hat{\eta}(t_1) \partial_{t_1} \eta(t_1) a / \Gamma_0,
\end{aligned} \tag{C21}$$

with

$$a = [J/k + 4J\rho(-J\eta^0 - H + k)] / k, \tag{C22}$$

as can be seen using that

$$e^{-k\Gamma_0(t_2-t_1)} \Theta(t_2 - t_1) = \frac{1}{2\pi} \int d\omega e^{i\omega(t_2-t_1)} / (k\Gamma_0 + i\omega), \tag{C23}$$

and

$$k\Gamma_0(t_2 - t_1) e^{-k\Gamma_0(t_2-t_1)} \Theta(t_2 - t_1) = \frac{1}{2\pi} \int d\omega e^{i\omega(t_2-t_1)} \frac{k\Gamma_0}{(k\Gamma_0 + i\omega)^2}. \tag{C24}$$

Eq. (C21) contributes to the “ $i\omega$ ” term in the propagator expressed in frequency space.

We have performed the above calculation for the case $H(t_1) = H(t_2)$. If instead one keeps $H(t_2) - H(t_1) = \Delta H \neq 0$ fixed as $\Omega \rightarrow 0$ (*i.e.* $t_2 - t_1 \rightarrow \infty$), one obtains

$$\lim_{\epsilon \rightarrow 0} \langle s_i(t_2) |_{H+\epsilon(t_2)} - s_i(t_2) |_H \rangle_f / \epsilon = J/k + 2J\rho(-J\eta^0(t_2) - H + k) \tag{C25}$$

up to dynamical corrections of the form $(\exp(-\Delta H \Gamma_0 / \Omega))$, which are negligible as $\Omega \rightarrow 0$. Consequently, the derivative with respect to $(-t_1)$ yields zero in this limit. Therefore there is no contribution to the action from these cases and the result converges to the expressions in eq. (C19) and eq. (C20) as $\Omega \rightarrow 0$.

c. The coefficients $u_{1,2}$, $u_{1,3}$ and $u_{2,0}$

The coefficients $u_{1,2}$ and $u_{1,3}$ at field H are calculated similarly. One obtains for the terms in the action corresponding to $u_{1,2}$ in the adiabatic limit:

$$\begin{aligned}
& \int d^d x \int_{-\infty}^{+\infty} dt \hat{\eta}(x, t) \left(w[\eta(x, t)]^2 + \int_{-\infty}^t dt_2 a(t, t_2, t_2) \eta(x, t_2) \partial_{t_2} \eta(x, t_2) \right. \\
& \quad \left. + \int_{-\infty}^t dt_2 \int_{-\infty}^{t_2} dt_1 a(t, t_1, t_2) \partial_{t_2} \eta(x, t_2) \partial_{t_1} \eta(x, t_1) \right).
\end{aligned} \tag{C26}$$

Here, $w = -2J^2\rho'(f_i = -J\eta^0 - H + k)$, and $a(t, t_1, t_2)$ is a transient function due to the relaxational dynamics of the system. It consists of terms proportional to $\exp\{-\Gamma_0(t - t_1)\}$ or $\exp\{-\Gamma_0(t - t_2)\}$. The transient terms proportional to $a(t, t_1, t_2)$ turn out to be irrelevant for the critical behavior observed on long length scales.

The static and the transient terms in the action contributed by $u_{1,3}$, are calculated similarly. Again, only the static part turns out to be relevant for the calculation of the exponents below the upper critical dimension. It is given by

$$\int d^d x \int_{-\infty}^{+\infty} dt u \hat{\eta}(x, t) [\eta(x, t)]^3, \quad (\text{C27})$$

with $u = 2J^3\rho''(f_i = -J\eta^0 - H + k)$.

Finally, the vertex $u_{2,0}(t_1, t_2) = \langle s_i(t_1)s_i(t_2) \rangle$ is calculated similarly. It is a local correlation function instead of a local response function. Therefore the times t_1 and t_2 can be infinitely far apart, i.e. even for $H(t_1) \neq H(t_2)$ the vertex $u_{2,0}$ is still nonzero. One obtains:

$$\begin{aligned} u_{2,0}(t_1, t_2) &= R^2/k^2 + \left(\int_{-\infty}^{-H(t_2)-\eta^0(t_2)+k} \rho(h)dh \right) \\ &\left(4 - 4 \int_{-H(t_2)-\eta^0(t_2)+k}^{-H(t_1)-\eta^0(t_1)+k} \rho(h)dh \right) \\ &- 4 \left(\int_{-\infty}^{-H(t_2)-\eta^0(t_2)+k} \rho(h)dh \right)^2 - 4 \left(\int_{-\infty}^{-H(t_2)-\eta^0(t_2)+k} (h/k)\rho(h)dh \right) \\ &- 2 \left(\int_{-H(t_2)-\eta^0(t_2)+k}^{-H(t_1)-\eta^0(t_1)+k} (h/k)\rho(h)dh \right), \end{aligned} \quad (\text{C28})$$

which is positive (or zero) for any normalized distribution $\rho(f)$.

2. Feynman Rules

In the following discussion we denote with u_{mn} the static part of $u_{mn}(t_1 \dots t_{m+n})$, i.e. the part which, (for $n \neq 0$, after taking the time derivative and integrating by parts) is not multiplied by any time derivative of the fields. This is usually the only part of the vertex which is not irrelevant under coarse graining (except for the propagator term, which also has a contribution proportional to $i\omega$). We formulate the Feynman rules in general terms,

although for our discussion only $u_{1,1} = \chi^{-1}/J + 1$, $u_{1,2} = w$, $u_{1,3} = u$ and $u_{2,0}$ come into play.

We introduce the following notation for the Feynman diagrams, which we will use in the perturbation expansion : A vertex $u_{1,n}$ is a dot with m outgoing arrows (one for each $\hat{\eta}$ operator) and n incoming arrows (one for each η operator.) Figure 17 (a) shows the graph for u as an example. The propagator can only connect $\hat{\eta}(t)$ and $\eta(t')$ operators. It is important to remember that causality must be obeyed, i.e. $t' > t$. Figure 17 (b) shows an example of a diagram which violates causality.

The vertex $u_{2,0}$ is denoted as shown in figure 17 (c). The black ellipse connects the two parts of the vertex that are taken at different times.

The symmetry factors for each diagram are obtained in the usual way [105,77] by drawing all topologically distinct graphs and counting their multiplicities. One must not forget to include the factors $1/(m!n!)$ that appear in the expansion (see eq. (60)).

In each diagram, momentum conservation requires that vertices should be connected by loops rather than a single, dead end propagator line. Figure 17 (d) shows an example of a diagram that is zero [78].

Each internal loop contributes an integral over the internal momentum-shell [53] (see also below)

$$\int_{\Lambda/b}^{\Lambda} d^d q / (q^2 - \chi^{-1}/J), \quad (\text{C29})$$

where Λ is the cutoff and $b > 1$.

Integration over time is already performed in eq. (C29). (In the low frequency approximation the propagator can be approximately taken to be $\delta(t - t')$, when we integrate out modes in the infinitesimal momentum shell $\Lambda/b < q < \Lambda$ [19].)

3. Implementation of the history

As we have mentioned in section VIC it turns out that on long length scales different magnetic fields decouple and the static critical exponents can be extracted from a renor-

malization group analysis performed at a single, fixed value of the external magnetic field H_0 due to a separation of time scales. In the following paragraph we will show that this statement is self-consistent using an argument by Narayan and Middleton in the context of the CDW depinning transition [20].

An expansion around mean-field theory in the way performed here corresponds to *first* increasing the magnetic field H within an infinite ranged model and *then* tuning the elastic coupling to a short ranged form, while the actual physical behavior corresponds to *first* tuning the elastic coupling to a short ranged form and *then* increasing the force within the short ranged model. The concern is that in the presence of many metastable states the critical behavior of the two approaches might not be the same. For example, spins might tend to flip backwards upon reduction of the interaction range in the expansion around mean-field theory. Although there will of course always be *some* spins for which this is the case, no such effects are expected on long length scales since the susceptibility is actually *more* divergent near the critical point for $d < 6$ than in mean-field theory:

$$(dm/dh)_{h=0} \sim r^{-\gamma} \tag{C30}$$

and

$$(dm/dh)_{r=0} \sim h^{1/\delta-1} \tag{C31}$$

with

$$\gamma(\text{in } d < 6) > \gamma(\text{in mean field theory}) \tag{C32}$$

and

$$(1 - 1/\delta)(\text{in } d < 6) > (1 - 1/\delta)(\text{in mean field theory}) \tag{C33}$$

as we learn from numerics and analytics. This suggests that on long length scales spins tend to flip *forward* rather than backward upon reduction of the coupling range. One would therefore expect the expansion around mean-field theory performed here to correctly describe the critical behavior.

Reassured by this self-consistency argument we now briefly discuss for separated time scales that the decoupling of the different magnetic fields is consistent also within the RG description. As discussed in appendix C 1 the response functions $u_{1,n}(t_1, \dots, t_{n+1})$ with fixed $H(t_1) \neq H(t_j)$ with $j \neq 1$ tend to zero in the adiabatic limit. However, the original action S of eq. (60) also contains terms of the form $u_{2,0}(H_1, H_2)$ which do couple different fields even as $\Omega \rightarrow 0$. These “multi-field” vertices however do not contribute to the renormalization of the vertices evaluated at a *single* value of the external magnetic field, because the propagator does not couple different field values. It turns out that the multi-field vertices are also irrelevant on long length scales: setting up the RG in section VII B we have treated $u_{2,0}(H_0, H_0)$ as a marginal variable. In fact, we have been choosing the rescaling $\gamma_{\hat{\phi}}$ of the fields $\hat{\eta}$ in $\hat{\eta}(x, t) = b^{-d/2-z-\gamma_{\hat{\phi}}/2}\hat{\eta}'(x, t)$ such that $u_{2,0}(H_0, H_0)$ remains marginal to all orders in perturbation theory. Similarly, the rescaling γ_{ϕ} of the fields η in $\eta(x, t) = b^{-d/2+2-\gamma_{\phi}/2}\eta'(x, t)$ is chosen such that the coefficient of the q^2 term remains marginal to all orders also. (These choices are made so that the rescaling of the response and the cluster correlation function under coarse graining immediately gives their respective power law dependence on momentum (see section VII A)). To decide what this implies for $u_{2,0}(H_1, H_2)$ at two *different* magnetic fields $H_1 \neq H_2$, we need consider two loop order corrections for $u_{2,0}(H_1, H_2)$. In figure 18 we have indicated the magnetic fields corresponding to the times at which the vertices are evaluated, taking into account that the propagators do not couple different fields. One finds the following recursion relation:

$$\begin{aligned} \frac{1}{2}u'_{2,0}(H_1, H_2) &= \frac{1}{2}u_{2,0}(H_1, H_2) & (C34) \\ &+ \frac{1}{2}u_{2,0}(H_1, H_2)(u_{2,0}(H_1, H_2)^2 - u_{2,0}(H_1)u_{2,0}(H_2)) \\ &+ \frac{1}{54}K_6^2(4\pi)^6\epsilon^2/(u_{2,0}(H_1)u_{2,0}(H_2))\ln b, \end{aligned}$$

with $u_{2,0}(H_1) \equiv u_{2,0}(H_1, H_1)$. The term that is subtracted stems from the second order correction to the rescaling of the fields $\hat{\eta}$ (from terms as depicted in figure 18 but with $H_1 = H_2$).

From eq. (C28) it follows that $u_{2,0}(H_1, H_2) \geq 0$. Furthermore, using the same equa-

tion one finds after some algebra that (for the special history considered here and for any distribution ρ of random fields, using the Cauchy-Schwartz inequality)

$$u_{2,0}(H_1, H_2)^2 - u_{2,0}(H_1)u_{2,0}(H_2) \leq 0. \quad (\text{C35})$$

In fact, for $H_1 \neq H_2$ (which excludes also H_1 and H_2 being both equal to $\pm\infty$, with the same sign), and $R \neq 0$ the expression in eq. (C35) is actually negative. This implies that for $R \neq 0$ the part in the quadratic action, which was coupling different magnetic fields, will be irrelevant at dimensions $d < 6$ under coarse graining. Its fixed point value is zero. In contrast, $u_{2,0}(H)$ stays constant under coarse graining.

What does this mean for the coarse grained action? If we leave out all the terms in the action that are zero or irrelevant at $d = 6 - \epsilon$, the different magnetic fields are completely decoupled, and the critical exponents (for $R \geq R_c$ at least) can be extracted from coarse graining the following action at fixed magnetic field H_0 :

$$\begin{aligned} \tilde{S}_{H_0} = & - \int d^d q \int dt \hat{\eta}(-q, t) (-1/\Gamma_0 \partial_t + q^2 - \chi^{-1}(H_0)/J) \eta(q, t) \\ & + 1/6 \int d^d x \int dt \hat{\eta}(x, t) (\eta(x, t))^3 u(H_0) \\ & + 1/2 \int d^d x \int dt_1 \int dt_2 u_{2,0}(H_0, H_0) \hat{\eta}(x, t_1) \hat{\eta}(x, t_2). \end{aligned} \quad (\text{C36})$$

(The index and argument H_0 serve as a reminder that all coefficients in this action are evaluated at the same magnetic field H_0 . The time integrals extend from $-\infty$ to ∞ . The constant coefficients of the ∂_t -term and the q^2 -term have been rescaled to 1 (see section VII A).

APPENDIX D: BOREL RESUMMATION

It is known [64,67] that the ϵ -expansion yields only asymptotic series for the critical exponents as functions of dimension. It is important to note that asymptotic series in general do not define a *unique* underlying function. In the following we will give a definition of an asymptotic series, discuss several examples and give the special conditions under

which there does exist a unique underlying function. So far it has not been possible to show that the ϵ -expansion would meet these conditions; we therefore cannot assume that it uniquely determines the critical exponents as functions of dimension. Applying the methods of reference [106] to our problem we Borel resum the perturbation series for our critical exponents to $O(\epsilon^5)$. A comparison of the result to the numerical values of the exponents in 3, 4, and 5 dimensions is given in the main text.

1. Definition of an asymptotic series

Let the variable z range over a sector S in the complex plane with the origin as a limit point (which may or may not belong to S):

$$\text{Arg}(z) \leq \alpha/2, |z| \leq |z_0|. \quad (\text{D1})$$

A power series $\sum_{k=0}^{\infty} f_k z^k$ is said to be asymptotic to the numerical function $f(z)$ defined on S as $z \rightarrow 0$

$$f(z) \sim \sum_{k=0}^{\infty} f_k z^k \quad (\text{D2})$$

if the approximation afforded by the first few terms of the series is better the closer z is to its limiting value, which is zero in this case [107]. Formally:

$$|f(z) - \sum_{k=0}^N f_k z^k| \ll |z|^N \quad (\text{D3})$$

as $z \rightarrow 0$ for every N (*i.e.* for any given $\epsilon > 0$ there exists a neighborhood U_ϵ of the origin so that

$$|f(z) - \sum_{k=0}^N f_k z^k| \leq \epsilon |z|^N \quad (\text{D4})$$

for all z common to U_ϵ and S).

This is equivalent to the statement that the remainder of the sum after summing the first N terms is of the order of the first neglected term and goes to zero rapidly as $z \rightarrow 0$:

$$\left(f(z) - \sum_{k=0}^N f_k z^k\right) \sim f_M z^M \quad (\text{D5})$$

for every N , where f_M is the first nonzero coefficient after f_N . As shown in [107] this implies that there exists a constant $C(N+1)$ (*i.e.* a number independent of z) and a neighborhood U of the origin such that

$$\left| \left(f(z) - \sum_{k=0}^N f_k z^k\right) \right| \leq |C(N+1)z^{(N+1)}| \quad (\text{D6})$$

for all z common to U and S .

Often the terms in the series at first decrease rapidly (the faster, the closer z approaches zero) but higher order terms start increasing again. If the series is truncated at the minimum term, one obtains usually the best possible truncated estimate for $f(z)$ with a finite error $E(z)$. If the coefficients $C(k)$ are of the form

$$C(k) \sim C(k!)^\beta A^{(-k)} \quad (\text{D7})$$

with $A > 0$, $\beta > 0$, and $C > 0$ real constants, the error $E(z)$ can be estimated explicitly [67] to

$$E(z) = \min_N C(k)|z|^k \sim \exp[-\beta(A/|z|)^{(1/\beta)}]. \quad (\text{D8})$$

which decreases rapidly as $|z| \rightarrow 0$. It determines a limit to the accuracy beyond which it is impossible to penetrate by straightforward summation of a finite number of terms of the series.

a. Non-uniqueness of $f(z)$

One sees that an asymptotic series does not in general define a unique analytic function $f(z)$ over S . Any other function $g(z)$ which is analytic in S and smaller than $E(z)$ in the whole sector can be added to $f(z)$ such that in S the series $\sum_{k=0}^{\infty} f_k z^k$ is asymptotic also to $g(z) + f(z)$. If however the sector is big enough, *i.e.* if $\alpha \geq \pi\beta$ then according to a classical theorem (Phragmen-Lindelöf) there exists no nonvanishing function over S that is

analytic in S and bounded by $E(z)$ in the whole sector. In that case the underlying function is uniquely determined by the series [67].

b. Examples

Let S_Δ be the sector $0 < |z| < \infty$, $\phi \equiv |\text{Arg}(z)| < \pi/2 - \Delta$ with $\Delta > 0$.

1. The function $\exp(-1/z)$ is asymptotic to $\sum_{n=0}^{\infty} 0 \cdot z^n = 0$ over S_Δ :

$$|\exp(-1/z) - 0| = \exp(-\cos(\phi)/|z|) < \exp(-\cos(\pi/2 - \Delta)/|z|) \ll |z|^N \quad (\text{D9})$$

for any N as $|z| \rightarrow 0$.

2. Similarly one can show that over S_Δ the series

$$\sum_{k=0}^{\infty} (-1)^{(k-1)} z^k \quad (\text{D10})$$

is asymptotic to the functions $1/(1 + z^{(-1)})$, $(1 + \exp(-1/z))/(1 + z^{(-1)})$ and $1/(1 + \exp(-\sqrt{(1/z)})) + z^{(-1)}$ as $z \rightarrow 0$ [107]. (A similar nonuniqueness is expected for the underlying functions of the ϵ -expansion.)

3. The Stirling series is one of the oldest and most venerable of asymptotic series. It expresses the asymptotic behavior of the factorial function $n!$ for large values of n

$$\Gamma(n) = (n-1)! \sim \left(\frac{2\pi}{n}\right)^{\frac{1}{2}} \left(\frac{n}{e}\right)^n \left(1 + \frac{A_1}{n} + \frac{A_2}{n^2} + \dots\right) \quad (\text{D11})$$

with $A_1 = 1/12$, $A_2 = 1/288$, etc. It becomes the full asymptotic expansion of the Gamma function $\Gamma(z)$ for complex argument z :

$$|\Gamma(z) - \left(\frac{2\pi}{n}\right)^{\frac{1}{2}} \left(\frac{z}{e}\right)^z \left(1 + \sum_{j=1}^N A_j z^{-j}\right)| \ll \left|\left(\frac{z}{e}\right)^z z^{-\frac{1}{2}-N}\right| \quad (\text{D12})$$

for $z \rightarrow \infty$ and $|\text{Arg}(z)| < \pi$ [90].

2. Borel resummation

The Borel summation is a technique for expressing an asymptotic series $\sum_{k=0}^{\infty} f_k z^k$ as the limit of a convergent integral. For an introduction to this technique see reference [90,107].

The idea is to modify the coefficients of the series such that for sufficiently small z it converges to a function $B(z)$, which can be calculated. In the simplest case

$$B(z) \equiv \sum_{k=0}^{\infty} f_k/k!z^k \quad (\text{D13})$$

would be appropriate. Suppose that also

$$f(x) \equiv \int_0^{\infty} \exp(-t)B(xt)dt \quad (\text{D14})$$

exists. Then, by expanding the integral $\int_0^{\infty} \exp(-t/x)B(t)dt/x$ for small x and integrating term by term, one finds [90] that $f(x) = \sum_{k=0}^{\infty} f_k x^k$ as $x \rightarrow 0^+$.

a. Example

The series $\sum f_k z^k = \sum_{n=0}^{\infty} n!(-x)^n$ diverges, but $B(x) \equiv \sum_{n=0}^{\infty} (-x)^n$ converges for $|x| \leq 1$ to $1/(1+x)$. Thus the Borel sum of $\sum_{n=0}^{\infty} n!(-x)^n$ is $f(x) = \int_0^{\infty} \exp(-t)/(1+xt)dt$. For z in the complex plane, $f(z)$ is asymptotic to $\sum (-z)^n n!$ over the sector S : $0 < |z| < \infty$, $|\text{Arg}(z)| \leq \pi - \epsilon$, $\epsilon > 0$. Since $|f_n| \sim n!$ we have $\beta = 1$ from eq. (D7), and since $\alpha > \pi$ for small enough ϵ , the uniqueness theorem of section D 1 a implies that $f(z)$ is the unique underlying analytic function of the series over S .

3. Borel resumming the ϵ -expansion

It is known [67], that the ϵ -expansion series is an asymptotic series. It has a zero radius of convergence. Lipatov, Brézin, LeGouillou, and Zinn-Justin have shown [108], that the coefficients of higher orders of the ϵ expansion $f(\epsilon) = \sum_k (-\epsilon)^k f_k$ (with $\epsilon = 4 - d$) have the asymptotic form $f_k \sim_{k \rightarrow \infty} k! a^k k^b c$. (The factorial growth of the coefficients reflects the zero radius of convergence.) Here, f stands for η or $1/\nu$ (or ω or g_0 , see [106]), and $a = 1/3$, $b = 7/2$ for η , and $a = 1/3$, $b = 9/2$ for $1/\nu$.

Using the newest results for the coefficients to $O(\epsilon^5)$ as given in Kleinert *et al.* [59] and the asymptotic form given above, we resum the coefficients to $O(\epsilon^5)$, using the method

discussed in reference [106,109] and reference [110]. The method is based on a modified Borel transformation:

$$f(\epsilon) = \int_0^\infty dx/(\epsilon a) \exp(-x/(\epsilon a))(x/(\epsilon a))^{(b+3/2)} B(x). \quad (\text{D15})$$

One obtains $B(x) = \sum_k (-x)^k B_k$, with $B_k = f_k/(a^k \Gamma(k + b + 5/2)) \sim_{k \rightarrow \infty} c/k^{3/2}$.

$B(x)$ is given by its Taylor series only for $|x| < 1$. It can be continued analytically beyond the unity convergence circle in the complex plane, using the conformal mapping [111] $x \rightarrow w$ with $w(x) = [(1+x)^{1/2} - 1]/[(1+x)^{1/2} + 1]$, or $x = 4w/(1-w)^2$. The integration interval $[0, \infty)$ then goes over into the interval $[0, 1]$ and the cut $(-\infty, -1]$ goes over in the boundary of the unit disk. The expansion of $B(x(w))$ in terms of w converges to $B(x)$ in the entire region of integration $w \in [0, 1]$. The coefficient of w^N is determined on the basis of the coefficients f_k for $k \leq N$ of the initial ϵ expansion. Neglecting the terms of $O(w^m)$, with $m > N$, one obtains an approximation $f_N(\epsilon)$ which takes into account the $O(\epsilon^N)$ corrections to f .

Since we are working with truncated rather than infinite series there is an arbitrariness in the reexpansion of $B(x)$ in terms of w [110,106]. Rather than expanding $B(x(w))$ directly, Vladimirov *et al.* actually expand $((1-w)^2)^\lambda B(x(w))/4 \equiv B^\lambda(w)$ in terms of w , so that (since $x = 4w/(1-w)^2$) the result for $B(x(w))$ is given by $B(x) \rightarrow x^\lambda B^\lambda(w) = (x/w)^\lambda \sum_k^N B_\lambda^{(k)} w^k$. λ is a parameter that must be chosen correctly, such that $f_N(\epsilon)$ is matched to the asymptotic form $f(\epsilon)$ as $\epsilon \rightarrow \infty$, given by: $f(\epsilon) \sim_{\epsilon \rightarrow \infty} (\epsilon)^\lambda$. Since the asymptotic form of the exponents relative to ϵ is unknown, it is argued in [109] and [110] that λ should be fixed from the condition of fastest convergence of f_N , i.e. it should minimize $\Delta_N = |1 - f_N(1)/f_{N-1}(1)|$. We have written a computer program that performs this procedure for the exponents $1/\nu$ and η using the following results for the ϵ -expansion to $O(\epsilon^5)$ from reference [59]:

$$1/\nu = 2 - \epsilon/3 - 0.1173\epsilon^2 + 0.1245\epsilon^3 - 0.307\epsilon^4 + 0.951\epsilon^5 + O(\epsilon^6), \quad (\text{D16})$$

$$\eta = 0.0185185\epsilon^2 + 0.01869\epsilon^3 - 0.00832876\epsilon^4 + 0.02566\epsilon^5 + O(\epsilon^6). \quad (\text{D17})$$

Through the perturbative mapping of our problem to the pure Ising model in two lower dimensions to all orders in ϵ these are also the results for the exponents in our system in $6 - \epsilon$ dimensions. Figure 14 shows the comparison between the Borel resummed exponents $1/\nu$, η , and $\beta\delta = \frac{\nu}{2}(d - 2\eta + \bar{\eta})$, and the corresponding numerical results at integer dimensions. We have used that in perturbation theory $\bar{\eta} = \eta$, as follows from the mapping to the equilibrium random field Ising model [60,62].

The standard Borel resummation has been modified in various ways specifically to resum the $4 - \epsilon$ expansion for the exponents of the pure Ising model. Le Guillou and Zinn-Justin [110] have developed a resummation prescription that takes into account that the critical exponents have a singularity at the lower critical dimension $d = 1$ (*i.e.* $\epsilon = 3$). In a more recent calculation [110], they treated the dimension of the singularity as a variational parameter to improve the apparent convergence of the expansion. They also imposed the exactly known values of the exponents in two dimensions. Their results agree (partly by design) very well with the numerical exponents of the pure equilibrium Ising model in two and three dimensions. Below two dimensions the apparent errors of their results are rapidly increasing.²¹

In our problem the lower critical dimension is probably 2 rather than 3, *i.e.* $\epsilon = 4$ rather than $\epsilon = 3$. In our Borel-resummation of the $6 - \epsilon$ expansion results for our critical exponents we have made no assumptions about a singularity for the critical exponents, nor did we impose any other information. Instead, we have applied the conventional Borel-resummation as adapted by Vladimirov *et al.*, which shows good agreement with our numerical data (see figure 14). Our resummation of corrections for ν up to order $O(\epsilon^5)$ has a pole around 2.3 dimensions. (In reality ν is expected to diverge at the lower critical dimension.) The pole did slowly increase with the order to which the resummation was performed. It is not clear

²¹We should note that their work was based on a form for the fifth order term which later turned out to be incorrect [59].

however whether this tendency persists at higher orders.

Figure 19 shows a comparison of our Borel resummation for ν with the results of LeGuillou and Zinn-Justin from 1987 [110]. It is believed that the "straightforward" Borel-resummation according to Vladimirov *et al.* [106,109] and the resummation according to LeGuillou and Zinn-Justin [110] which treats the dimension of the singularity in the exponents as a variational parameter, should both at high enough orders converge to the pure Ising exponents, although this has not been proven. Unfortunately, the curve from LeGuillou and Zinn-Justin [110] shown in figure 19 has been obtained using an epsilon expansion for the critical exponents, which later turned out to be incorrect in the 5th order term [59]. Our own Borel-resummation however, which is also shown in figure 19, is based on the newest, presumably correct result for the fifth order term [59]. We are currently trying to duplicate the variable-pole analysis of LeGuillou and Zinn-Justin with the correct fifth order term.

As we have already mentioned, there is no known reason to assume that the ϵ -expansion is Borel-summable, *i.e.* that the values of the exponents would be uniquely determined as functions of dimension by the Borel summation of their asymptotic ϵ -expansion. At this stage we do not know the size of the section of analyticity for the various Borel sums [110]. Hence we expect the ϵ -expansion to give the correct value of the exponents only asymptotically as $\epsilon \rightarrow 0$, even after Borel resummation. There is no reason to expect that its extrapolation to $\epsilon = 3$ can be used to determine the lower critical dimension, *i.e.* the dimension where ν has a pole, and where the transition disappears or loses its universality (see also section VIII B in the text).

APPENDIX E: INFINITE AVALANCHE LINE

In most of this paper we have focussed on the critical endpoint $(R_c, H_c(R_c))$, in particular as it is approached from $R \geq R_c$. In this appendix we discuss the onset of the infinite avalanche for $R < R_c$. Our ϵ -expansion can be applied to the entire line $H_c(R)$, $R < R_c$ at which the infinite avalanche occurs (with some reservations which we will discuss later). In

mean-field theory the approach to this line is continuous with a power law divergence of the susceptibility $\chi \sim dM/dH$ and precursor avalanches on all scales (see appendix A). From

$$S_H = - \sum_{j,l} \int dt J_{jl}^{-1} J \hat{\eta}_j(t) \eta_l(t) - \sum_j \int dt \hat{\eta}_j(t) [-\partial_t/\Gamma_0 - u_{11}^{stat}] \eta_j(t) \quad (E1)$$

$$+ \sum_j (1/6) \int dt \hat{\eta}_j(t) (\eta_j(t))^3 u + (1/2) \sum_j \int dt_1 \int dt_2 \hat{\eta}_j(t_1) \hat{\eta}_j(t_2) u_{2,0},$$

quoted from in eq. (65), and from the rescaling of the vertices given in eq. (82)

$$u'_{m,n} = b^{[-(m+n)+2]d/2+2n} u_{m,n}. \quad (E2)$$

one sees that on long length scales the effective action is purely quadratic above 8 dimensions. This suggests that there is a *continuous* transition (as H approaches $H_c(R)$) with mean-field critical exponents and a diverging correlation length $\xi(\chi^{-1})$ with the scaling behavior $\xi(\chi^{-1}) = b\xi(b^2\chi^{-1})$, *i.e.* $\xi \sim (\chi^{-1})^{-1/2}$. Since $\chi^{-1} \sim \sqrt{|H - H_c(R)|}$ (see appendix A) it follows that $\xi \sim |H - H_c(R)|^{-\nu_h}$ with $\nu_h = 1/4$ for $d > 8$.²²

For $d = 8 - \tilde{\epsilon}$ ($\tilde{\epsilon} > 0$) the vertex w in the action S_H becomes relevant. In contrast to the critical endpoint where $\chi^{-1} = 0$ and $w = 0$, the infinite avalanche line is characterized by the “bare values ” $\chi^{-1} = 0$ and $w = -2J^2\rho'(-JM(H_c(R)) - H_c(R) + k) \neq 0$. Figure 20 shows the lowest order the correction to vertex w . With the Feynman-rules of appendix C 2 and section VII B 1 the recursion relation to the same order becomes

$$w'/2 = b^{(-d/2+4)} \left\{ w/2 + (u_{2,0}/2)(w/2)^3 8/(4\pi)^4 \int_{\Lambda/b}^{\Lambda} dq 1/(q^2 - \chi^{-1}/J)^4 \right\}. \quad (E3)$$

Performing the integral over the momentum shell $\Lambda/b < q < \Lambda$ and writing $b^{(-d/2+4)} = b^{(\tilde{\epsilon}/2)} = 1 + \tilde{\epsilon}/2 \log b$ we find

²²If the Harris-criterion is not violated through the presence of large rare nonperturbative fluctuations in an infinite system, such as a preexisting interface (for a discussion see appendix G), *i.e.* if $\nu_h \geq 2/d$ is a valid exponent-inequality, then the mean-field critical exponents with $\nu_h = 1/4$ are only correct for $d \geq 8$, which is consistent with our result from perturbation theory.

$$w'/2 = w/2 + (w/2)\left(\tilde{\epsilon}/2 + u_{2,0}(w/2)^2 4/(4\pi)^4 \log b\right). \quad (\text{E4})$$

Since $u_{2,0} > 0$, this equation has only two fixed points w^* with $w' = w$ for $\tilde{\epsilon} > 0$: either $w^* = 0$ or $w^* = \infty$. Any system with bare value $w \neq 0$ will have effectively larger w on longer length scales. The system flows to the strong coupling limit. We interpret this as indication that in perturbation theory the transition is of first-order type below 8 dimensions. Indeed, our numerical simulation suggests an abrupt onset of the infinite avalanche in 2, 3, 4, 5 and 7 dimensions, but smooth in 9 dimensions [45].

As we discuss in appendix G there are some questions as to whether in an infinite system the onset of the infinite avalanche would be abrupt in *any* finite dimension due to large rare preexisting clusters of flipped spins which provide a preexisting interface that might be able to advance *before* the perturbatively calculated critical field $H_c(R)$ is reached. These large rare fluctuations might be nonperturbative contributions which are not taken into account by our ϵ -expansion. The progression of a preexisting interface has been studied previously in the framework of depinning transitions [30,29,28]. Our preliminary numerical simulation results in 9 dimensions do however seem to show a continuous transition at the onset of the infinite avalanche as predicted by the RG calculation [45].

APPENDIX F: DETAILS FOR THE ϵ -EXPANSION OF THE AVALANCHE EXPONENTS

1. The second moment of the avalanche size distribution

In this section we show that the second moment $\langle S^2 \rangle_f$ of the avalanche size distribution $D(S, r, h)$ scales in the adiabatic limit as

$$\langle S^2 \rangle_f \sim \int dt_1 \int dt_\alpha dt_\beta d^d x_\alpha d^d x_\beta \langle \hat{s}^\alpha(t_\alpha, x_\alpha) s^\alpha(t_0, x_\alpha) \hat{s}^\beta(t_\beta, x_0) s^\beta(t_1, x_\beta) \rangle_f. \quad (\text{F1})$$

where α and β specify the corresponding replica that have identical configurations of random fields and are exposed to the same external magnetic field $H(t) = H_0 + \Omega t$, with $\Omega \rightarrow 0$.²³

We start by computing the (not yet random field averaged) expression

$$\begin{aligned} & \int dt_\alpha d^d x_\alpha dt_\beta d^d x_\beta \{ \hat{s}^\alpha(t_\alpha, x_\alpha) s^\alpha(t_0, x_\alpha) \hat{s}^\beta(t_\beta, x_0) s^\beta(t_1, x_\beta) \} \\ & = \int dt_\alpha d^d x_\alpha \{ \hat{s}^\alpha(t_\alpha, x_\alpha) s^\alpha(t_0, x_\alpha) \} \int dt_\beta d^d x_\beta \{ \hat{s}^\beta(t_\beta, x_0) s^\beta(t_1, x_\beta) \} \end{aligned} \quad (\text{F2})$$

where $\{ \}$ stands for the path integral over the product with the δ -function weight in Z that singles out the correct path through the space of possible states for the given configuration of random fields and the given history. In eq. (F2) the two replicas are uncoupled since we have not yet averaged over the random fields. As we have seen in appendix C

$$\begin{aligned} (\Delta S / \Delta H)_\alpha & \equiv \int dt_\alpha d^d x_\alpha \{ \hat{s}^\alpha(t_\alpha, x_\alpha) s^\alpha(t_0, x_\alpha) \} = \\ & \int dt_\alpha d^d x_\alpha \frac{\partial}{\partial t_\alpha} \lim_{\Delta H \rightarrow 0} \\ & \left(s^\alpha(t_0, x_\alpha) |_{H_{x_0}(t_0)=H(t_0)+\Delta H \Theta(t_0-t_\alpha)} - s^\alpha(t_0, x_\alpha) |_{H_{x_0}(t_0)=H(t_0)} \right) / \Delta H \end{aligned} \quad (\text{F3})$$

is the response of replica α to a perturbing pulse of amplitude ΔH applied at field $H(t_\alpha)$ at site x_0 integrated over the entire system.

If no spin flips in response to the perturbation, the total response will be

$$(\Delta S / \Delta H) = \Delta S_{\text{harmonic}} / \Delta H = C_2 \quad (\text{F4})$$

where C_2 is a constant that depends only on the parameters k , J , and the coordination number z of the lattice.

If, on the other hand the perturbation triggers an avalanche of spin flips from the lower to the upper potential well, $\Delta S = S_{\text{flip}} \equiv S_\alpha$ will be of the order of the number of spins participating in the avalanche (see also appendix C 1).²⁴

²³A heuristic justification of this was given in section IX together with an explanation of why replicas are necessary.

²⁴ S_α is not exactly equal to the number of spins flipping in the avalanche. It contains also the

The expression in eq. (F2) is the product of the total response to the same perturbation at site x_0 measured in replica α at time t_0 and in replica β at time t_1 . At finite sweeping rate Ω/k the corresponding values $((\Delta S)_\alpha/\Delta H)$ and $((\Delta S)_\beta/\Delta H)$ do not have to be the same, since the responses are measured at potentially different values of the external magnetic field ($H_0 \equiv H(t_0)$ and $H_1 \equiv H(t_1)$ respectively). (We only consider the adiabatic case, in which the sweeping rate Ω/k is small compared to the relaxation rate $\Gamma_0 k$, so that the magnetic field can be assumed to be constant during the course of an avalanche.²⁵)

Without loss of generality let us assume that $H(t_1) \geq H(t_0)$. First we discuss the case that there is an avalanche S_α triggered by the perturbation of amplitude ΔH in replica α at field H_0 . We further assume that t_1 is much bigger than t_0 , such that $H_1 \geq H_0 + \Delta H$. In this case the response to the pulse in replica β will be substantially different from the response S_α in replica α . The spins that are pushed over the brink by the *perturbation* at field H_0 in replica α , will in replica β be triggered by the increased external magnetic field *before* it reaches the bigger value H_1 at which the response is measured. For Ω/Γ_0 , ΔH , and $H_1 - H_0$ small enough, the response in replica β at field H_1 will then be just the harmonic response

harmonic response that each spin flip causes through the coupling to the neighboring spins. This harmonic response couples back to the original spin and propagates to the next-nearest neighbors with an amplitude damped by the factor J_{ij}/k and so on. Occasionally it may cause an avalanche to continue which would otherwise (in the hard spin model) have come to a halt. However since this is a short-ranged effect, we do not expect it to be of any relevance to the scaling behavior on long length scales. In mean-field theory the harmonic response only amounts to a constant factor relating S_α to the number of spins participating in the avalanche.

²⁵We take the adiabatic limit $\Omega \rightarrow 0$ at finite correlation length ξ , *before* approaching the critical point of diverging avalanche size and time to avoid triggering a new avalanche before the previous one has come to a halt. This is consistent with our computer simulations at finite system sizes where avalanches occur only sequentially.

C_2 or a *different* avalanche. If it is the harmonic response, the expression in eq. (F2) takes the form

$$(\Delta S/\Delta H)_\alpha(\Delta S/\Delta H)_\beta = (S_\alpha/\Delta H)C_2. \quad (\text{F5})$$

Similarly one might imagine scenarios in which there is an avalanche S_β triggered only in replica β , i.e.

$$(\Delta S/\Delta H)_\alpha(\Delta S/\Delta H)_\beta = (S_\beta/\Delta H)C_2, \quad (\text{F6})$$

or where there is no avalanche happening at either field value

$$(\Delta S/\Delta H)_\alpha(\Delta S/\Delta H)_\beta = (C_2)^2. \quad (\text{F7})$$

It is also possible that two *different* avalanches are triggered in the two replicas:

$$(\Delta S/\Delta H)_\alpha(\Delta S/\Delta H)_\beta = (S_\alpha/\Delta H)(S_\beta/\Delta H) \quad (\text{F8})$$

with $S_\alpha \neq S_\beta$.

We are interested however in contributions due to the *same avalanche* response in both replicas

$$(\Delta S/\Delta H)_\alpha(\Delta S/\Delta H)_\beta = (S_\alpha/\Delta H)(S_\beta/\Delta H) \quad (\text{F9})$$

with $S_\alpha = S_\beta$. As we have seen, a necessary condition is that $H_0 - \Delta H \leq H_1 \leq H_0 + \Delta H$. We denote with $P_{flip} = c_0 \Delta H + o((\Delta H)^2)$ (with c_0 a constant in the critical regime) the fraction of all possible configurations of random fields in which a local perturbation of amplitude ΔH at field H , applied at site x_0 , causes at least one spin to flip. For Ω and ΔH small enough the fraction of all possible configurations of random fields in which the local perturbation will lead to the same initial spin flip triggering the same avalanche S in replica α and replica β , is to leading order in ΔH proportional to the size of the overlap P_{flip}^{both} of the two intervals $[H_0, H_0 + \Delta H]$ and $[H_1, H_1 + \Delta H]$, multiplied by P_{flip} , with

$$P_{flip}^{both} = (1 - \Theta(|H_1 - H_0| - \Delta H))(\Delta H - |H_1 - H_0|)/\Delta H \quad (\text{F10})$$

(see figure 21). We can now compute the random-field average of the expression in eq. (F2), denoted by $\langle \rangle_f$ to leading order in ΔH

$$\begin{aligned} \left\langle \frac{\Delta S}{\Delta H_\alpha} \frac{\Delta S}{\Delta H_\beta} \right\rangle_f &= \bar{C}_1 \frac{\langle S^2 \rangle_f}{\Delta H^2} P_{flip}^{both} P_{flip} + \bar{C}_2 \frac{\langle S \rangle_f}{\Delta H} (1 - P_{flip}^{both}) P_{flip} \\ &+ (C_2)^2 + \langle S_\alpha S_\beta \rangle / (\Delta H)^2 P_{flip}^2 (1 - P_{flip}^{both}), \end{aligned} \quad (\text{F11})$$

where $\langle S^2 \rangle_f$ is the mean square avalanche size, and $\langle S \rangle_f$ is the mean avalanche size, and \bar{C}_1 and \bar{C}_2 are constants in the critical regime. The last term accounts for cases in which two different avalanches $S_\alpha \neq S_\beta$ are triggered in the two replicas.

The last three terms in eq. (F11) approach a constant as $\Delta H \rightarrow 0$, since $P_{flip} \sim \Delta H$. We will now analyze the first term, which is proportional to $\langle S^2 \rangle$ in more detail. The function multiplying $\langle S^2 \rangle_f$ is sharply peaked around $H_0 = H_1$ (see figure 21). Since $P_{flip} \sim \Delta H$ it is proportional to $P_{flip}^{both} / \Delta H$. From eq. (F10) we have

$$\int_{H_0 - \Delta H}^{H_0 + \Delta H} dH_1 P_{flip}^{both} / \Delta H = 1 \quad (\text{F12})$$

independent of ΔH . The same integral applied to the other terms in eq. (F11) yields contributions of order $O(\Delta H)$ which are negligible compared to the first term as ΔH is chosen small. With $H_1 = H_0 + \Omega t$ we can express the integral in terms of time

$$\int_{-\Delta H/\Omega}^{\Delta H/\Omega} \Omega dt_1 P_{flip}^{both} / \Delta H = 1. \quad (\text{F13})$$

We then obtain

$$\lim_{\Delta H \rightarrow 0} \lim_{\Omega \rightarrow 0} \int_{-\Delta H/\Omega}^{\Delta H/\Omega} \Omega dt_1 \left\langle \frac{\Delta S}{\Delta H_\alpha} \frac{\Delta S}{\Delta H_\beta} \right\rangle_f = \bar{C}_1 \langle S^2 \rangle_f. \quad (\text{F14})$$

With eq. (F3) this leads to the scaling relation

$$\langle S^2 \rangle_f \sim \int dt_1 \int dt_\alpha dt_\beta d^d x_\alpha d^d x_\beta \langle \hat{s}^\alpha(t_\alpha, x_\alpha) s^\alpha(t_0, x_\alpha) \hat{s}^\beta(t_\beta, x_\beta) s^\beta(t_1, x_\beta) \rangle_f. \quad (\text{F15})$$

which was to be shown. In this notation we have suppressed the factor Ω and the various limits for clarity. The integrals over time extend from $-\infty$ to $+\infty$ with an infinitesimal associated change in magnetic field.

2. Feynman rules for two replicas

We study the behavior of $S^{\alpha\beta}$ of eq. (161) under coarse graining analogously to the calculation done before for just one replica, with the difference that instead of two, there are now four fields to be considered (two for each replica).²⁶ In the following section we briefly describe the associated Feynman rules. This section may be skipped by the reader uninterested in the details, since it turns out that there are no loop corrections to $O(\epsilon)$ to $\langle S^2 \rangle$.

In the Feynman graphs for the loop corrections, the fields of the α replica are symbolized by arrows on full lines, whereas those for the β replica are symbolized by arrows on dashed lines. A vertex u_{mnpq} has then m outgoing arrows on full lines, n incoming arrows on full lines, p outgoing arrows on dashed lines and q incoming arrows on dashed lines. In this notation, the fact that $u_{0npq} = 0$ if $n \neq 0$, $u_{mn0q} = 0$ if $q \neq 0$ and $u_{0n0q} = 0$, which we discussed in section IX B, means that any vertex with incoming arrows of a certain replica must have at least one outgoing arrow of the same type of replica, i.e. there are no “sinks”, with only incoming lines of a certain replica. Furthermore, since the spins from different replica do not interact directly, and since $u_{0,1,1,0} = u_{1,0,0,1} = 0$, there are only two kinds of propagators, one for each replica. In other words, in any diagram, an outgoing line can be connected only to an incoming line of the same replica.

Using the above rules and causality, one finds that corrections to vertices with lines of only one replica, can only receive corrections from vertices of the *same* replica. There are no contributions from diagrams that also involve the other replicas. That means that our results for the magnetization and other quantities that can be calculated using only one replica, are unaffected by the introduction of a second replica.

“Pure” (or one-replica) vertices which depend on more than one time usually have several

²⁶In section IX B we already derived the appropriate partition function. In this appendix we use the notation introduced there.

different contributions. For example the vertex $u_{2,2}(t_1, t_2, t_3, t_4)$ has two main contributions that are obtained by partial integration of the corresponding term in the action as discussed in appendix C. One contribution is derived from $u_{2,2}(t_1, t_2, t_3, t_4)$ and has $t_1 = t_3^+$ and $t_2 = t_4^+$. The other contribution is derived from $u_{2,2}(t_1, t_2, t_3, t_4)$ and has $t_1 = t_3^+$ and $t_1 = t_4^+$. If we have two replicas, there are *different* “mixed” vertices each of which corresponds to one such the individual contribution to a pure vertex. Each of them has the same bare value as such a pure counterpart, since both are obtained in the same way from mean-field theory. With “corresponding” we mean that the times associated with the different legs of the mixed vertex, are assigned in the same way to the legs of the corresponding part of a pure vertex. The part of a pure vertex formally corresponding to $u_{1,1,1,1}$, for example, is given by that contribution to $u_{2,2}(t_1, t_2, t_3, t_4)$, which has $t_1 = t_3^+$ and $t_2 = t_4^+$. Conversely the part of a pure vertex corresponding to $u_{1,2,1,0}$ is given by that contribution to $u_{2,2}(t_1, t_2, t_3, t_4)$, which has $t_1 = t_3^+$ and $t_1 = t_4^+$. Notice, that in any mixed vertex all legs carrying a certain time label (one outgoing and any number of incoming arrows), must belong to the same replica. In contrast to the different contributions to one pure vertex, the corresponding mixed vertices do not add up to a single mixed vertex, since they are multiplied by field from different replicas $\eta^\alpha \neq \eta^\beta$.

The loop corrections to mixed vertices formally look the same as those the corresponding parts of the pure vertices. For each loop correction to a mixed vertex there is a matching correction to the corresponding *part* of the pure vertex and vice versa. The combinatoric factors are also the same. This implies in particular that choosing the same spin rescaling for both replica as we did before in the case of only one replica, renders marginal not only $u_{2,0}^\alpha$ and $u_{2,0}^\beta$, but also $u_{1,0,1,0}$.

3. Scaling of the second moment of the avalanche size distribution

We need to find the scaling behavior of the “Greens function”

$$\langle \hat{s}^\alpha(t_\alpha, x_0) s^\alpha(t_0, x_\alpha) \hat{s}^\beta(t_\beta, x_0) s^\beta(t_1, x_\beta) \rangle_f \quad (\text{F16})$$

from its behavior under coarse graining. The topology of the diagrams permits no $O(\epsilon)$ loop corrections to the corresponding vertex function.

One finds the canonical dimensions of the fields [105] (where “dimension of” is denoted by “[]” and Λ is the upper cutoff in momentum): $[\eta(p, \omega)] = \Lambda^{-d/2-2-z}$, $[\hat{\eta}(p, \omega)] \sim \Lambda^{-d/2}$.

For calculating Greens functions one introduces source terms in the action. From the (functional) derivative with respect to the source fields, one obtains the corresponding average correlation functions. In the end the source fields are taken to zero again, since usually they have no physical significance. In our case the following three source terms are needed: $\int d^d q \int d\omega L(q, \omega)\eta(q, \omega)$, $\int d^d q \int d\omega \hat{L}(q, \omega)\hat{\eta}(q, \omega)$, and the term needed for the calculation of the (spacially) composite operator in $\langle S^2 \rangle_f$, given by

$$\int d^d q \int d\omega_1 \int d\omega_2 L_2(q, \omega_1, \omega_2) \int d^d q \hat{\eta}(q, \omega_1) \hat{\eta}(p - q, \omega_2). \quad (\text{F17})$$

L , \hat{L} and L_2 are the respective source fields: the corresponding canonical dimensions are $[L(q, \omega)] \sim \Lambda^{-d/2+2}$, and $[\delta/\delta L(q, \omega)] \sim \Lambda^{(d/2-2)}\Lambda^{(-d-z)} \sim \Lambda^{-d/2-2-z}$. Similarly $[\hat{L}(q, \omega)] \sim \Lambda^{-d/2-z}$, and $[\delta/\delta \hat{L}(q, \omega)] \sim \Lambda^{-d/2}$. And also $[L_2(p, \Omega)] \sim \Lambda^{(d-2z)}$, and $[\delta/\delta L_2(p, \Omega)] \sim \Lambda^0$. From eq. (164) and the fact that Greens functions in the fields η and $\hat{\eta}$ scale in the same way as those in terms of s and \hat{s} (see section VIB), we then find (without loop corrections) that $\langle S^2 \rangle_f \sim \Lambda^{-(4+z)}$. Below the upper critical dimension, the canonical dimensions of the fields $\eta(q, \omega)$ and $\hat{\eta}(q, \omega)$ are corrected by $\Lambda^{(\eta/2)}$ and $\Lambda^{(\eta-\bar{\eta}/2)}$ respectively. With $\eta = \bar{\eta}$ from the mapping to the pure Ising model [60], one obtains (to $O(\epsilon)$) $\langle S^2 \rangle_f \sim \Lambda^{-(z+(2-\eta)^2)}$. Similarly, one finds for the higher moments $\langle S^n \rangle_f \sim \Lambda^{-((n-1)z+(2-\eta)^n)}$ to $O(\epsilon)$. In section IX D this result is compared to the scaling behavior of $\langle S^2 \rangle$ as obtained from the scaling form of the avalanche size distribution

$$\langle S^2 \rangle \sim r^{(\tau-3)/\sigma} \mathcal{S}_{\pm}^{(2)}(h/r^{\beta\delta}) \quad (\text{F18})$$

(with the appropriate scaling function \mathcal{S}_{\pm}) to extract the results for $1/\sigma$ and τ . There we obtain

$$1/\sigma = 2 + \epsilon/3 + O(\epsilon^2). \quad (\text{F19})$$

and

$$\tau = 3/2 + O(\epsilon^2). \tag{F20}$$

APPENDIX G: RELATED PROBLEMS

1. Comparison with depinning transitions

a. Relation to fluid invasion in porous media

Much progress has been made in the study of fluid invasion of porous media [112,27,28]. A preexisting fluid in the porous medium, for example oil in rock, is displaced by an invading fluid (water), which is driven by an applied pressure P . The interface between the two fluids is pinned at pressures lower than a threshold value P_c and advances continuously at higher pressures. The interface depinning transition is accompanied by a diverging correlation length, critical fluctuations and universal exponents. There are three different universality classes for the associated critical exponents, corresponding to low, intermediate and high disorder in the system. At low disorder the marginally stable interface at P_c is faceted, at intermediate disorder it is self-affine and at high disorder it is self-similar.

Already before we did our work on hysteresis, Robbins, Cieplak, Ji and Koiller have pointed out the analogy of fluid invasion to the physics of domain wall motion in Ising ferromagnets [28,30,29]. There, the interface separates regions of up and down spins. As the magnetic field is ramped, one domain grows at the expense of the other — the interface is pushed forward. Quenched disorder may be due to random fields or random bonds. The authors study the zero temperature nonequilibrium RFIM with a *rectangular distribution* of random fields of width Δ and a preexisting flat interface separating up spins from down spins. They increase the external magnetic field adiabatically and study avalanches of spin flips that are triggered by flipping spins at the interface. As in our system a spin in such an avalanche flips up if its local effective field becomes positive. *The main difference is that*

in their system no spins are allowed to flip ahead of the interface. Each spin flip can be interpreted as an advancement of the pre-existing system-spanning interface. The value of the magnetic field at which any part of the interface reaches the other side of the system is the critical field which corresponds to the threshold pressure P_c in fluid invasion in porous media. As in fluid invasion, Ji and Robbins find in 3 dimensions a faceted regime at low disorder Δ , a self-affine regime at intermediate Δ and a percolation regime at large Δ . At a critical width $\Delta_2^c = 3.41J$, which separates the self-affine regime from the self-similar regime, a diverging length scale in a bulk quantity (“fingerwidth”) is observed. The critical exponents associated with the interface depinning transition in the self affine regime have also been calculated in an ϵ -expansion [30,29]. They are the same for random-field and random-bond disorder [29].

We expect that in our system it would be possible to observe the same critical behavior at the onset of the infinite avalanche in large enough systems with less than critical disorder ($R < R_c$). If the system is big enough, there will certainly be somewhere a rare large cluster of flipped spins, even at relatively low magnetic fields. As the field is slowly raised, the surface of such a cluster is expected to act as a preexisting interface analogously to Ji and Robbins system. The small clusters that are flipped ahead of the interface probably have no influence on the long length scale behavior and the critical exponents associated with interface progression such as roughening exponents. The onset field for the infinite avalanche in an infinite system corresponds to the threshold field at which a preexisting interface gets depinned in Ji and Robbins system.

Numerical and analytical studies [19,20,29,30,28,21,22,31,23] leave no doubt that the interface depinning transition has an associated diverging height-height correlation length and critical fluctuations. There are scaling forms for quantities related to the shape of the interface and its progression, which suggest that the interface gets depinned in a second order transition. Nevertheless in our system (in three dimensions) we have called the onset of the infinite avalanche in systems with less than critical disorder an abrupt or “*first order*” transition. What’s come over us ? Our numerical simulations in three dimensions clearly

show a kink in the magnetization curve at the threshold field $H_c(R)$, rather than power law behavior as expected in continuous transitions. This is not a contradiction. One has to be careful about which quantities are measured: The critical fluctuations at the interface yield no contribution to bulk quantities (*e.g.* the magnetization), which are measured per unit volume. In references [126,128] we propose an experimental setup that would allow one to observe bulk and interface fluctuations simultaneously. In the conventional setup for measuring magnetic hysteresis loops discussed in this paper however, the second order depinning transition with a diverging height-height correlation function at the interface discussed by Robbins *et al.* is buried invisibly inside the line of abrupt (“first order”) transitions seen in our magnetization curves in sufficiently low dimensions. Note that this connection can only be established for large enough systems, where rare large fluctuations provide a preexisting interface of flipped spins. In smaller systems, disorder induced nucleation effects will determine the size of the onset field for the infinite avalanche in our hysteresis model.

At the critical disorder Δ_2^c , separating the self-affine regime from the self-similar regime, Ji and Robbins find a diverging bulk length scale, the “fingerwidth” of regions of flipped spins. The critical exponents associated with this transition are different from the exponents seen at our critical endpoint $(R_c, H_c(R_c))$. This is not too surprising: unlike the case for $R < R_c$, near R_c a large advancing interface in our problem runs into pre-existing flipped regions *of all sizes* — presumably changing the universality class. Also we have several infinite fronts at R_c . Ji and Robbins report that for a bounded nonanalytic distribution of random fields the corresponding exponents are nonuniversal in the depinning problem, but depend on the analytic form of the edges of the distribution of random fields. However, for an analytic distribution they presumably take universal values [113]. In our problem we use an analytic distribution and ν is universal, as is shown by the RG calculation. It has been shown [57] however that the exponents are different for a rectangular distribution of random fields in our system also. Perhaps it would not be universal in our problem either for rectangular distributions of random fields [57] (or other distributions with singularities at their tails). In section G 2 this issue will be discussed in more detail.

Above a critical amount of disorder, using single interface dynamics, Ji and Robbins see a self-similar regime, where the interface grows to a percolating cluster at a certain “threshold field” $H_c^{single}(R)$. In our dynamics in an infinite system such a percolating cluster might occur already at a lower value of the external magnetic field, because it is probably easier to connect preexisting clusters of flipped spins to form a percolating cluster than it is to push a domain wall through the system all the way till it reaches the the opposite side. One would expect the same argument to apply for $R \leq R_c$, *i.e.* $H_c(R) \leq H_c^{single}(R)$. In references [126,129] we discuss four potential experimental setups for measuring Barkhausen noise (or avalanche size distributions in general), explaining for each case whether the single interface model of Ji and Robbins or our model with many interfaces and domain nucleation is expected to apply.

2. Other models

a. Adiabatic models for hysteresis

There are several numerical studies of related hysteresis models, which we discuss in more detail in reference [126,128]. Here we only list a few closely related models.

Maslov and Olami [57] have simulated the same model as we have studied, but for a rectangular distribution of random fields [57] rather than a Gaussian. The authors find different critical exponents than ours in 3 dimensions and in mean-field theory. They report that their numerical results speak in favor of the upper critical dimensions being $d_c = 6$. They claim that the model does not belong to any known universality class.²⁷

²⁷Presumably in each dimension there will be a critical power law for the tails of a bounded distribution, so that distributions with a power law larger than this critical value will lead to different critical exponents. In this sense the tails of a rectangular distribution can be thought of as an infinite power law, and conceivably might lead to a different universality class than ours in

Koiller, Ji and Robbins [28] point out that for a rectangular distribution at $R < R_c$ there is a close connection to diffusion percolation and bootstrap percolation in 2 and also in 3 dimensions [113], which are modified percolation models in which the occupation of a site depends on its environment [114].

Coram, Jacobs, and Heinig [115] have studied the zero temperature nonequilibrium random bond Ising models, both spin glasses (SG) and random ferromagnets (RFM) with nearest neighbor interactions in one, two and three dimensions. They report power law sensitivity to single-spin-flip perturbations in 2 and 3 dimensional random ferromagnets, if, starting from the spin state with all spins pointing down (ground state at $H = 0$) the field has been raised to a positive critical value. The associated critical exponents are $\tau = 1.37$ in 2 dimensions, and $\tau = 2.8$ in three dimensions. It is likely that the value of the exponent τ would be different for a Gaussian distribution of random bonds (see footnote 27 on page 108).

Vives *et al.* [50] have studied that case for a negative mean of the Gaussian bond distribution. They trigger avalanches by a slowly increasing homogeneous external magnetic field (as in our model). For the avalanche size distribution integrated over one branch of the hysteresis curve they find $\tau + \sigma\beta\delta = 2.0 \pm 0.2$ in three dimensions and $\tau + \sigma\beta\delta = 1.45 \pm 0.1$ in two dimensions, which are rather close to the values of the nonequilibrium RFIM (see section G 2 c). One would expect the value the exponent τ to be smaller than $\tau + \sigma\beta\delta$, *i.e.* their result seems to deviate from the number obtained by Coram *et al.* for a rectangular distribution of ferromagnetic bonds with strengths between 0 and 1. That is not surprising if we consider the differences in the two approaches. It might be interesting to compare the shape of the hysteresis loops of the two models at various values of the relevant tunable parameters. A similar comparison of our hysteresis loops to those of Maslov and Olami's RFIM with a rectangular distribution of random fields [57] revealed marked differences of

all dimensions.

the two models. For example, in our model at less than critical randomness, there were precursors to the infinite avalanche, while in Maslov and Olami's model there were none.

Bertotti and Pasquale [118] have studied hysteresis phenomena in the Sherrington-Kirkpatrick spin glass model [117] with N Ising spins $s_i = \pm 1$ on a lattice with random infinite range interactions that are distributed according to a Gaussian with mean zero. They used a slightly generalized dynamics that allows for temperature like fluctuations at a finite sweeping frequency Ω with $H = \Omega t$. They report power law scaling of the power spectrum due to avalanches of spin flips near the central part of the saturation hysteresis loop, where the rate of change of the magnetization dM/dt is approximately constant. The authors note that this scaling behavior as well as the associated shape $F(\omega)/\Omega$ very much resembles the behavior observed in Barkhausen effect experiments in soft magnetic materials [119].

For sweeping rate $\Omega \rightarrow 0$ we can think of their model without random fields as an infinite range mean-field theory for the nonequilibrium random bond Ising model, simulated by Vives *et al.* [50]. Vives *et al.* found that in two and three dimensions the nonequilibrium RFIM does reveal a critical point of the kind we found in the nonequilibrium RFIM. It would be interesting to look for the same kind of critical point in Bertotti *et al.*'s nonequilibrium SK-model (with and without random fields), for example by setting the mean J_0 of the distribution of random bonds to a nonzero value and tuning the widths of distributions of random fields and random bonds.

Rudyak [37] has suggested a theory for dielectric hysteresis in ferroelectrics which leads to the same picture as our hard-spin mean-field theory for $R < R_c$.

b. Dynamical and other hysteresis models

There are several studies of scaling behavior of the area of the hysteresis loop as a function of driving frequency Ω and amplitude H_0 of the of the external magnetic field $H(t) = H_0 \sin \Omega t$, and other dynamical effects [120,118,121]. Most of these model contin-

uum and lattice spin systems do incorporate temperature effects, but no quenched disorder. Rao, Krishnamurthy and Pandit give a nice review and discussion of previous (empirical) hysteresis models such as the Preisach model and mean-field types of theories like the Stoner-Wohlfarth theory and others [121].

c. Conjectures about other models in the same universality class

Recently Vives, Goicoechea, Ortín, and Planes found [50] that the numerical exponents ν , β , τ , and z in the nonequilibrium zero temperature RFIM and the RBIM (random bond Ising model) have very similar values in two and three dimensions. In two dimensions, the exponents for the RFBE (random field Blume-Emery-Griffiths model [122]) seem to be similar also. In this interesting paper the authors suggest that these models might actually be in the same universality class. Admiring their work, we however have some concerns as to whether their critical exponents will remain unchanged for larger system sizes: they used systems of linear size up to $L = 100$; we used much larger systems, up to 7000^2 and 800^3 for the RFIM, and found that finite size effects are actually quite prominent and lead to shifted results for the exponents. Although the *equilibrium* versions of these models are not in the same universality class, it is known [30,29], however, that the nonequilibrium *single interface depinning* transitions of the RFIM and the RBIM do have the same critical exponents.

In the following section we will discuss some symmetry arguments, that would indeed speak in favor of Vives *et al.*'s conjecture and would suggest that the universality class of our model extends even beyond just the RBIM. A large universality class would also explain the surprisingly good agreement with experiments discussed in section X. Generally one may ask how robust the universality class of our model is against the introduction of other kinds of disorder, other symmetries for the order parameter, long range interactions, different dimensions, and altered dynamics. The variation with dimension has already been discussed at the appropriate places in this paper (see for example section X).

Other forms of disorder and symmetries

If a new kind of disorder in an otherwise unaltered system changes neither the symmetries, nor the interaction range, nor the dynamics, nor the relevant dimensions, we may be hopeful that it does not lead to a different universality class.

Random fields and random bonds: Uncorrelated fluctuations in the nearest neighbor coupling strengths (random bonds) in the presence of random field disorder do not break any new symmetries. Our random field Ising model fulfills two Harris criteria $\nu/\beta\delta \geq 2/d$ and $\nu \geq 2/d$. Adding random bond disorder cannot destroy the fixed point in the Harris criterion sense through added statistical fluctuations, because the random field disorder has already broken the relevant (translational) symmetry. It then seems plausible that systems with random bonds and random fields are in the same universality class as systems with random fields only. The ultimate justification for this conjecture may be drawn from the renormalization group picture. If the change in the generating functional due to the added new disorder turns out to be irrelevant under coarse graining, it will not affect the critical behavior on long length scales. Some preliminary studies seem to indicate that this would be case for random bonds in the presence of random fields. Further elaborations on this issue will be presented elsewhere [128].

Random bonds only: Similarly one might expect systems with random bonds only to be in the same universality class also. Because the critical magnetization $M_c \equiv M(H_c(R_c))$ is nonzero, the time reversal invariance will be broken at the critical point, just as it is broken in the case of random fields. The symmetries of the random field model and the random bond model would then be the same. In a soft spin model the dynamics could also be defined in the same way, using relaxational dynamics. One would then expect to see the same critical behavior on long length scales. In fact, in the random bond model one may consider the spins that flip outside the critical region to act as random fields for the spins that participate in the large avalanches near the critical point. We have already suggested that random bonds in the presence of random fields do not change the critical behavior. It

then seems plausible that the random bond problem would be in the same universality class also, as numerical simulations seem to confirm [50]. As a warning to the enthusiastic reader we should mention that the simplest mean field theory for this problem has some sicknesses that make it difficult to verify this conjecture in the RG framework. We believe, however, that these subtleties occur only in the infinite range mean-field theory, and that they are unimportant for the behavior in finite dimensions. Some simulations of the infinite range model with random bonds are reported in [118,116].

Random anisotropies: Realistic models of Barkhausen noise in polycrystalline magnets usually involve random anisotropies rather than random fields. In the same way it appears plausible that a nonequilibrium $O(n)$ model with random anisotropies [7,35,123] may be in the same universality class as the nonequilibrium RFIM. The external magnetic driving field breaks the rotational symmetry and time reversal invariance, just as in the case of random bonds. Again, spins that do not flip in the critical region may act as random fields for the spins participating in avalanches near the critical point, so that the essential features are the same as in our model, and one may expect to see the same critical exponents.²⁸ The $O(n)$ model with random anisotropies is very similar to a continuous scalar spin model with random couplings to the external magnetic field (random “g-factors”). The mean-field theory for the random g-factor model turns out to have the same critical exponents as our random-field Ising model. There are no new terms generated in the RG description of this model either, it is therefore expected to be in the same universality class as our model. By symmetry we would neither expect any change in the exponents if there was randomness added through a distribution in the soft-spin potential well curvatures k (see our definition

²⁸It may be that in some strong coupling limit the system will lose the ability to avalanche and all spins will smoothly rotate from down to up as the external magnetic field is increased. Our discussion above refers to the case where the coupling is weaker and avalanches do occur, as of course they do experimentally.

of the soft-spin potential $V(s_i)$ in eq. (31)), nor if random bonds are added to the system, as may be the case in real experimental systems.

The RG formalism developed in this paper can be used as a convenient tool to verify these conjectures. One can write down the most general generating functional and verify for each of these models whether on long length scales the same kinds of terms become important or irrelevant as in our model.

Long range interactions:

The question about the effect of long range interactions is of equal importance. Depending on the sample shape, dipole-dipole interactions can lead to long-range, antiferromagnetic interaction forces which are the reason for the breakup of the magnetization into Weiss-domains in conventional magnets [35,7]. In the case of martensites there are long range antiferroelastic strain fields present [58,8]. In references [126,129] we give an example of a critical exponent in a system with long range forces (from avalanche duration measurements in martensites [13]) that appears to be quite different from the corresponding exponent in our model. On the other hand, measurements of Barkhausen-noise distributions in magnets in the presence of long range demagnetizing fields seem to yield a critical exponent quite close to the corresponding exponent in our model [97].

In a recent preprint [97] Urbach, Madison and Markert study a model for a *single* moving domain wall without overhangs in the presence of infinite range antiferromagnetic interactions and quenched (random field) disorder. In an infinite system their model self-organizes²⁹ without necessary parameter tuning to the same critical state seen in the absence of the infinite range interactions right at the interface depinning threshold [28]. An analysis [124] of our ferromagnetic RFIM in the presence of infinite range antiferromagnetic interactions leads to an unchanged critical behavior except for a tilt of the entire magnetization curve in the

²⁹This self-organization to the critical point is similar to the trivial self-organization expected in an experiment in the presence of a gradient field, which we proposed in references [126,129]

(M, H) plane: here too it does not change the critical properties. It would be interesting to see how these results would change for more physical long-range interactions. Dipole-dipole interactions decaying with distance as $1/x^3$, for example, might be appropriate.

3. Thermal fluctuations

(a) The equilibrium random field Ising model:

The equilibrium properties of the random field Ising model, in particular the phase transition from paramagnetic to ferromagnetic (long range ordered) behavior, have been the subject of much controversy since the 1970s [62]. The reason is intriguing: experimental and theoretical studies of the approach to equilibrium show that near the critical temperature there seems to appear a “glassy” regime where relaxation to equilibrium becomes very slow. Activated by thermal fluctuations the system tumbles over free energy barriers to lower and lower valleys in the free energy landscape, until it has reached the lowest possible state, the equilibrium or ground state. The higher those barriers are compared to the typical energy of thermal fluctuations, the longer the relaxation process takes. At low temperatures, due to the effect of disorder, some of these barriers are so large (diverging in an infinite system), that the system gets stuck in some metastable state and never reaches true equilibrium on measurement time scales. On long length scales (and experimental time scales) thermal fluctuations become irrelevant and collective behavior emerges. When driven by an external field, the system moves through a local valley in the free energy landscape, and collective behavior in the form of avalanches is found when the system reaches a descending slope in the free energy surface. The present state of the system depends on its history — a phenomenon commonly observed as hysteresis.

(b) The nonequilibrium random field Ising model:

We have studied this hysteresis in the zero temperature random field Ising model, far from equilibrium and in the absence of any thermal fluctuations. We found a critical point, at which the shape of the hysteresis loops (magnetization versus magnetic field) changes

continuously from displaying a jump in the magnetization to a smooth curve. Interestingly, the nonequilibrium critical exponents associated with the universal behavior near this point in $d = 3$ dimensions seem to match those obtained from 3 dimensional simulations of the equilibrium phase transition point approximately within the error bars (see table I). This is surprising, since the physical starting points of the two systems are very different. Furthermore, our perturbation expansion in $\epsilon = 6 - d$ for nonequilibrium critical exponents can be mapped onto the expansion for the equilibrium problem to all orders in ϵ . Our expansion stems from a dynamical systems description of a deterministic process, which takes into account the history of the system and is designed to single out the correct metastable state, while the calculation for the equilibrium problem involves temperature fluctuations and no history dependence at all.

(c) The crossover:

It would be interesting to see if there is actually a deeper connection between the nonequilibrium and equilibrium critical points, and whether the calculation for the nonequilibrium model could be used to resolve long-standing difficulties with the perturbation expansion for the equilibrium model. The idea is to introduce temperature fluctuations in the nonequilibrium calculation, and at the same time a finite sweeping frequency for the external driving force. The lower the sweeping frequency Ω at fixed temperature, the more equilibrated the system and the longer the length scale above which nonequilibrium behavior emerges. Tuning Ω would allow one to explore the whole crossover region between the two extreme cases that are found in the literature (far from and close to equilibrium). Contrary to previous treatments of relaxation, the history dependence that is so essential in experimental realizations, emerges naturally from this approach. At fixed temperature, but for progressively lower sweeping frequencies, one expects to see smaller and smaller hysteresis loops, asymptotically attaining a universal shape at low enough frequencies. The tails of these hysteresis loops will match the equilibrium magnetization curve. In the limit of zero frequency, the hysteresis loop shrinks to a point, and equilibrium is expected at all values of the

external magnetic field. On the other hand, taking temperature to zero first, should yield nonequilibrium behavior as seen in our recent work. The prospect of relating equilibrium and nonequilibrium critical behavior as two limits at opposite edges of the experimentally relevant crossover regime is an exciting challenge.

REFERENCES

- [1] J.P. Sethna, J.D. Shore, M. Huang *Phys. Rev. B* **44**, 4943 (1991), and references therein; J.D. Shore, Ph.D. thesis, Cornell University (1992), and references therein; T. Riste and D. Sherrington “Phase Transitions and Relaxation in Systems with Competing Energy Scales”, *Proc. at NATO Adv. Study Inst.*, April 13-23 1993, Geilo, Norway, and references therein; M. Mézard, G. Parisi, M.A. Virasoro “Spin Glass Theory And Beyond”, World Scientific (1987), and references therein; K.H. Fischer and J.A. Hertz “Spin Glasses”, Cambridge University Press (1993), and references therein.
- [2] J. Villain, *Phys. Rev. Lett.* **29**, 6389, (1984); J. Villain *Proc. at NATO Adv. Study Inst.*, April 8-19 1985, Geilo, Norway, and references therein; M. Mézard and A.P. Young, *Europhys. Lett.* **18**, 653 (1992), and references therein.
- [3] G. Grinstein and J.F. Fernandez *Phys. Rev. B* **29**, 6389 (1984); J. Villain, *Phys. Rev. Lett.* **52**, 1543 (1984).
- [4] A. J. Bray and M. A. Moore, *Journal of Physics C* **18**, L927 (1985).
- [5] D. S. Fisher *Phys. Rev. Lett.* **56**, 416 (1986).
- [6] J. C. McClure, Jr. and K. Schröder, *CRC Crit. Rev. Solid State Sci.* **6**, 45 (1976).
- [7] D. Jiles “Introduction to Magnetism and Magnetic Materials”, Chapman and Hall, 1991.
- [8] “Martensite”, G. B. Olson and W. S. Owen, eds., ASM International; A.D. Bruce and R.A. Cowley, “Structural Phase Transitions”, Taylor and Francis, London (1981); P.F. Gobin and G. Guenin, “Solid State Phase Transformations in Metals and Alloys”, Aussois summer school, September 3-15, 1978, Les Éditions de Physique, Orsay, (1978).
- [9] D. Sornette, *J. Phys. I France* **4**, 209 (1994).
- [10] references 16-25 in D. Sornette, *J. Phys. I France* **4**, 209 (1994); R.L. Smith, S.L.

- Phoenix, M.R. Greenfields, R.B. Hengstenburg, R.E. Pitt, *Proc. R. Soc. Lond A* **388**, 353 (1983) and references therein; P.C. Hemmer and A. Hansen *Theor. Phys. Seminar Trondheim*, **4** (1991).
- [11] P. J. Cote and L. V. Meisel, *Phys. Rev. Lett.* **67**, 1334, 1991; L.V. Meisel and P.J. Cote, *Phys. Rev. B* **46**, 10822, 1992.
- [12] S. Field, J. Witt, F. Nori, and X. Ling, *Phys. Rev. Lett.* **74**, 1206 (1995).
- [13] E. Vives, J. Ortín, L. Mañosa, I. Ràfols, R. Pérez-Magrané, and A. Planes *Phys. Rev. Lett.* **72**, 1694 (1994).
- [14] C.F. Richter *Ann. Geophys.* **9** 1 (1956).
- [15] K.M. Godshalk and R.B. Hallock, *Phys. Rev. B* **36**, 8294 (1987); M.P. Lilly, P.T. Finley, and R.B. Hallock *Phys. Rev. Lett.* **71**, 4186 (1993).
- [16] S.N. Coppersmith *Phys. Rev. Lett.* **65**, 1044 (1990) has shown that on sufficiently large length scales the elastic theory always breaks down.
- [17] D.S. Fisher, *Phys. Rev. B* **31**, 1396 (1985).
- [18] “Charge Density Waves in Solids”, edited by Gy. Hutiray and J. Sólyom, Lecture Notes in Physics Vol. 217 (Springer-Verlag, Berlin, 1984); and “Charge Density Waves in Solids”, edited by L.P. Gorkov and G. Grüner (Elsevier, Amsterdam, 1989).
- [19] O. Narayan and D. S. Fisher, *Phys. Rev. Lett.* **68**, 3615 (1992) and *Phys. Rev. B* **46**, 11520 (1992)
- [20] O. Narayan and A.A. Middleton *Phys. Rev. B* **49**, 244 (1994).
- [21] C. Myers and J.P. Sethna *Phys. Rev. B* **47**, 11171 (1993), and *Phys. Rev. B* **47**, 11194 (1993) (CDW).
- [22] A.A. Middleton and D.S. Fisher *Phys. Rev. Lett.* **66**, 92 (1991), and references therein;

- Phys. Rev. B* **47**, 3530 (1993) (CDW).
- [23] A.I. Larkin and Yu.N. Ovchinnikov, *J. Low Temp. Phys.* **34**, 409 (1979) (flux lattice).
- [24] M.V. Feigel'man and V.M. Vinokur, *Phys. Rev. B* **41**, 8986.
- [25] D.S. Fisher, and D.A. Huse, *Phys. Rev. B* **43**, 130 (1991) and references therein.
- [26] D. Ertas and M. Kardar (preprint 1994).
- [27] M.A. Rubio, C. Edwards, A. Dougherty, and J.P. Gollup, *Phys. Rev. Lett.* **63**, 1685 (1989); **65**, 1339 (1990); V.K. Horvath, F. Family, and T. Vicsek, *Phys. Rev. Lett.* **65**, 1388 (1990); *J. Phys. A* **24**, L25 (1991); M.A. Rubio, A. Dougherty, and J.P. Gollup, *ibid* **65**, 1389 (1990); V.K. Horvath, F. Family, and T. Vicsek, *ibid* **67**, 3207 (1991); S. He, G.L.M.K.S. Kahanda, and P-Z. Wong, *ibid* **69**, 3731 (1992).
- [28] M. Cieplak and M.O. Robbins, *Phys. Rev. Lett.* **60**, 2042 (1988), and *Phys. Rev. B* **41**, 11508 (1990); N. Martys, M. Cieplak, and M.O. Robbins, *Phys. Rev. Lett.* **66**, 1058 (1991); N. Martys, M.O. Robbins, and M. Cieplak, *Phys. Rev. B* **44**, 12294 (1991); B. Koiller, H. Ji, and M.O. Robbins, *ibid* **45**, 7762 (1992) (fluid invasion); H. Ji and M.O. Robbins *ibid* **46**, 14519 (1992); B. Koiller, H. Ji, M.O. Robbins, *Phys. Rev. B* **46**, 5258 (1992) (domain wall in random magnets).
- [29] O. Narayan and D.S. Fisher *Phys. Rev. B* **48**, 7030 (1993).
- [30] T. Nattermann, S. Stepanow, L.H. Tang and H.Leschhorn *J. Phys. II France* **2**, 1483 (1992)
- [31] D. Ertas and M. Kardar, *Phys. Rev. E* **49**, R2532 (1994); J.F. Joanny and M.O. Robbins, *J. Chem. Phys.* **92**, 3206 (1990) (contact lines).
- [32] A. Brass, H.J. Jensen, and A.J. Berlinsky, *Phys. Rev. B* **39**, 102 (1989).
- [33] R. Lenormand and C. Zircon, *Phys. Rev. Lett.* **54**, 2226 (1985).

- [34] O. Narayan and D.S. Fisher *Phys. Rev. B* **49**, 9469 (1994), and references therein.
- [35] S. Chikazumi, “Physics of Magnetism”, Wiley, New York (1964).
- [36] Aizu K., *Phys. Rev. B* **2**, 754 (1970), *J. Phys. Soc. Japan* **44**, 334 and 683 (1978);
Martin “Die Ferroelektrika”, Leipzig 1964.
- [37] V.M. Rudyak, *Bull. Acad. Sci. USSR Phys. Ser.* **57**, 955 (1993) and references therein;
V.M. Rudyak *Bull. Acad. Sci. USSR Phys. Ser.* **45**, 1 (1981).
- [38] G.L. Vasconcelos, M. de Sousa-Vieira, S.R. Nagel *Physica A* **191**, 69 (1992).
- [39] R. Burridge and L. Knopoff *Bull. Seismol. Soc. Am.* **57**, 341 (1967); P.Bak and C.
Tang, *J. Geophys. Res.* **94** 15635 (1989); Z. Olami, H.J.S. Feder, and K. Christensen,
Phys. Rev. Lett. **68**, 1244 (1992); K. Christensen and Z. Olami *Phys. Rev. A* **46**, 1829
(1992); L. Pietronero, P. Tartaglia and Y.C. Zhang *Physica (Amsterdam)* **137A**, 22
(1991); E.J. Ding, Y.N. Lu *Phys. Rev Lett.* **70**, 3627 (1993).
- [40] J.M. Carlson and J.S. Langer *Phys. Rev. Lett.* **62**, 2632 (1989).
- [41] J.P. Sethna, K. Dahmen, S. Kartha, J.A. Krumhansl, B.W. Roberts, and J.D. Shore,
Phys. Rev. Lett. **70**, 3347 (1993); K. Dahmen, S. Kartha, J.A. Krumhansl, B.W.
Roberts, J.P. Sethna, and J.D. Shore, *J. Appl. Phys.* **75**, 5946 (1994).
- [42] K. Dahmen and J.P. Sethna, *Phys. Rev. Lett.* **71**, 3222 (1993).
- [43] F. Preisach, *Z. Phys.* **94**,277 (1935); M. Krasnoselskii and A. Pokrovskii, *Systems with
Hysteresis*, (Nauka, Moscow, 1983), I. D. Mayergoyz, *J. Appl. Phys.* **57**, 3803 (1985);
Mathematical Models of Hysteresis, (Springer-Verlag,1991); P.C. Clapp, *Materials Sci-
ence and Engineering* **A127**, 189-95 (1990).
- [44] K.P. O’Brien and M.B. Weissman, *Phys. Rev. E* **50**, 3446 (1994) and references therein;
K.P. O’Brien and M.B. Weissman, *Phys. Rev. A* **46**, R4475 (1992).
- [45] O. Perković, K.A. Dahmen, and J.P. Sethna, (simulations: preprint in preparation).

- [46] V. Raghavan in *Martensite*, G. B. Olson and W. S. Owen, eds., (ASM International), 1992, p. 197.
- [47] A. Berger, unpublished.
- [48] Details about the experimental setup used by Berger are given in A.W. Pang, A. Berger, and H. Hopster, *Phys. Rev. B* **50**, 6457 (1994); A. Berger, A.W. Pang, H. Hopster, *J. Magn. Magn. Mat.* **137**, L1 (1994); A. Berger, A.W. Pang, and H. Hopster, *Phys. Rev. B* **52** (1995, in print).
- [49] W. Wu and P.W. Adams, *Phys. Rev. Lett.* **74**, 610 (1995).
- [50] E. Vives and A. Planes *Phys. Rev. B* **50**, 3839 (1994) (simulations of the two-dimensional random bond Ising model); E. Vives, J. Goicoechea, J. Ortín and A. Planes, preprint (1994) (simulations of the RFIM and the RBIM in two and three dimensions, and of the Blume-Emery-Griffiths model in two dimensions).
- [51] L. Chayes, private communication.
- [52] Return point memory has been seen in ferromagnetism: D. C. Jiles, D. L. Atherton, *J. Appl. Phys.* **55**, 2115 (1984); J.A. Barker, D.E. Schreiber, B.G. Huth, and D.H. Everett, *Proc. R. Soc. London A* **386**, 251-261 (1983). Martensitic transformations (thermally and stress-induced) of metallic alloys J. Ortín *J. Appl. Phys.* **71**, 1454 (1992); *J. de Phys. IV*, colloq. C4, **1**, C-65 (1991) and references therein. In ammonium chloride: Smits *et al.* *Z. Phys. Chem. A* **166**, 97 (1933); **175**, 359 (1936); *Z. Phys. Chem. B* **41**, 215 (1938). Spin transitions: E.W. Müller, H. Spiering, and P. Gülich, *J. Chem. Phys.* **79**, 1439 (1983). Adsorption of gases by porous solids: J. Katz, *J. Phys. (Colloid) Chem.* **53**, 1166 (1949); Emmett and Cines, *J. Phys. (Colloid) Chem.*, **51**, 1248 (1947). Charge-density waves: Z. Z. Wang and N. P. Ong, *Phys. Rev. B* **34**, 5967, 1986. Cellular Automata: J. Goicoechea and J. Ortín, *Phys. Rev. Lett* **72**, 2203 (1994), and references therein.

- [53] N. Goldenfeld, “Lectures on Phase transitions and the Renormalization Group”, Addison Wesley 1992, p.383.
- [54] J.M. Yeomans “Statistical Mechanics of Phase Transformations” Clarendon Press, Oxford (1992).
- [55] In this paper we consider a lattice of classical spins. For an illustrative quantum mechanical description of magnetic moments in an external magnetic field see also S. Brandt and H.D. Dahmen “The Picture Book of Quantum Mechanics”, second edition, Springer Verlag, New York 1995.
- [56] N.G. van Kampen “Stochastic Processes in Physics and Chemistry”, North Holland 1990.
- [57] S. Maslov and Z.Olami, preprint (1993).
- [58] S. Kartha, Ph.D. thesis, Cornell University (1994).
- [59] H. Kleinert, J. Neu, V. Schulte-Frohlinde, and K.G. Chetyrkin, *Phys. Lett. B* **272**, 39 (1991).
- [60] U. Krey, *J. Phys. C* **17**, L545-L549 (1984), U. Krey, *J. Phys. C* **18**, 1455-1463 (1985), U. Krey and H. Ostermeier, *Z. Phys. B* **66**, 219 (1987).
- [61] D. Stauffer and A. Aharony “Introduction to Percolation Theory”, Taylor and Francis (1992).
- [62] T. Nattermann and J. Villain, *Phase Transitions* 1988, Vol. 11, pp 5-51, Gordon and Breach Science publishers Inc. (1988), and references therein; T. Nattermann and P. Rujan *Inter. J. Mod. Phys. B* **3**, 1597 (1989); D. P. Belanger and A. P. Young, *J. Magn. Magn. Mat.* **100**, 272 (1991); E.B. Kolomeisky, in *JETP Lett.* **52**, No.10, 538 (1990).
- [63] M. Schwartz, and A. Soffer, *Phys. Rev. Lett.* **55**, 2499 (1985).

- [64] J.J. Binney, N.J. Dowrick, A.J. Fisher, M.E.J. Newman, “The Theory of Critical Phenomena”, Clarendon Press, Oxford (1992).
- [65] S.K. Ma “Modern Theory of Critical Phenomena”, Benjamin/Cummings Publishing Company Inc Reading, (1976).
- [66] M. Fisher “Critical Phenomena”, Proc. Stellenbosch, South Africa 1982, Springer Verlag (1982).
- [67] J. Zinn-Justin “Quantum Field Theory and Critical Phenomena”, 2nd edition, Clarendon Press, Oxford (1993).
- [68] D.J. Amit “Field Theory, the Renormalization Group, and Critical Phenomena”, World Scientific, 1984.
- [69] P.C. Hohenberg, B.I. Halperin “Theory of dynamic critical phenomena” *Rev. Mod. Phys.* **49**, 435 (1977).
- [70] For a review of the real-space renormalization group, which we do not employ here, see also R. J. Creswick, H. A. Farach, and C. P. Poole, Jr., “Introduction to Renormalization–Group Methods in Physics”, John Wiley and Sons, New York, (1992).
- [71] A. Brooks Harris and T.C. Lubensky, *Phys. Rev. Lett.* **33**, 1540 (1974); T.C. Lubensky, *Phys. Rev. B* **11**, 3573 (1975).
- [72] A.A. Middleton *Phys. Rev. B*, **45**, 9465 (1992).
- [73] P. C. Martin, E. Siggia and H. Rose, *Phys. Rev. A* **8**, 423 (1973); C. De Dominicis, *Phys. Rev. B* **18**, 4913 (1978); H. Sompolinsky and A. Zippelius, *Phys. Rev. B* **25**, 6860 (1982); A. Zippelius, *Phys. Rev. B* **29**, 2717 (1984).
- [74] R. Bausch, H.K. Janssen, and H. Wagner, *Z. Phys. B* **24**, 113 (1976); U.C. Täuber and F. Schwabl, *Phys. Rev. B* **46**, 3337 (1992) and references therein.
- [75] C. De Dominicis, *Phys. Rev. B* **18**, 4913 (1978).

- [76] H. Sompolinsky and A. Zippelius, *Phys. Rev. B* **25**, 6860 (1982); A. Zippelius, *Phys. Rev. B* **29**, 2717 (1984).
- [77] P. Ramond “Field Theory: A modern primer”, Addison-Wesley Publishing Company, Inc., 1990.
- [78] K. G. Wilson and J. Kogut, *Physics Reports* **12C**, 76 (1974).
- [79] C. Domb, M.S. Green, “Phase Transitions and Critical Phenomena”, Vol 6, Academic Press (1976).
- [80] E. Brézin, D.J. Wallace, and K.G. Wilson, *Phys. Rev. Lett.* **29**, 591 (1972), and *Phys. Rev. B* **7**, 232 (1973); D. J. Wallace and R.P.K. Zia *J. Phys. C: Solid Sstate Phys.* **7**, 3480 (1974).
- [81] A. Aharony, Y. Imry, S.K. Ma, *Phys. Rev. Lett.* **37**, 1364 (1976); A.P. Young, *J. Phys. A* **10**, L 257 (1977); G. Parisi and N. Sourlas *Phys. Rev. Lett.* **43**, 744 (1979).
- [82] G. Parisi, lectures given at the 1982 Les Houches summer school XXXIX “Recent advances in field theory and statistical mechanics” (North Holland), and references therein.
- [83] B. Tadic *Z. Phys.* **41**, 13 (1981).
- [84] From the RG description one deduces that the exponents β and δ are related to ν , η , and $\bar{\eta}$ by the relations $\beta = \frac{\nu}{2}(d - 4 + \bar{\eta})$, $\delta = (d - 2\eta + \bar{\eta})/(d - 4 + \bar{\eta})$, just as in the equilibrium model [62,125]. Using these relations one finds that the inequality $\nu/\beta\delta \geq 2/d$ goes over into the Schwartz-Soffer inequality $\bar{\eta} \leq 2\eta$ that has been derived for the corresponding equilibrium model [63].
- [85] R.B. Griffiths, *Phys. Rev.* **158**, 176 (1967).
- [86] A. Maritan, M. Cieplak, M.R. Swift and J. Banavar, *Phys. Rev. Lett.* **72**, 946 (1994); J.P. Sethna, K. Dahmen, S. Kartha, J.A. Krumhansl, O. Perković, B.W. Roberts, and

- J.D. Shore, *Phys. Rev. Lett.* **72**, 947 (1994).
- [87] A.P. Young and M. Nauenberg *Phys. Rev. Lett.* **54**, 2429, 1985; A.T. Ogielski and D.A. Huse *Phys. Rev. Lett.* **56**, 1298, 1986.
- [88] M.E.J. Newman and G.T. Barkema, Cornell Theory Center preprint # CTC95TR218 (1995), submitted to *Phys. Rev. E* for publication.
- [89] I. Dayan, M. Schwartz, and A.P. Young, *J. Phys. A* **26**, 3093 (1993).
- [90] C. Bender, S.A. Orszag, “Advanced mathematical methods for scientists and engineers”, Mc Graw Hill (1978).
- [91] K. Stierstadt and W. Boeckh, *Z. Physik* **186**, 154 (1965) (in German). The results quoted here are extracted from replotting the data of figure 4 in the form of histograms of the pulse areas recorded withing a small interval of the external magnetic field H .
- [92] G. Bertotti, G. Durin, and A. Magni *J. Appl. Phys.* **75**, 5490 (1994).
- [93] H. Bittel *IEEE Trans. Magn.* **5**, 359 (1969).
- [94] U. Lieneweg *IEEE Trans. Magn.* **10**, 118 (1974).
- [95] U. Lieneweg and W. Grosse-Nobis *Intern. J. Magnetism* **3**, 11 (1972).
- [96] G. Bertotti, F. Fiorillo, and A. Montorsi *J. Appl. Phys.* **67**, 5574 (1990).
- [97] J.S. Urbach, R.C. Madison, and J.T. Markert, preprint 1994.
- [98] K.A. Dahmen, O. Perković, and J.P. Sethna, preprint 1994, submitted for publication.
- [99] G. Montalenti *Z. angew. Physik* **28**, 295 (1970).
- [100] B.W. Roberts, Ph.D. thesis, Cornell University (1995), and references therein.
- [101] M. E. J. Newman, B. W. Roberts, G. T. Barkema, and J. P. Sethna, *Phys. Rev. B* **48**, 16533 (1993), and references therein.

- [102] J.Z. Imbrie *Phys. Rev. Lett.* **53**, 1747 (1984); *Commun. Math. Phys.* **98**, 145 (1985); *Physica* **140 A**, 291 (1986).
- [103] J. Bricmont and A. Kupiainen, *Phys. Rev. Lett.* **59**, 1829 (1987); *Commun. Math. Phys.* **116**, 539 (1988).
- [104] J.T. Chayes, L. Chayes, D.S. Fisher, and T. Spencer. *Phys Rev. Lett.* **57**, 2999, (1986).
- [105] L.H. Ryder, “Quantum Field Theory”, Cambridge University Press (1985).
- [106] A. A. Vladimirov, D. I. Kazakov, and O. V. Tarasov, *Sov. Phys. JETP* **50** (3), 521 (1979) and references therein.
- [107] A. Erdélyi “Asymptotic expansions”, Dover Publications, Inc., New York.
- [108] J.C. Le Guillou and J. Zinn-Justin “Large-Order Behaviour of Perturbation Theory”, North Holland (1990).
- [109] D.I. Kazakov, O.V. Tarasov, and D.v. Shirkov, *Teor. Mat. Fiz.* **38**, 15 (1979).
- [110] J.C. LeGuillou and J. Zinn-Justin *Phys. Rev. B* **21**, 3976 (1980); J.C. LeGuillou and J. Zinn-Justin *J. Physique Lett.* **46**, L137 (1985); J.C. LeGuillou and J. Zinn-Justin, *J. Physique* **48**, 19 (1987).
- [111] J.J. Loeffel, Workshop on Padé Approximants, (eds. D. Bessis, J. Gilewicz, and P. Merry), CEA (1976) and E. Brézin, Review talk, European Particle Physics conference, Budapest (1977).
- [112] J. Feder, “Fractals”, Plenum, New York, 1988; R. Lenormand and S. Bories, *C.R. Acad. Sci. Ser. B* **291**, 279 (1980); R. Chandler, J. Koplik, K. Lerman, and J.F. Willemsen, *J. Fluid Mech.* **119**, 249 (1982); R. Lenormand, *J. Phys.:Cond. Mat.* **2**, SA79 (1990); R. Lenormand, and C. Zarcone, *Phys. Rev. Lett.* **54**, 2226 (1985); J.P. Stokes, D.A. Weitz, J.P. Gollub, A. Dougherty, M.O. Robbins, P.M. Chaikin, and H.M. Lindsay, *Phys. Rev. Lett* **57**, 1718 (1986); J.P. Stokes, A.P. Kushnik, and M.O. Robbins, *Phys.*

- Rev. Lett.* **60**, 1386 (1988).
- [113] M. Robbins, private communication.
- [114] J. Adler and A. Aharony, *J. Phys. A: Math. Gen* **21**, 1387 (1988); J. Adler, *Physica A* **171**, 453 (1991) and references therein; N.S. Branco, R.R. dos Santos, and S.L.A. de Queiroz, *J. Phys. C* **21**, 2463 (1988).
- [115] C.M. Coram, A. Jacobs, N. Heinig, and K. B. Winterbon, *Phys. Rev. B* **40**, 6992 (1989).
- [116] G. Bertotti and M. Pasquale *J. Appl. Phys.* **69**, 5066 (1991).
- [117] D. Sherrington and S. Kirkpatrick, *Phys. Rev. Lett.* **35**, 1792 (1975).
- [118] G. Bertotti and M. Pasquale *J. Appl. Phys.* **67**, 5255 (1990).
- [119] B. Alessandro, G. Bertotti, A. Montorsi, *J. Phys. (Paris) Colloq.* **49** C8, 1907 (1988).
- [120] D. Dhar and P.B. Thomas *J. Phys. A* **25**, 4967 (1992); P.B. Thomas and D. Dhar *J. Phys. A: Math. Gen.*, **26**, 3973 (1993); S. Gupta, preprint 1993; J. Zemmouri, B. Ségard, W. Sergent, and B. Macke, *Phys. Rev. Lett.* **70**, 1135 (1993).
- [121] M. Rao, H.R. Krishnamurthy, and R. Pandit *Phys. Rev. B* **42**, 856 (1990) and references therein.
- [122] M. Blume, V.J. Emery, and R.B. Griffiths, *Phys. Rev. A* **4**, 1071 (1971).
- [123] N.W. Ashcroft, N.D. Mermin, “Solid State Physics” W.B. Saunders Company (1976).
- [124] B.W. Roberts and J.P. Sethna (unpublished).
- [125] H. Rieger and A.P. Young, *J. Phys. A: Math. Gen.*, **26**, 5279 (1993).
- [126] K.A. Dahmen, Ph.D. thesis, Cornell University (1995).
- [127] G. Parisi and L. Pietronero, *Europhys. Lett.* **16**, 321 (1991).

- [128] K.A. Dahmen, O. Perkovic, B.W. Roberts, and J.P. Sethna, preprint in preparation.
- [129] K.A. Dahmen, O. Perkovic, and J.P. Sethna, preprint in preparation.
- [130] The $O(\epsilon^2)$ diagram which we constructed in reference [42] and had argued to lead to different results in $O(\epsilon^2)$ for the two models, turned actually out to be irrelevant, as all other diagrams which are different from the equilibrium model.
- [131] Further information is available via World Wide Web:
http://www.lassp.cornell.edu/LASSP_Science.html.

FIGURES

FIG. 1. **Experiment: Magnetic hysteresis loops of a 60 nm thick Gd film for various annealing temperatures** (as indicated next to each loop) and constant annealing time (3 minutes each). All measurements are performed at $200 \pm 5K$. The sweeping frequency of the external magnetic field is 0.5 Hz (from A. Berger, unpublished).

FIG. 2. **Experiment: Distribution of pulse areas (p), integrated over the hysteresis loop for 81% Ni-Fe wires after various heat treatments.** The originally hard drawn wires have been subjected to a one-hour heat treatment in high vacuum at temperatures of $240^\circ C$ or $460^\circ C$ and cooled down in the furnace. (From U. Lieneweg and W. Grosse-Nobis, *Int. J. Magn* **3**, 11 (1972).)

FIG. 3. **Equilibrium magnetization curve $M(H)$** for the pure Ising model at zero temperature.

FIG. 4. **Nonequilibrium magnetization curve $M(H)$** in the pure Ising model at zero temperature for the dynamics defined in the text.

FIG. 5. **Mean-field magnetization curves** for the nonequilibrium zero temperature random field Ising model at various values of the disorder $R = 0.6J < R_c$ (a), $R = R_c = \sqrt{(2/\pi)}J = 0.798J$ (b), and $R = J > R_c$ (c).

FIG. 6. **Mean-field magnetization curves for the soft-spin version** of the zero temperature random field Ising model at various values of the disorder $R = 1.3J < R_c$ (a), $R = R_c = 2kJ/((k - J)\sqrt{2\pi}) = 1.6J$ (see appendix A 6) (b), and $R = 2J > R_c$ (c).

FIG. 7. **Mean-field phase diagram** for the nonequilibrium zero temperature random field Ising model. The critical point studied in this paper is at $R = R_c$, $H = H_c(R_c)$, with $H_c(R_c) = 0$ in the hard-spin mean field theory. There are two relevant directions $r = (R_c - R)/R$ and $h = H - H_c(R_c)$ near this critical point. The bold line indicates the threshold field $H_c^u(R)$ for the onset of the infinite avalanche upon monotonically increasing the external magnetic field. The dashed line describes $H_c^l(R)$ for a decreasing external magnetic field. The three dotted vertical lines marked (a), (b), and (c) describe the paths in parameter space which lead to the corresponding hysteresis loops shown in figure 5.

FIG. 8. **Mean-field phase diagram for the soft-spin version** of the nonequilibrium zero temperature random field Ising model. The diagram is plotted analogously to figure 7. Magnetic field sweeps along the lines (a), (b) and (c) lead to the corresponding soft-spin hysteresis curves shown in figure 6. Note that here, in contrast to the hard-spin model the value of the critical field, $H_c(R_c)$ does depend on the history of the system: for monotonically increasing external magnetic field $H_c(R_c) = H_c^u(R_c) = k - J$, and for monotonically decreasing external magnetic field $H_c(R_c) = H_c^l(R_c) = -(k - J)$ (see appendix A 6). This implies that in contrast to the hard-spin mean-field theory of figure 7, the soft-spin mean-field theory displays hysteresis for *all* finite disorder values, *i.e.* even at $R \geq R_c$.

FIG. 9. **Simulated hysteresis curves for two small realizations of the nonequilibrium RFIM in three dimensions.** Each sample consists of only 5^3 spins, with periodic boundary conditions. The two systems have different configurations of random fields that are taken from the same distribution $\rho(f)$ with standard deviation $R = 5J > R_c$. (In 3 dimensions $R_c = (2.16 \pm 0.03)J$ [45].) Note that here, as in all plots of numerical simulation results in finite dimensions J denotes the strength of the nearest neighbor coupling J_{ij} , which differs from its definition in the analytical calculation by the coordination number z – see footnote 4 on page 16.

FIG. 10. **Mean-field avalanche size distribution** integrated over the hysteresis loop for systems with 1000000 spins at various disorder values $R > R_c = 0.798J$: (a) $R = 1.46J$ (averaged over 10 different configurations of random fields), (b) $R = 1.069J$ (averaged over 5 different configurations of random fields), and (c) $R = 0.912J$ (averaged over 10 different configurations of random fields). Each curve is a histogram of all avalanche sizes found as the magnetic field is raised from $-\infty$ to $+\infty$, normalized by the number of spins in the system. For small $|r| = |R_c - R|/R$ the distribution roughly follows a power law $D(S, r) \sim S^{-(\tau + \sigma\beta\delta)}$ up to a certain cutoff size $S_{max} \sim |r|^{-1/\sigma}$ which scales to infinity as r is taken to zero. The straight line above the three data curves in the figure represents an extrapolation to the critical point $R = R_c$ in an infinite system, where one expects to see a pure power law distribution on all length scales $D(S, r) \sim S^{-(\tau + \sigma\beta\delta)}$ with the mean field values of the corresponding exponents $\tau + \sigma\beta\delta = 2.25$.

FIG. 11. **Feynman diagrams.** The relevant corrections to first order in $\epsilon = 6 - d$ for the constant part χ^{-1}/J in the propagator (a), and for the vertex u (b). Figure (c) shows an example of a diagram forbidden by causality.

FIG. 12. **Phase diagram and flows (schematic).** (a) The vertical axis is the external field H , responsible for pulling the system from down to up. The horizontal axis is the width of the random-field distribution R . The bold line is $H_c(R)$, the location of the infinite avalanche (assuming an initial condition with all spins down and a slowly increasing external field). The critical point we study is the end point of the infinite avalanche line ($R_c, H_c(R_c)$).

Using the analogy with the Ising model (see text) we also show the RG flows around the critical point. Here we ignore the RG motion of the critical point itself: equivalently, the figure can represent a section through the critical fixed point tangent to the two unstable eigenvectors (labeled h and r). Two systems on the same RG trajectory (dashed thin lines) have the same long-wavelength properties (correlation functions ...) except for an overall change in length scale, leading to the scaling collapse of equation (9). The r eigendirection to the left extends along the infinite avalanche line; to the right, we speculate that it lies along the percolation threshold for up spins.

(b) $O(\epsilon)$ RG flows below 6 dimensions in the (χ^{-1}, u) plane (see text). Linearization around the Wilson-Fisher (WF) fixed point yields the exponents given to $O(\epsilon)$ in the table. In the vicinity of the repulsive $u = 0 = \chi^{-1}$ (MFT) fixed points one obtains the old mean-field exponents.

FIG. 13. **Feynman diagram.** The correction to $O(\tilde{\epsilon})$ to the vertex w in an expansion about 8 dimensions, see eq. (110) in the text.

FIG. 14. **Borel resummed critical exponents and simulation results.** Shown are the numerical values of the exponents $1/\nu$, η , and $\beta\delta = \nu(d - \eta)/2$ (triangles, diamonds, and circles respectively) in 3, 4, and 5 dimensions and in mean field theory (dimension 6 and higher). The error bars denote systematic errors in finding the exponents from collapses of curves at different values of disorder R . Statistical errors are smaller. The dashed lines are the Borel sums to fifth order in ϵ for the same exponents (see text).

FIG. 15. **Comparison to numerical results.** Numerical values (filled symbols) of the exponents $\tau + \sigma\beta\delta$, τ , $1/\nu$, $\sigma\nu z$, and $\sigma\nu$ (circles, diamond, triangles up, squares, and triangle left) in 2, 3, 4, and 5 dimensions. The empty symbols are values for these exponents in mean field (dimension 6). Note that the value of τ in 2d was not measured. The empty diamond represents the expected value [98,129]. The numerical results are courtesy of Olga Perković [45,98] from simulations of sizes up to 7000^2 , 1000^3 , 80^4 , and 50^5 spins, where for 320^3 for example, more than 700 different random field configurations were measured. The long-dashed lines are the ϵ expansions to first order for the exponents $\tau + \sigma\beta\delta$, τ , $\sigma\nu z$, and $\sigma\nu$. They are: $\tau + \sigma\beta\delta = \frac{9}{4} - \frac{\epsilon}{8}$, $\tau = \frac{3}{2} + O(\epsilon^2)$, and $\sigma\nu z = \frac{1}{2} + O(\epsilon^2)$, and $\sigma\nu = \frac{1}{4} + O(\epsilon^2)$ where $\epsilon = 6 - d$ and d is the dimension. The short-dashed line is the Borel sum for $1/\nu$ to fifth order in ϵ . The other exponents can be obtained from exponent equalities (see section IVI in the text). The error bars denote systematic errors in finding the exponents from collapses of curves at different values of disorder R . Statistical errors are smaller.

FIG. 16. **Contour lines for the correlation length** in the (r', h') plane (schematic). The tilted coordinate axes indicate the physical directions (r, h) . Since $\nu/(\beta\delta) < \nu$, the correlation length ξ changes faster in the $(0, h')$ direction than in the $(r', 0)$ direction.

FIG. 17. **Feynman diagrams.** The perturbative expansion about mean-field theory is presented here by Feynman diagrams. (a) Graph for the vertex u . Incoming arrows denote η fields, outgoing arrows denote $\hat{\eta}$ fields. (b) Example of a diagram which violates causality and is therefore forbidden. (c) Graph for the vertex $u_{2,0}$. (d) Example of a diagram that is zero due to momentum conservation [78].

FIG. 18. **Feynman diagram** for the lowest order correction to $u_{2,0}(H_1, H_2)$. The magnetic fields corresponding to the times at which the vertices are evaluated are indicated. The propagators do not couple different fields.

FIG. 19. **Different Borel-resummations for ν .** Borel resummation of the perturbation series for ν to $O(\epsilon^5)$ in $6 - \epsilon$ dimensions using (a) the method of Vladimirov, Kazakov, and Tarasov [106], which does not impose a pole for ν or any other independent information, and (b) the results of Le Guillou and Zinn-Justin [110], which are obtained by explicitly assuming a singularity for ν at a (variationally determined) critical value of ϵ and by imposing the exactly known value in two dimensions. Curve (b) is based on an old result for the epsilon-expansion which later turned out to have the wrong 5th order term [59]. Our own Borel-resummation (curve (a)) on the other hand has been obtained using the newest, presumably correct result for the fifth order term [59]. Partly by design, curve (b) agrees very well with the value of ν in the equilibrium pure Ising model in $d - 2$ dimensions. Le Guillou and Zinn-Justin quote an error due to truncation of the series, which is increasingly larger than 10% below 2.5 dimensions. Curve (a) agrees better with the numerical results in our zero-temperature avalanche model, indicated for the respective dimensions by the black diamonds with error bars [45]. It is believed that the two resummation methods should converge to the same results if taken to high enough order, though this has never been proven. Also shown are values for ν for the *equilibrium* random field Ising model in three dimensions (circles) from different sources [87,88].

FIG. 20. **Feynman diagram.** The correction to $O(\tilde{\epsilon})$ to the vertex w in an expansion about 8 dimensions, see eq. (E3) in the text.

FIG. 21. **The function P_{flip}^{both}** defined in equation (F10), plotted as a function of H_1 . In the figure, dH denotes the amplitude which is called ΔH in the text.

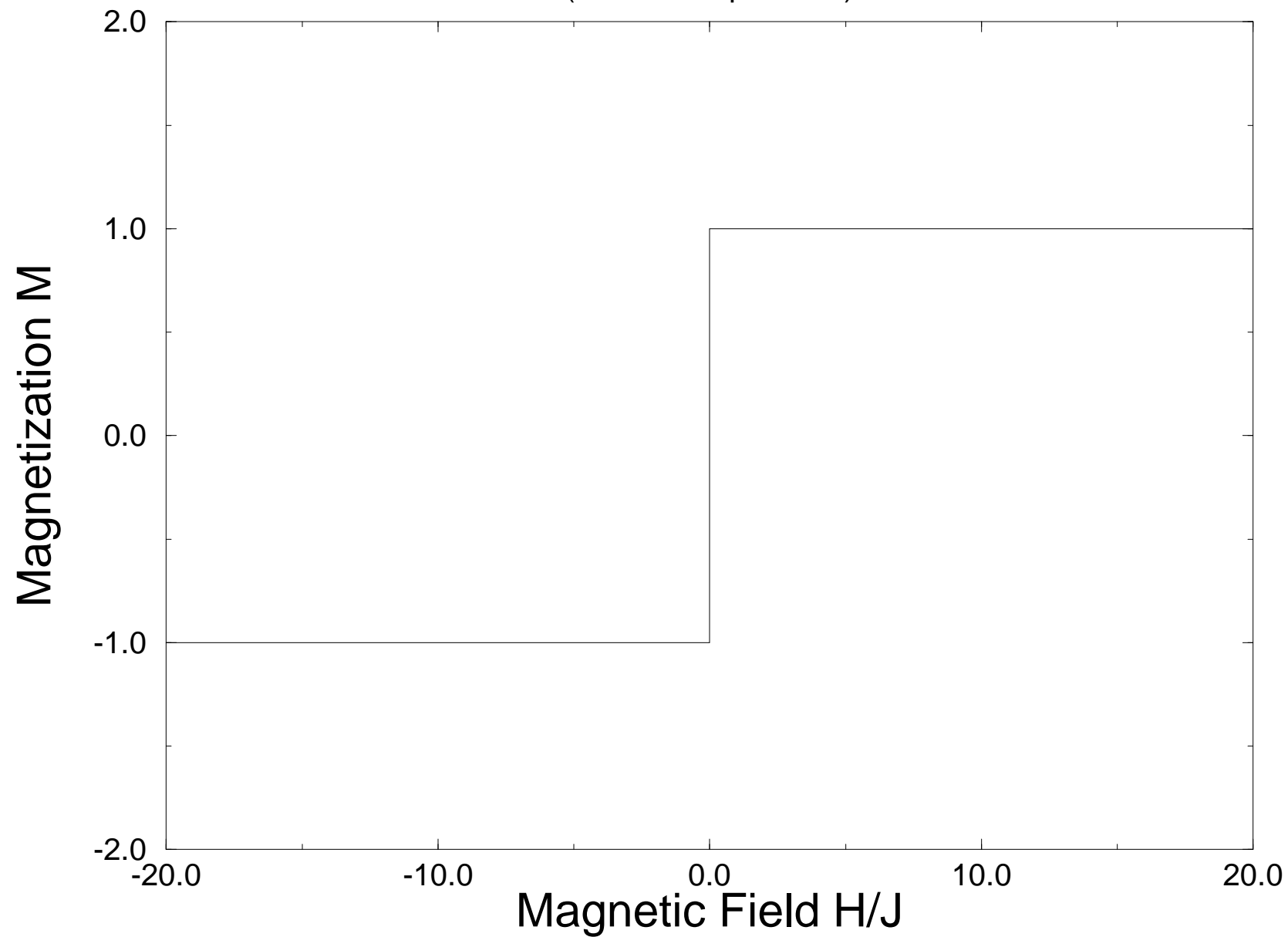
TABLES

TABLE I. **Numerical results for the critical exponents in three dimensions** for our hysteresis model [45,98] and for the equilibrium zero temperature random field Ising model [62,87,88]. The breakdown of hyperscaling exponent $\tilde{\theta}$ is calculated for the the hysteresis model from the relation $\beta + \beta\delta = (d - \tilde{\theta})\nu$ (see section a and references [126,129]). The values of the critical exponents of the two models remain within each other's errorbars (except for ν and perhaps η , although Dayan, Schwartz, and Young [89] found that $\nu \simeq 1.4$ in the three dimensional equilibrium random-field Ising model from real space renormalization group calculations); the equality of the exponents was conjectured by Maritan *et al* [86]. The numerical agreement may not be so surprising, if one remembers that the $6 - \epsilon$ expansion is the same for all exponents of the two models. Nevertheless there is always room for nonperturbative corrections, so that the exponents might still be different in 3 dimensions (see section VIII B, and figure 19). Physically, the agreement is rather unexpected, since the nature of the two models is very different. While the hysteresis model is far from equilibrium, occupying a history dependent, metastable state, the equilibrium RFIM is always in the lowest free energy state. One may speculate, however, about a presumably universal crossover from our hysteresis model to the equilibrium random field Ising model as temperature fluctuations and a finite field-sweeping frequency Ω are introduced (see appendix G 3).

exponents	Hysteresis loop [45] in 3 dimensions (courtesy Olga Perković)	Equilibrium RFIM [87,88] in 3 dimensions
ν	1.42 ± 0.17	0.97, 1.30, 1.02 ± 0.06
β	0.0 ± 0.43	-0.1, 0.05, 0.06 ± 0.07
$\beta\delta$	1.81 ± 0.36	1.6, 1.9 ± 0.4 , 1.83 ± 0.18
η	0.79 ± 0.29	0.25, 0.5 ± 0.5 , 0.14 ± 0.067
$\tilde{\theta}$	1.5 ± 0.5	1.45, 1.5 ± 0.45 , 1.851 ± 0.067
R_c (Gaussian)	2.16 ± 0.03	2.3 ± 0.2 [88]
$H_c(R_c)$	1.435 ± 0.004	0 (by symmetry)

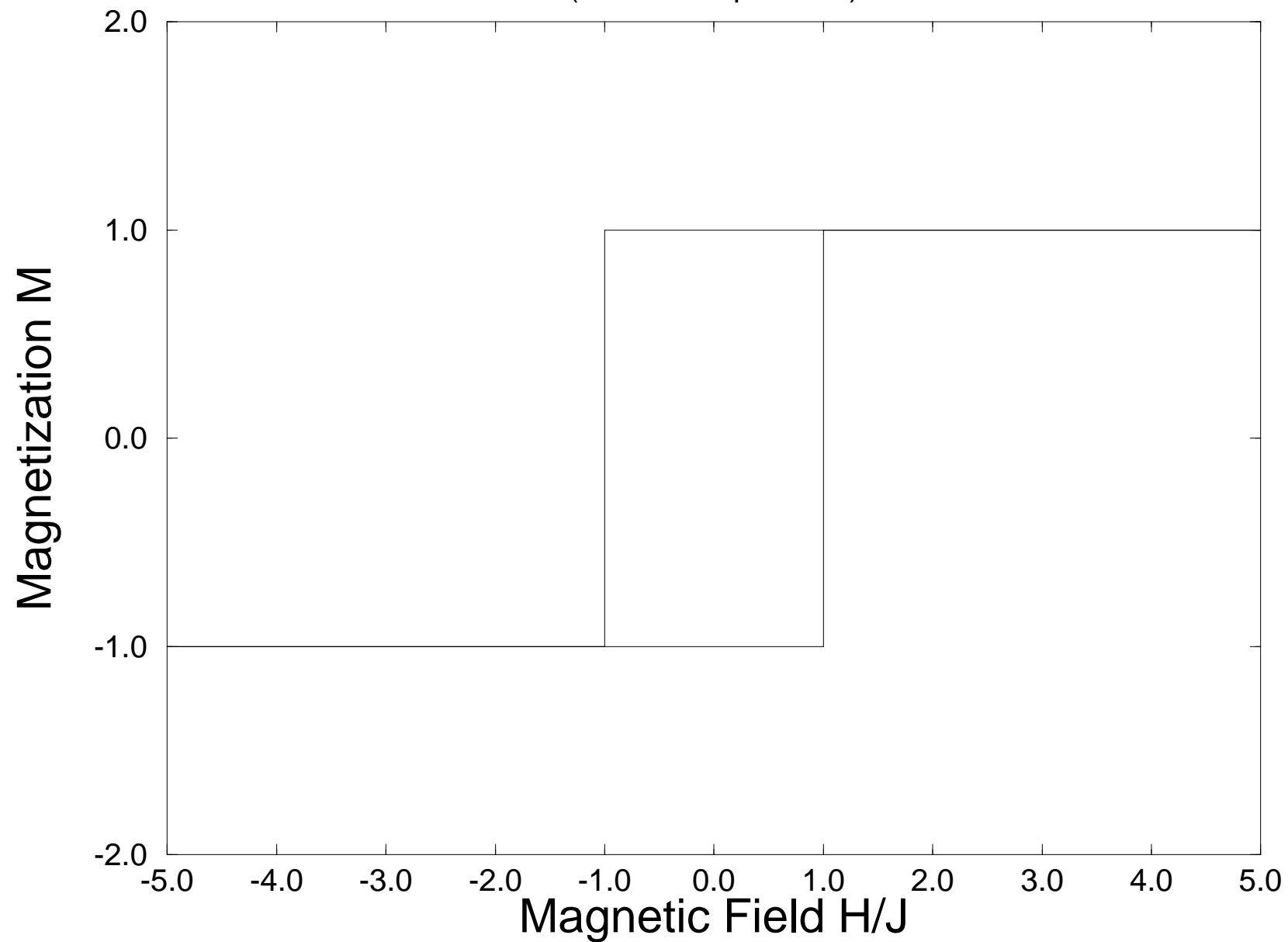
M(H) for the pure Ising model in equilibrium

(at zero temperature)



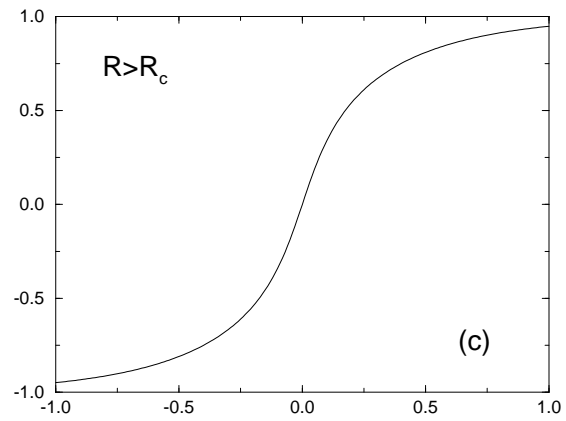
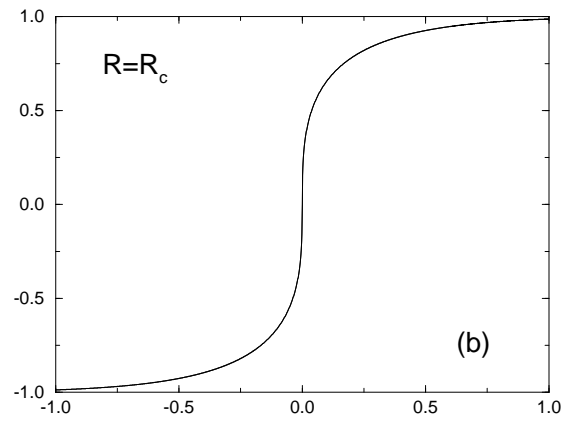
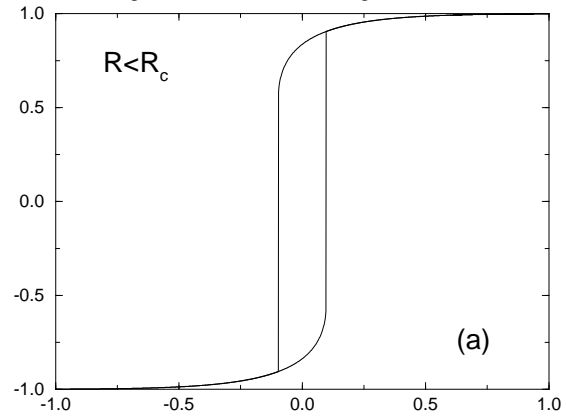
M(H) for the nonequilibrium pure Ising model

(at zero temperature)



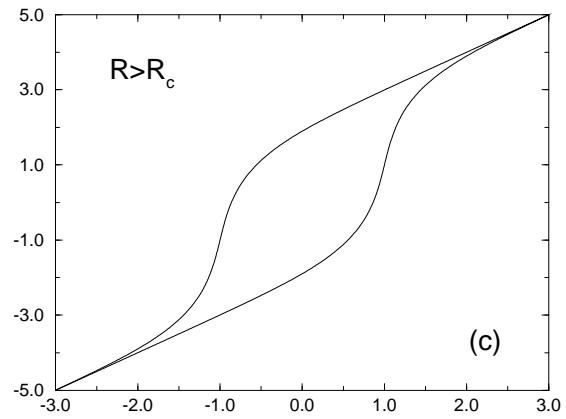
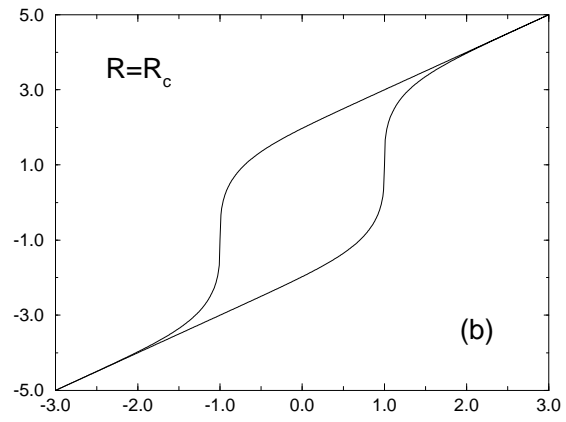
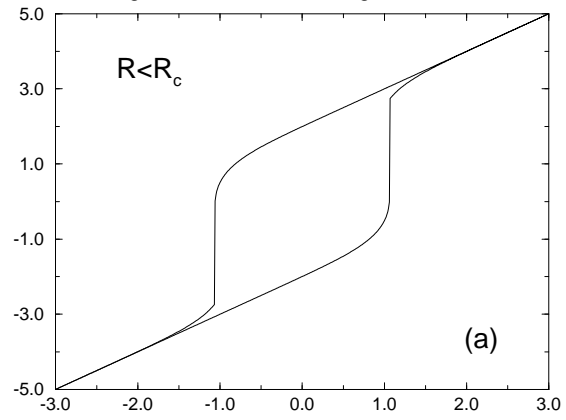
Hard-spin mean-field magnetization curve

Magnetization M versus Magnetic Field H/J

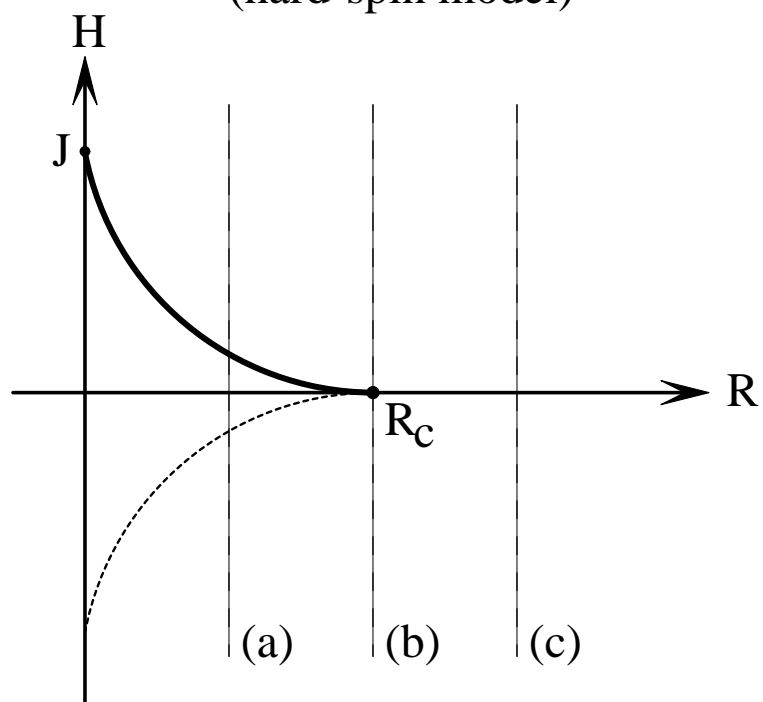


Soft-spin mean-field magnetization curve

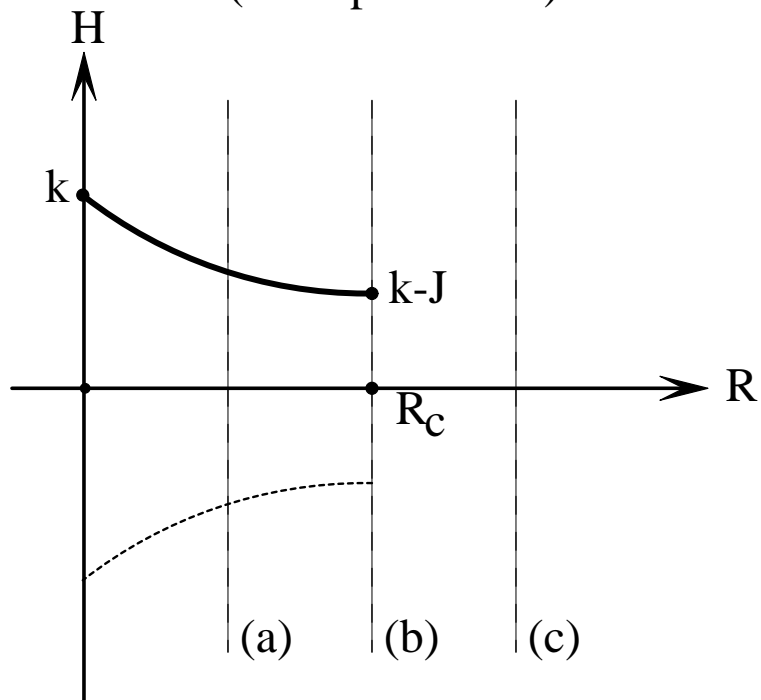
Magnetization M versus Magnetic Field H/J

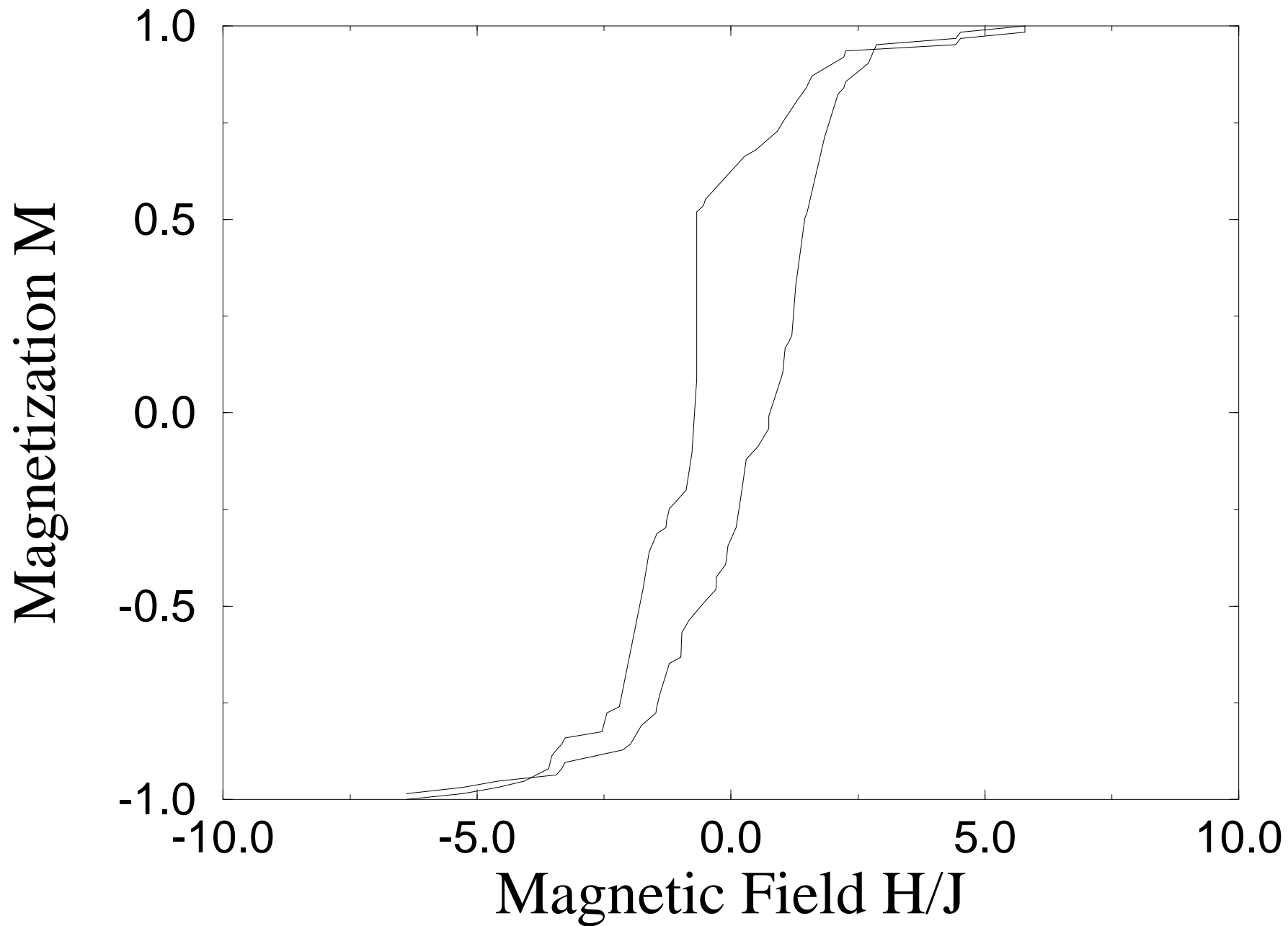


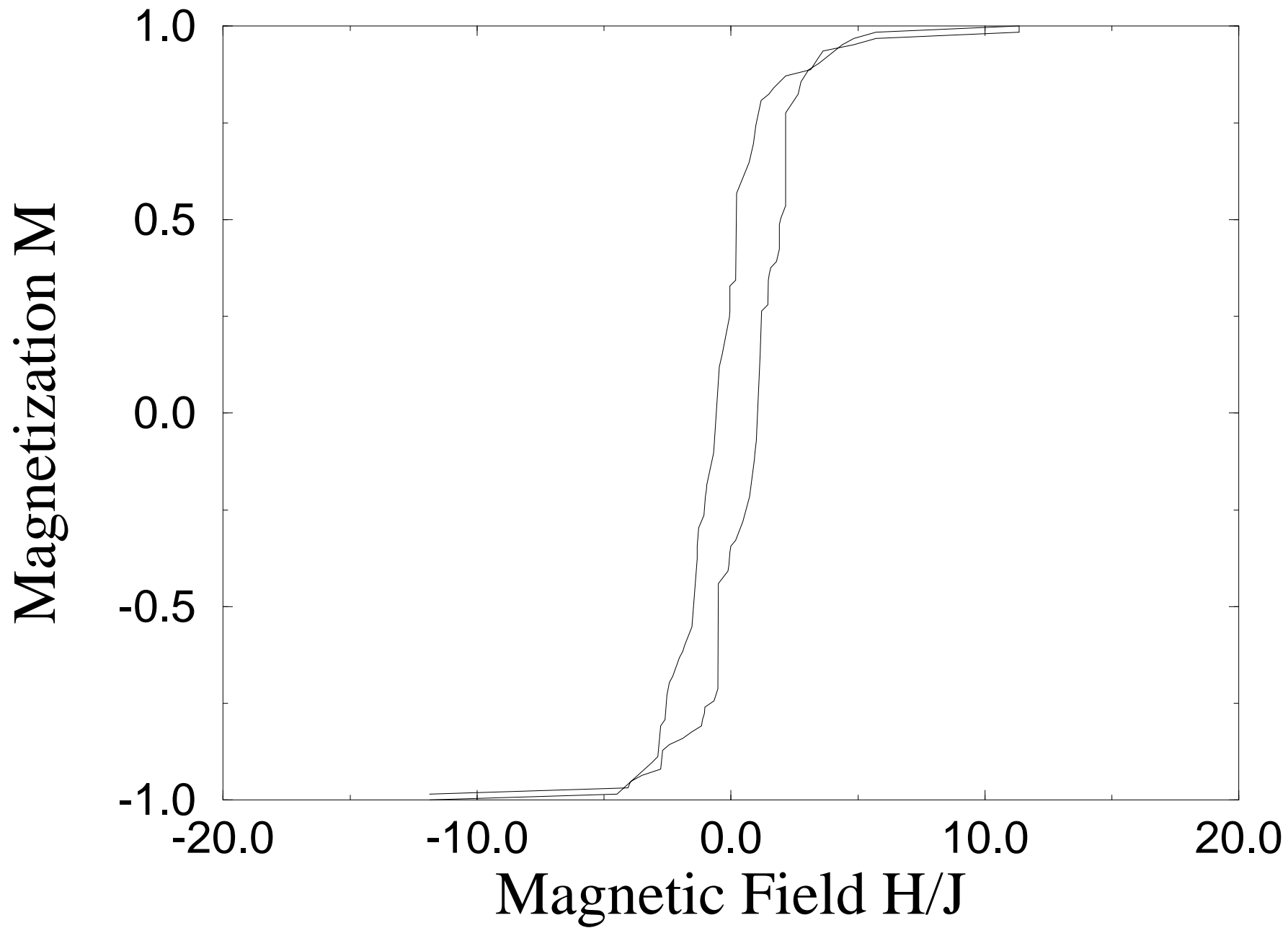
Phase Diagram in Mean-Field Theory
(hard-spin model)

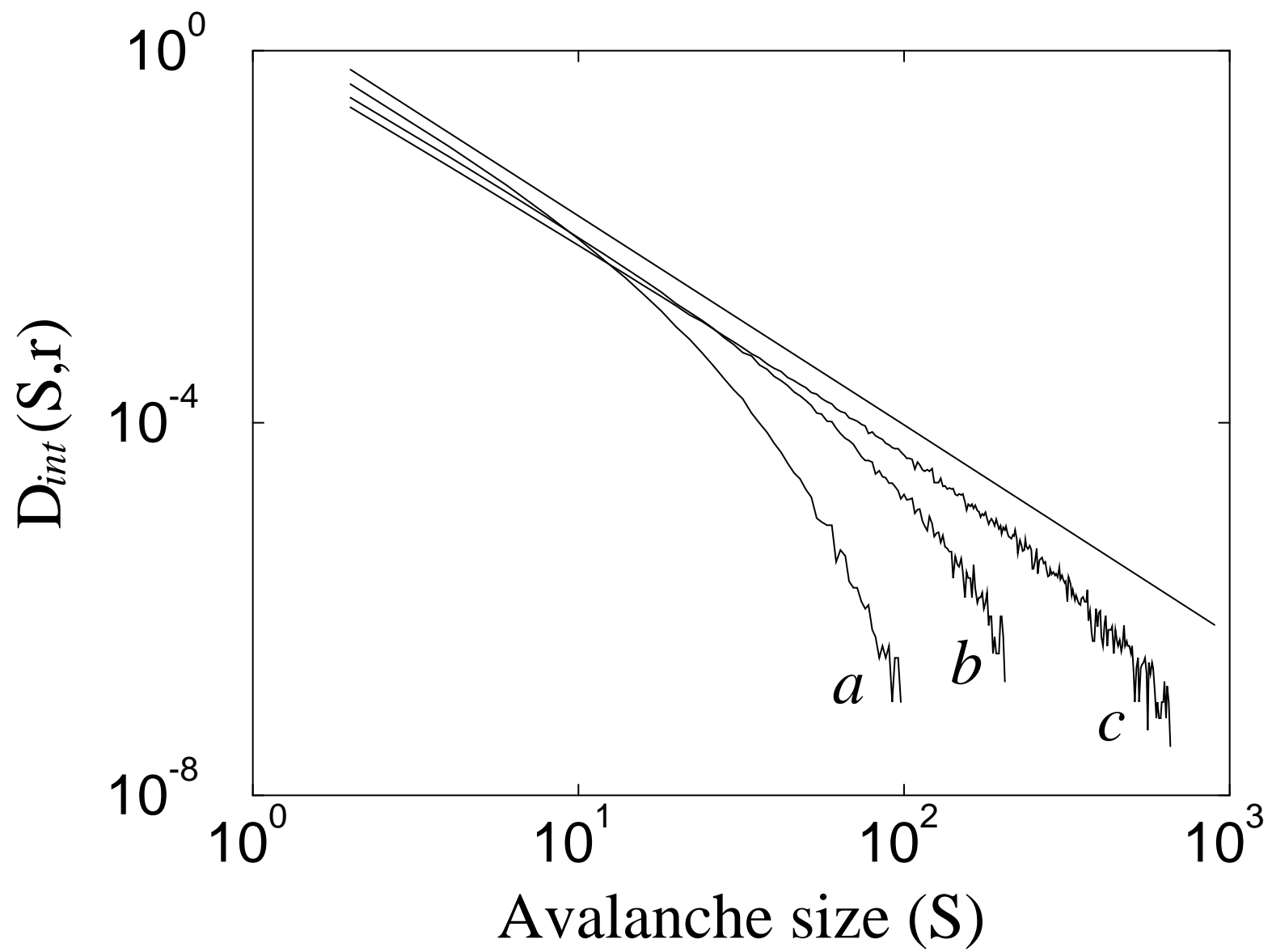


Phase Diagram in Mean-Field Theory
(soft-spin model)

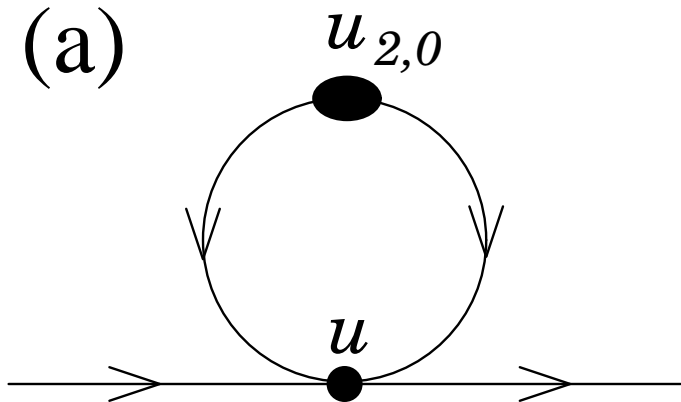




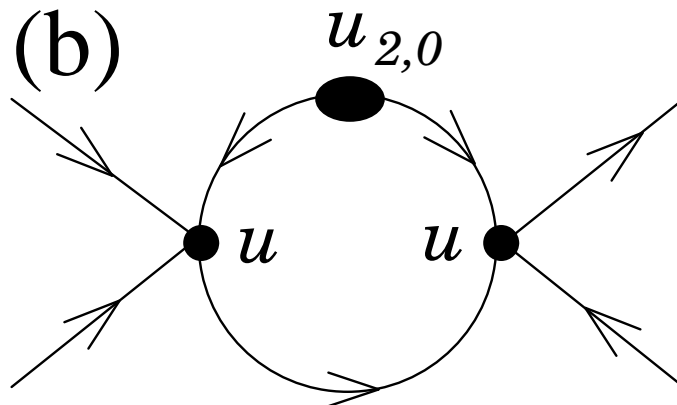




(a)



(b)



(c)

